SCIENTIFIC RESEARCH OF THE SCO COUNTRIES: SYNERGY AND INTEGRATION

上合组织国家的科学研究：协同和一体化

Proceedings of the International Conference

Date: June 8

Beijing, China 2022

上合组织国家的科学研究：协同和一体化国际会议

参与者的英文报告

International Conference “Scientific research of the SCO countries: synergy and integration”

Part 2: Participants’ reports in English

2022年6月8日。中国北京
June 8, 2022. Beijing, PRC

Proceedings of the International Conference
“Scientific research of the SCO countries: synergy and integration”. Part 2 - Reports in English

(June 8, 2022. Beijing, PRC)

ISBN 978-5-905695-82-7

这些会议文集结合了会议的材料 – 研究论文和科学工作者的论文报告。 它考察了职业化人格的技术和社会学问题。一些文章涉及人格职业化研究问题的理论和方法论方法和原则。
作者对所引用的出版物，事实，数字，引用，统计数据，专有名称和其他信息的准确性负责

These Conference Proceedings combine materials of the conference – research papers and thesis reports of scientific workers. They examine technical, juridical and sociological aspects of research issues. Some articles deal with theoretical and methodological approaches and principles of research questions of personality professionalization.

Authors are responsible for the accuracy of cited publications, facts, figures, quotations, statistics, proper names and other information.

.

ISBN 978-5-905695-82-7

CONTENTS

MEDICAL SCIENCES

AGRICULTURAL SCIENCES

TECHNICAL SCIENCE

PHYSICS AND MATHEMATICS

DOI 10.34660/INF.2022.72.96.274

婴儿严重合并颅脑外伤后每分钟血液循环量的变化
CHANGES IN MINUTE VOLUME OF BLOOD CIRCULATION IN SEVERE CONCOMITANT TRAUMATIC BRAIN INJURY IN INFANTS

Muhitdinova Hura Nuritdinovna
Doctor of Medical Sciences, Full Professor
Center for the Development of Professional Qualifications of Medical Workers, Doctor of Medical Sciences
Krasnenkova Marianna Borisovna
Candidate of Medical Sciences, Associate Professor
Tashkent Medical Academy

抽象的。 在第一天，所有三岁以下的 STBI 儿童都有高动力型的血流动力学。 器官和系统功能响应极端暴露的适应性变化在本质上是波动的，代表心脏功能活动增加和减少的交替变化，随着 CO 的变化，波动周期为 4-5 天。 至每天 1 升。 考虑到婴儿期代偿机制的适应性资源和功能活动，夜间是最脆弱的，这是对3岁以下受伤儿童STBI急性期矫正治疗有效性的确认之一。 被认为是最小化 CO 昼夜节律反转的持续时间。

关键词：昼夜节律，血流动力学，严重合并颅脑损伤，儿童。

Abstract. *On the first day, all children with STBI under the age of three years had a hyperdynamic type of hemodynamics. Adaptive changes in the function of organs and systems in response to extreme exposure were undulating in nature, representing an alternation of an increase and a decrease in the functional activity of the heart with a period of fluctuations of 4-5 days with changes in CO up to 1 liter per day. Taking into account that for adaptive resources and functional activity of compensatory mechanisms in infancy, the night time is the most vulnerable, one of the confirmations of the effectiveness of corrective therapy in the acute period of STBI in injured children under the age of 3 years can be considered the minimization of the duration of CO circadian rhythm inversion.*

Keywords: *circadian rhythm, hemodynamics, severe concomitant traumatic brain injury, children.*

Relevance

One of the leading extracranial factors aggravating the consequences of SCT-

BI is unstable hemodynamics, which may be the result of compensatory reactions aimed at maintaining brain tissue oxygenation in conditions of traumatic shock, inflammatory response, increased intracranial pressure (ICP) and other mechanisms, usually observed in associated trauma. The circulatory and tissue hypoxia that develops most early in severe TBI may be a consequence of circulatory inefficiency and, at the same time, factors aggravating subsequent cerebral ischemia. External respiratory disorders of the peripheral type caused by traumatic injury usually develop in patients with STBI, accompanied by impaired consciousness and bulbar disorders, significantly impairing the compensatory mechanisms of systemic hemodynamics, leading to depletion of the energy resources of the circulatory system as a whole. However, there is not enough information in the literature on the features of changes in cardiac output in the acute period of SCTBI in infants [1-3].

Purpose of the work

To study and evaluate changes in cardiac output in severe concomitant traumatic brain injury in infants.

Material and research methods

A detailed analysis of reliably significant deviations, intergroup differences in the studied hemodynamic parameters was carried out. The results were obtained by monitoring with hourly recording of body temperature, heart rate (HR), systolic (SBP), diastolic (DBP) blood pressure, cardiac output (CO). The calculation of the stroke volume index was carried out according to the formula: CO=SV*HR/1000, l per minute.

The research data were processed by the method of variation statistics using the Excel program by calculating the arithmetic mean values (M) and the errors of the means (m). To assess the significance of differences between the two values, Student's parametric test (t) was used. The relationship between the dynamics of the studied indicators was determined by the method of pair correlations. The critical level of significance in this case was taken equal to 0.05.

Of the 18 children (tab. 1) diagnosed with severe concomitant traumatic brain injury (SCTBI) admitted to the Republican Center for Emergency Medical Care in infancy, 7 patients were intensively treated in the ICU for 5.9 ± 1.3 days, 6 patients for 14±1.7 days, 7 children for 31.2±5.3 days, which served as the basis for creating randomized groups according to the severity of the condition. The difference is significant ($p<0.05$).

Table 1.

Characteristics of SCTBI patients admitted before the age of 3 years

Groups	Num. of days in ICU	Num. of patients	Gender male	Age	RTA	Catatrauma	Traum. shock of the 2 degree	Operated on admission	Number of days in hospital
1	5.9±1.3	7	4.	20.8±7.8	71% (5)	29% (2)	71% (5)	71% (5)	15.2±7
2	14±1.7	6	4	23.1±4.7	50% (3)	50% (3)	83% (5)	66% (4)	20±4
3	31.2±5.3	5	3	18.2±4.6	80% (4)	20% (1)	100% (5)	100% (5)	37.4±5.3

In group 1, the frequency of closed traumatic brain injury (CTBI) (71%), concussion (28%) prevailed, the number of operations on the first day after injury was 71%. In the 2nd more severe group, the number of open traumatic brain injury (OTBI) prevailed - 66%, the frequency of severe brain contusion (SBC) - 50%, fracture of the parietotemporal bone with the transition to the base of the skull 48%, severe traumatic shock was observed in all patients. In the most severe group 3, 100% of the severity of the condition at admission was due to CTBI, SBC, subarachnoid hemorrhage (SAH), traumatic shock. In group 1, out of 5.9±1.3 days spent in the ICU, only 1 patient out of 7 was on mechanical ventilation for 3 days in CMV mode, followed by extubation upon restoration of spontaneous breathing. In groups 2 and 3, all patients were transferred to mechanical ventilation upon admission according to indications. Subsequently, out of 14.6 ± 1.7 days spent in the ICU, the average rate of mechanical ventilation in CMV mode in group 2 was carried out for 6.8 ± 2.2 days, SIMV 1.75±0.8, CPAP in 1 patient - 1 day, the duration of spontaneous breathing was 7±1.6 days. In group 3, mechanical ventilation in the CMV mode was performed for three patients for 17±3 days, SIMV 9.5±4.6 days, CPAP 2.5±1.5 days, spontaneous breathing 34±9.5 days.

Results and discussion

The phase structure of the CO circadian rhythm in the acute period of SCTBI in infancy was studied and assessed. Table 2 shows changes in the mesor of the circadian rhythm CO depending on the severity of the injury by groups.

Table 2.

Dynamics of the mesor of the circadian rhythm CO in the acute period of SCTBI in children under 3 years of age

Days	Group 1	Group 2	Group 3
1	4.2±0.7	5.3±0.9	4.0±0.4
2	4.5±0.4	5.5±0.4	3.9±0.3
3	4.1±0.3	4.7±0.4	3.7±0.4
4	4.0±0.5	4.4±0.4	3.8±0.3
5	3.3±0.2	3.6±0.2*	3.2±0.2*
6	3.2±0.4	3.5±0.2*	3.7±0.2
7	3.3±0.3	3.6±0.2*	3.9±0.3
8		3.4±0.2*	3.7±0.2
9		3.7±0.2*	3.9±0.2
10		3.9±0.2*	3.8±0.3
11		4.5±0.4	4.1±0.2
12		4.4±0.2	3.4±0.3
13		5.0±0.3	3.9±0.4
14		4.5±0.3	3.7±0.3
15		4.3±0.4	3.3±0.4
16			3.5±0.2
17			3.5±0.3
18			3.2±0.3*
19			3.3±0.2*
20			4.1±0.2
21			3.3±0.3
22			3.2±0.3*
23			3.4±0.3
24			3.9±0.3
25			3.5±0.3
26			3.8±0.4
27			3.9±0.4
28			3.6±0.3
29			4.0±0.4
30			4.1±0.4

*-the change is significant relative to the indicator in 1 day

On the first day, all examined children revealed a hyperdynamic type of hemodynamics, as evidenced by the excess of the mesor of the circadian rhythm CO of the age normative values presented in the literature (tab. 1). A decrease in CO on the 5th day by 32% in group 2, by 20% in group 3 ($p<0.05$, respectively) and trends towards a decrease in CO in group 1 indicated an effective stress-limiting therapy, aimed at preventing acute heart failure due to an energy-deficient state, naturally present in the early stages after a severe injury. So, in the 2nd group, the mesor of the circadian rhythm CO remained less than the initial one on days 6-9, with a tendency to increase in the following days (fig. 1). In the 3rd group of children, a repeated decrease in the mesor of the circadian rhythm CO was revealed on days 18, 19, 22 by an average of 20% ($p<0.05$, respectively) relative to the initial level. The wave-like change in CO in the acute period of SCTBI, apparently, is of a compensatory nature in the process of adaptation under conditions of serious deviations in the parameters of homeostasis systems during the period of an acute systemic inflammatory reaction, the severity of which creates a risk of developing functional failure of organs and systems due to the integrative effect of tissue energy deficiency. conditions, including the cardiovascular system (fig. 1).

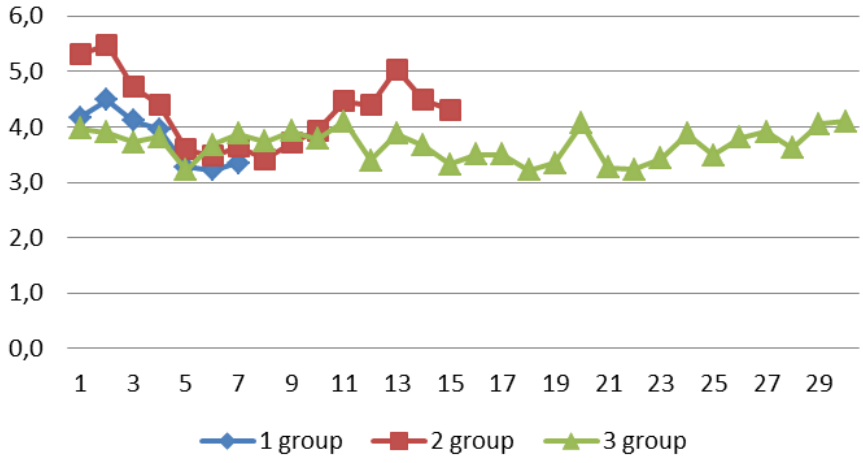

Figure 1. *Dynamics of the mesor of circadian rhythm CO*

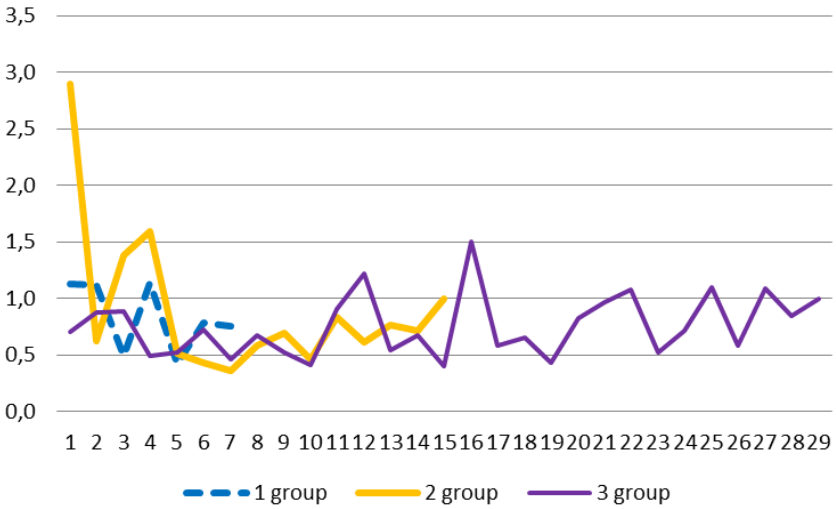

Figure 2. *Dynamics of the amplitude of the circadian rhythm CO*

The instability of hemodynamics on the first day was the most significant in children of the 2nd group, when the amplitude of the circadian rhythm of CO was 2.8 l/min, while in group 1 - 1.2 l/min, in group 3 it turned out to be the smallest - 0.6 l/min (fig. 2).

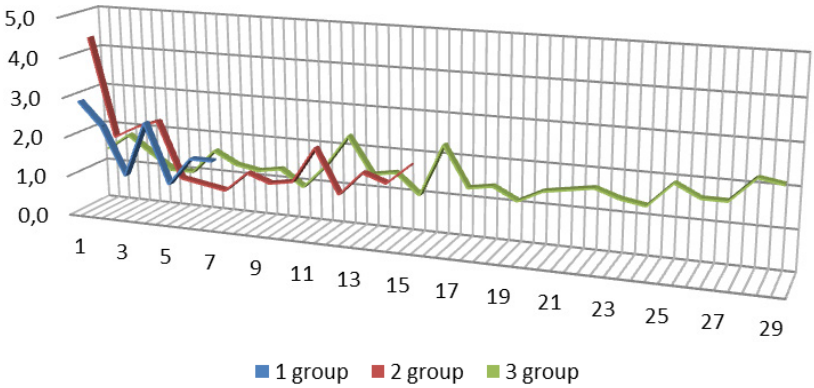

Figure 3. *Change in diurnal CO fluctuations at SCTBI up to 3 years*

The range of daily fluctuations in CO on the first day corresponded to the deviations of the amplitude indicator, that is, it was the largest in group 2 and the minimum in group 3 (fig. 3). In the following days, the oscillatory nature of CO changes persisted. Wave-like changes in CO during the acute period of SCTBI represented the dynamics of adaptive restructuring of the physiological regulators of the function of the cardiovascular system, which worked even in conditions of severe brain damage in infancy. Adaptive changes in the function of organs and systems in response to extreme exposure were undulating in nature, representing an alternation of an increase and a decrease in the functional activity of the heart with a period of fluctuations of 4-5 days with changes in CO up to 1 liter per day.

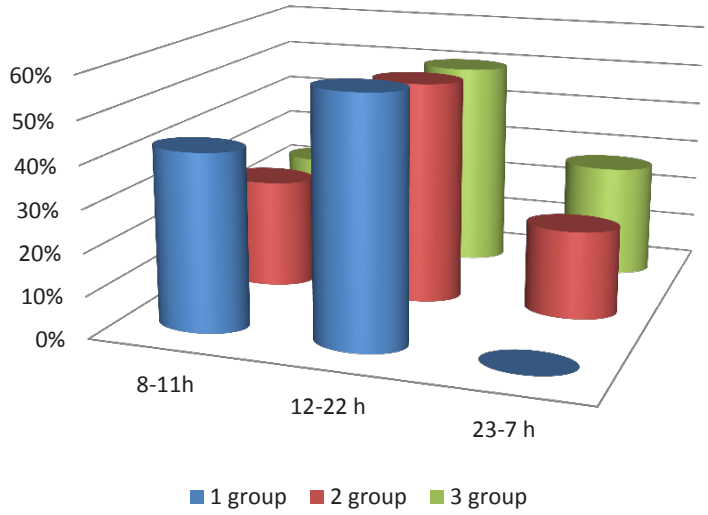

Figure 4. *Duration of CO acrophase shifts in the acute period of SCTBI up to 3 years*

In all groups of injured children, a moderate shift of the acrophase peak within the daylight hours prevailed over a longer period (fig. 4), amounting to 58% in group 1, 53% in group 2, and 50% in group 3. Thus, considering that for adaptive resources and functional activity of compensatory mechanisms for infancy, the most vulnerable is night time, one of the confirmations of the effectiveness of corrective therapy in the acute period of STBI in injured children under the age of 3 years can be considered the minimization of the duration of CO circadian rhythm inversion.

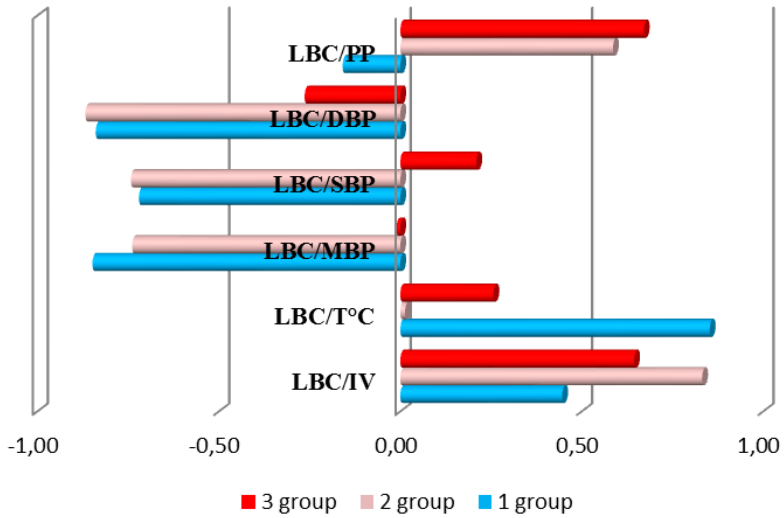

Figure 5. *Correlation links of CO*

As shown in fig. 5, compensatory hemodynamic reactions were found, expressed in inverse correlations of CO with DBP, CO with SBP, CO with MBP in the 1st group of children, which were practically absent in the most severe patients. A tendency to increase CO with an increase in temperature was found only in children of the 1st group. One of the components of the increase in CO in children under 3 years old was the SV value, this relationship was most significant in group 2 and the smallest in children of group 1.

Conclusion

On the first day, all children with STBI under the age of three years had a hyperdynamic type of hemodynamics. Adaptive changes in the function of organs and systems in response to extreme exposure were undulating in nature, representing an alternation of an increase and a decrease in the functional activity of the heart with a period of fluctuations of 4-5 days with changes in CO up to 1 liter per day. Taking into account that for the adaptive resources and functional activity of compensatory mechanisms for infancy, the night time is the most vulnerable, one of the confirmations of the effectiveness of corrective therapy in the acute period of STBI in injured children under the age of 3 years can be considered the minimization of the duration of CO circadian rhythm inversion.

References

1. *https://profmedik.ru/napravleniya/nevrologiya/cherepno-mozgovye-travmy/metodika-borby-s-rasstrojstvami-krovoobrashcheniya-pri-cherepno-mozgovoj-travme*
2. *http://medbiol.ru/medbiol/har_nevr/000869ee.htm*
3. *https://userdocs.ru/medicina/143308/index.html*

DOI 10.34660/INF.2022.57.32.275

3岁以下儿童严重合并颅脑损伤急性期一般外周血管阻力昼夜节律变化

CHANGES IN THE CIRCADIAN RHYTHM OF THE GENERAL PERIPHERAL VASCULAR RESISTANCE IN THE ACUTE PERIOD OF SEVERE CONCOMITANT TRAUMATIC BRAIN INJURY IN CHILDREN UNDER 3 YEARS OF AGE

Muhitdinova Hura Nuritdinovna
Doctor of Medical Sciences, Full Professor
Center for the Development of Professional Qualifications of Medical Workers, Doctor of Medical Sciences

抽象的。 在受伤当天，第 2 组的昼夜节律 GPVR 中值显着高于第 1 组和第 3 组 40%。 胸部、腹腔、输血的颅外损伤严重程度占主导地位，导致第 2 组儿童心血管系统的代偿性高动力得到更大的动员。 GPVR 和 SV、GPVR 和 CO 的负相关表明血流动力学参数的函数关系的高动力学性质。 GPVR 对高热反应的代偿性降低在第 1 组和第 2 组中最为显着，在第 3 组最严重的儿童中几乎没有。

关键词：昼夜节律，总血管阻力，伴随的颅脑损伤，儿童。

Abstract. *On the day of injury, the mesor of the circadian rhythm GPVR in group 2 was significantly higher than in groups 1 and 3 by 40%. The predominance of the severity of extracranial injuries of the chest, abdominal cavity, blood transfusion, led to greater mobilization of compensatory hyperdynamia of the cardiovascular system in children of the 2nd group. The inverse correlation of GPVR and SV, GPVR and CO indicate the hyperdynamic nature of the functional relationship of hemodynamic parameters. The compensatory decrease in GPVR to the hyperthermic reaction was most significant in groups 1 and 2, almost absent in the most severe children of group 3.*

Keywords: *circadian rhythm, total vascular resistance, concomitant traumatic brain injury, children.*

Relevance

One of the leading extracranial factors that aggravate the consequences of SCTBI is unstable hemodynamics, which may be a consequence or cause of increased intracranial pressure (ICP) and other mechanisms, as a rule, observed in concomitant trauma. The average person has approximately 40 billion capillaries. The effective exchange surface of the capillaries is approximately 1000 m2 in

total. The density of capillaries in different organs is not the same. It is 4-5 times greater than the "average" (average) value in the brain, myocardium, and kidneys. This means that with violations of microcirculation in vital organs, the likelihood of their edema in relation to bone, connective and adipose tissue increases. External respiratory disorders caused by traumatic injury significantly worsen the compensatory mechanisms of systemic hemodynamics, leading to the depletion of the energy resources of the circulatory system as a whole. However, there is insufficient information in the literature on the characteristics of changes in general peripheral vascular resistance (GPVR) in the acute period of SCTBI in infants [1-3].

Purpose of the work

To study and evaluate the effect of severe concomitant injury on the circadian rhythm of peripheral vascular resistance in infants in the acute period.

Material and research methods

A detailed analysis of reliably significant deviations, intergroup differences in the studied parameters of the phase structure of circadian rhythms of hemodynamics was carried out. The results were obtained by hourly monitoring of body temperature, heart rate (HR), systolic (SBP), diastolic (DBP) blood pressure, general peripheral vascular resistance (GPVR). Under normal physiological conditions, GPVR ranges from 1200 to 1700 dyn*s*cm^{-5}, with arterial hypertension this value can double against the norm and be equal to 2200-3000 dyn*s*cm^{-5}.

The research data were processed by the method of variation statistics using the Excel program by calculating the arithmetic mean values (M) and the errors of the means (m). To assess the significance of differences between the two values, Student's parametric test (t) was used. The relationship between the dynamics of the studied indicators was determined by the method of pair correlations. The critical level of significance in this case was taken equal to 0.05.

Of the 18 children (tab. 1) diagnosed with severe concomitant traumatic brain injury (SCTBI) admitted to the Republican Center for Emergency Medical Care in infancy, 7 patients received intensive care in the ICU for 5.9 ± 1.3 days, 6 patients for 14±1.7 days, 7 children for 31.2±5.3 days. The difference is significant ($p<0.05$).

Table 1.

Characteristics of SCTBI patients admitted before the age of 3 years

Groups	Num. of patients	Num. of patients	Gender male	Age	RTA	Catatrauma	Traum. shock of the 2 degree	Operated on admission	Number of days in hospital
1	5.9±1.3	7	4.	20.8±7.8	71% (5)	29% (2)	71% (5)	71% (5)	15.2±7
2	14±1.7	6	4	23.1±4.7	50% (3)	50% (3)	83% (5)	66% (4)	20±4
3	31.2±5.3	5	3	18.2±4.6	80% (4)	20% (1)	100% (5)	100% (5)	37.4±5.3

In group 1, the frequency of closed traumatic brain injury (CTBI) (71%), concussion (28%) prevailed, the number of operations on the first day after injury was 71%. In the 2nd more severe group, the number of open traumatic brain injury (OTBI) prevailed - 66%, the frequency of severe brain contusion (SBC) - 50%, fracture of the parietotemporal bone with the transition to the base of the skull 48%, severe traumatic shock was observed in all patients. In the most severe group 3, 100% of the severity of the condition at admission was due to CTBI, SBC, subarachnoid hemorrhage (SAH), traumatic shock. The second group differed from the first and third ones in the predominance of catatrauma almost twice. In group 1, out of 5.9±1.3 days spent in the ICU, only 1 patient out of 7 was on mechanical ventilation for 3 days in CMV mode, followed by extubation upon restoration of spontaneous breathing. In groups 2 and 3, all patients were transferred to mechanical ventilation upon admission according to indications. Subsequently, out of 14.6 ± 1.7 days spent in the ICU, the average rate of mechanical ventilation in CMV mode in group 2 was carried out for 6.8 ± 2.2 days, SIMV 1.75±0.8, CPAP in 1 patient - 1 day, the duration of spontaneous breathing was 7±1.6 days. In group 3, mechanical ventilation in the CMV mode was performed for three patients for 17±3 days, SIMV 9.5±4.6 days, CPAP 2.5±1.5 days, spontaneous breathing 34±9.5 days.

Results and discussion

The phase structure of the GPVR circadian rhythm in the acute period of SCTBI in infancy has been studied and evaluated. Table 2 shows changes in the GPVR circadian rhythm mesor index depending on the severity of the injury by groups.

Table 2.

*Dynamics of the mesor of the circadian rhythm GPVR up to 3 years, dyn/s*cm -5.*

Days	Group 1	Group 2	Group 3
1	717±122	1208±231*	711±94‴
2	698±90	1188±103*	763±92‴
3	742±78	1321±74*	757±98‴
4	713±87	1478±159*	752±75‴
5	782±61	1780±137*	769±60‴
6	821±88	1792±126* °	703±57‴
7	751±84	1730±104* °	701±87‴
8		2041±226 °	733±56‴
9		1690±113 °	670±38‴
10		1600±145 °	789±76‴
11		1545±256	659±64‴
12		1640±73 °	920±82‴
13		1597±114	711±93‴
14		1813±146 °	742±51‴
15		1759±129 °	821±103‴
16			768±46
17			809±129
18			796±84
19			808±67
20			633±40
21			829±110
22			827±77
23			751±61
24			646±62
25			724±52
26			676±52
27			753±53
28			770±52
29			660±69
30			625±66

*-the deviation is significant relative to the indicator in group 1

‴-the deviation is significant relative to the indicator in group 2

°-the deviation is significant relative to the indicator on the first day

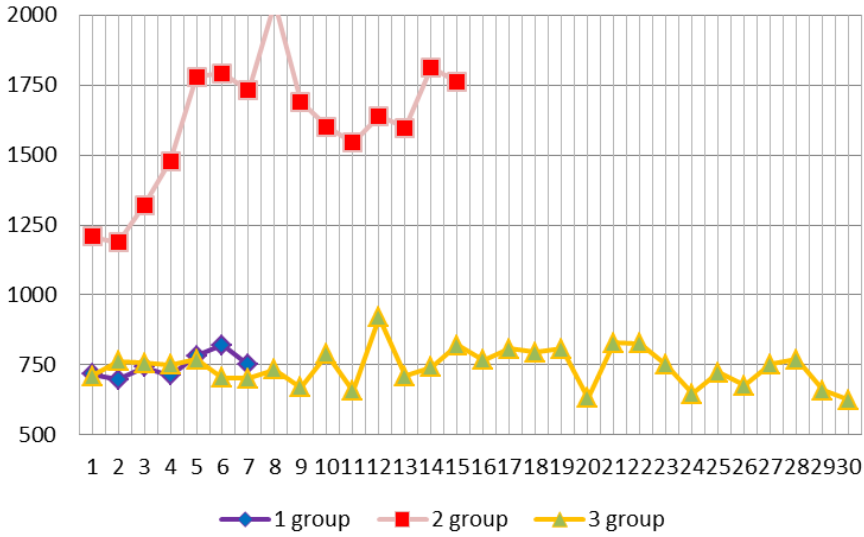

Figure 1. *Dynamics of the mesor of the circadian rhythm GPVR with SCTBI up to 3 years*

As can be seen from the data presented in tab. 1 and fig. 2, on the day of injury, the mesor of the circadian rhythm GPVR in group 2 was significantly higher than in groups 1 and 3 by 40% ($p<0.05$).

Given the decrease in CO on the first day of 5.3 l/min by the fifth day to 3.5 l/min in group 2 to 3 l/min - the level of the indicator in groups 1 and 3, an increase in GPVR on day 5 by 40%, and on day 8 by 60% compared to the initially increased by 25% ($p<0.05$, respectively), it should be assumed that critical disorders of central and peripheral hemodynamics in the first week after injury were tolerated by children of group 2. In this group, along with severe OTBI, there is also severe damage to the respiratory system, liver rupture. That is, in group 2, the severity of extracranial injuries of the organs of the chest, abdominal cavity, which led to greater mobilization of compensatory hyperdynamia of the cardiovascular system, prevailed. Timely effective therapeutic corrective measures caused, compared with the 3rd group, to get out of a serious condition in a shorter time, despite the continuing more pronounced hyperkinetic type of blood circulation on the 15th day of acute SCTBI.

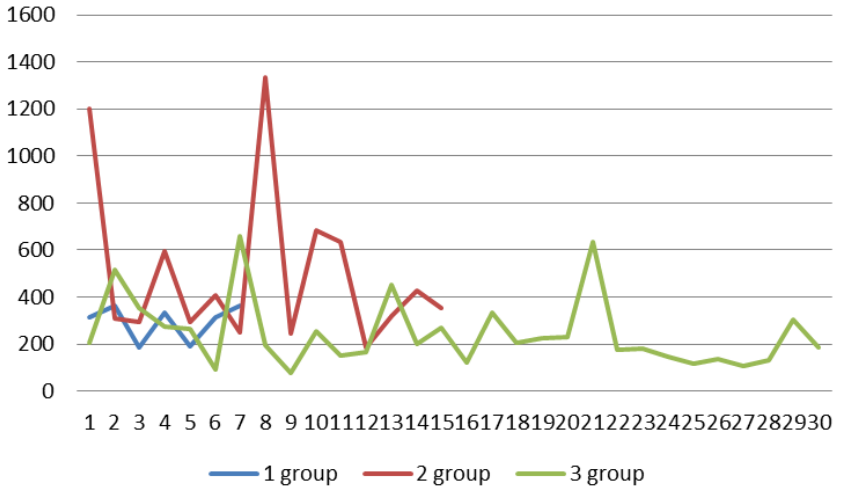

Figure 2. *Dynamics of the amplitude of the circadian rhythm GPVR up to 3 years*

The predominance of instability of homeostasis systems was expressed in group 2 by the largest amplitude of the GPVR circadian rhythm on days 1, 8, and 10 (fig. 2).

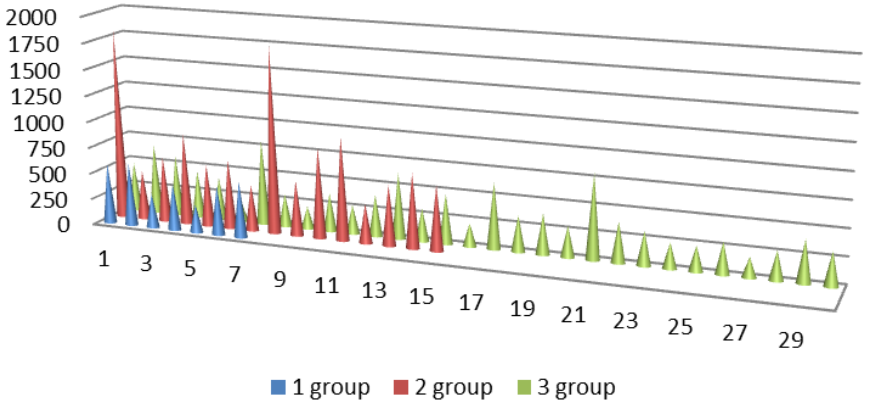

Figure 3. *Scope of diurnal GPVR fluctuations*

Confirmation of the pronounced instability of peripheral vascular tone is the largest differences in GPVR in 1, 8,10 days, exceeding the figures in groups 1 and 3 (fig.3).

The longest inversion of the circadian rhythm GPVR was detected in groups 3 and 2, which amounted to 9 and 8 days (tab. 3). While in percentage terms, the duration of the inversion of the circadian rhythm was 31% in group 3, 39% in group 1, and 53% in group 2 (fig. 5).

Table 3.

Duration and severity of shifts in the peak of the acrophase of the circadian rhythm GPVR in the acute period of SCTBI in children under 3 years of age.

Groups	Norm	Moderate shift	Inversion
	8-11 hours	12-22 hours	23-7 hours
1	14% (1)	57% (4)	39% (2)
2	7% (1)	40% (6)	53% (8)
3	33% (10)	36% (11)	31% (9)

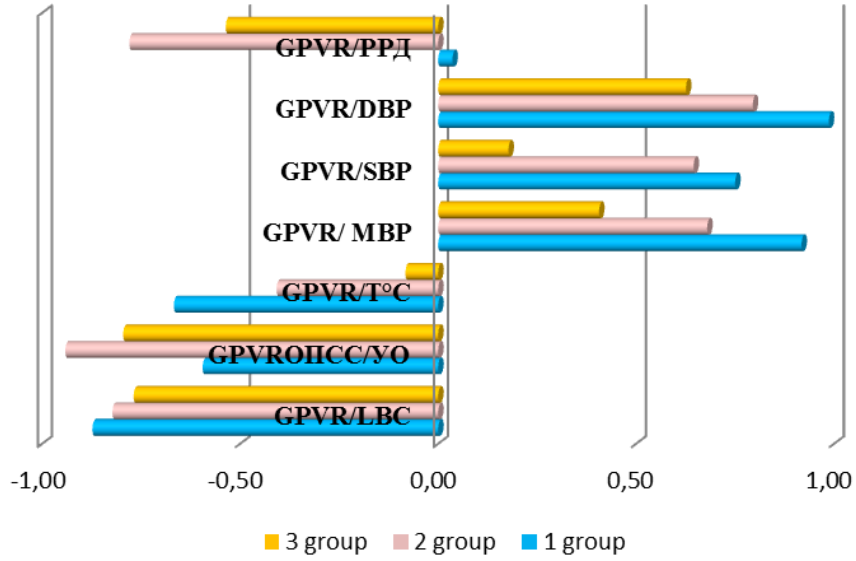

Figure 4. *Correlation links of GPVR*

A direct correlation of varying degrees of severity of changes in GPVR and DBP, GPVR and SBP, GPVR and MBP was found, indicating the most active compensatory reaction in groups 1 and 2 and the least significant in children of group 3. The inverse correlation of GPVR and SV, GPVR and CO indicates the hyperdynamic nature of the relationship between hemodynamic parameters. The compensatory decrease in GPVR to the hyperthermic reaction was most significant in groups 1 and 2, almost disappearing in the most severe children of group 3.

Conclusion

On the day of injury, the mesor of the circadian rhythm GPVR in group 2 was significantly higher than in groups 1 and 3 by 40%. The predominance of the severity of extracranial injuries of the chest, abdominal cavity, blood transfusion, led to greater mobilization of compensatory hyperdynamia of the cardiovascular system in children of the 2nd group. The inverse correlation of GPVR and SV, GPVR and CO indicate the hyperdynamic nature of the functional relationship of hemodynamic parameters. The compensatory decrease in GPVR to the hyperthermic reaction was most significant in groups 1 and 2, almost absent in the most severe children of group 3.

References

1. *https://www.youtube.com/watch?v=https:accounts.google.comServiceLogin*
2. *https://heal-cardio.ru/2017/03/17/chto-takoe-opss-v-kardiologii/*
3. *https://diseases.medelement.com/material*

DOI 10.34660/INF.2022.44.59.276

婴儿急性合并外伤性脑损伤心肌需氧量的变化
CHANGES IN MYOCARDIAL OXYGEN DEMAND IN ACUTE CONCOMITANT TRAUMATIC BRAIN INJURY IN INFANTS

Muhitdinova Hura Nuritdinovna
Doctor of Medical Sciences, Full Professor
Center for the Development of Professional Qualifications of Medical Workers, Doctor of Medical Sciences

抽象的。在所有 3 岁以下受伤儿童中，第 1 天的昼夜节律 TNMO 中值平均增加了 34%。 TNMO 的增加是由高热反应引起的，第 1 组的 CO 代偿性增加，而在第 3 组的儿童中，TNMO 与体温之间的直接关系降至 0.5。 TNMO 最显着的波动发生在第 3 组的波中，振荡周期为 6、5、6、5、5、6 天。在第 3 组受伤的婴儿中，SBP、DBP、MBP 的更显着增加，已经显着增加，导致 TNMO 显着增加，增加了缺氧恶化的风险，这是一种心肌能量不足的状态。一种更有效的应激保护疗法旨在通过引入能量底物来预防与心肌缺氧相关的急性心力衰竭，建议在 SCTBI 急性期预防第 3 组儿童的急性线粒体心肌功能不全。

关键词：心肌需氧量，伴随颅脑损伤，儿童。

Abstract. *The mesor of the circadian rhythm TNMO on day 1 was increased by an average of 34% in all injured children under the age of 3 years. An increase in TNMO was caused by a hyperthermic reaction, with a compensatory increase in CO in group 1, while in children of group 3, the direct relationship between TNMO and body temperature decreased to 0.5. The most significant fluctuations in TNMO occurred in waves in group 3 with an oscillation period of 6, 5, 6, 5, 5, 6 days. In injured infants of the 3rd group, a more significant increase in SBP, DBP, MBP, which was already significantly increased, caused a significantly significant increase in TNMO, increasing the risk of worsening hypoxia, an energy-deficient state of the myocardium. A more effective stress-protective therapy aimed at the prevention of acute heart failure associated with myocardial hypoxia by the introduction of energy substrates, the prevention of acute mitochondrial myocardial insufficiency in children of the 3rd group in the acute period of SCTBI is advisable.*

Keywords: *myocardial oxygen demand, concomitant traumatic brain injury, children.*

Relevance

One of the leading extracranial factors that aggravate the consequences of SCTBI is unstable hemodynamics, which may be the result of compensatory reactions aimed at maintaining brain tissue oxygenation in conditions of traumatic shock, inflammatory response, increased intracranial pressure (ICP) and other mechanisms, as a rule, observed in combined trauma. It is known that unstable hemodynamics is one of the leading factors contributing to an increase in the load of the myocardium, resulting in an energy-deficient state of the myocardium, creating a high risk of developing acute heart failure. Circulatory and tissue hypoxia that develops most early in severe TBI may be due to inefficiency of blood circulation and, at the same time, factors that aggravate subsequent cerebral ischemia. External respiratory disorders caused by traumatic injury, usually developing in patients with SCTBI, accompanied by impairment of consciousness and bulbar disorders, significantly reduce the effectiveness of compensatory reactions of systemic hemodynamics, leading to depletion of energy resources both in the myocardium and the circulatory system as a whole. However, there is insufficient information in the literature on the peculiarities of changes in myocardial oxygen demand in the acute period of SCTBI in infants [1-5].

Purpose of the work

To study and evaluate the effect of severe concomitant injury on myocardial oxygen consumption in infants in the acute period.

Material and research methods

A detailed analysis of reliably significant deviations, intergroup differences in the studied hemodynamic parameters was carried out. The results were obtained by hourly monitoring of body temperature, heart rate (HR), systolic (SBP), diastolic (DBP) blood pressure, cardiac output (CO), the need of myocardium in oxygen (TNMO). The research data were processed by the method of variation statistics using the Excel program by calculating the arithmetic mean values (M) and the errors of the means (m). To assess the significance of differences between the two values, Student's parametric test (t) was used. The relationship between the dynamics of the studied indicators was determined by the method of pair correlations. The critical level of significance in this case was taken equal to 0.05.

Results and discussion

Of the 18 children (tab. 1) diagnosed with severe concomitant traumatic brain injury (SCTBI) admitted to the Republican Center for Emergency Medical Care in infancy, 7 patients received intensive care in the ICU for 5.9 ± 1.3 days, 6 patients 14±1.7 days, 7 children for 31.2±5.3 days, which served as the basis for the creation of randomized groups according to the severity of the condition. The difference is significant ($p<0.05$).

Table 1.

Characteristics of SCTBI patients admitted before the age of 3 years

Groups	Num. of patients	Num. of patients	Gender male	Age	RTA	Catatrauma	Traum. shock of the 2 degree	Operated on admission	Number of days in hospital
1	5.9±1.3	7	4.	20.8±7.8	71% (5)	29% (2)	71% (5)	71% (5)	15.2±7
2	14±1.7	6	4	23.1±4.7	50% (3)	50% (3)	83% (5)	66% (4)	20±4
3	31.2±5.3	5	3	18.2±4.6	80% (4)	20% (1)	100% (5)	100% (5)	37.4±5.3

Table 2.

Dynamics of the mesor of the circadian rhythm TNMO in the acute period of SCTBI in children under 3 years old in %.

Days	Group 1	Group 2	Group 3
1	130±8	143±14	130±15
2	130±5	141±9	140±7
3	127±4	129±4	145±9*
4	127±4	139±6*	140±5*
5	123±8	125±6	142±9*
6	127±4	123±6	131±7
7	123±4	124±5°	137±4‴
8		133±8	143±7
9		118±6°	139±6‴
10		121±4°	144±7‴
11		116±5°	129±6‴
12		120±4°	147±6‴
13		113±6°	135±5‴
14		103±4°	131±6‴
15		114±5°	126±10
16			123±8
17			118±8

18			118±5
19			124±6
20			128±7
21			110±6
22			117±5
23			121±6
24			121±5
25			117±5
26			129±6
27			162±13°
28			140±4
29			135±4
30			139±5

*- the deviation is significant relative to the indicator in group 1.

‴-significant relative to the indicator in group 2

°-significantly relative to the indicator on the first day.

As can be seen from the data presented in tab. 2, the mesor of the circadian rhythm TNMO on day 1 was increased by an average of 34% in all injured children. In group 1, no significant changes were observed during the observation period. In group 2, a significantly significant decrease in TNMO was noted on days 7, 9-15 by 13%, by 17-20% ($p<0.05$, respectively), that is, almost to normal levels. In group 3, an increase in TNMO was detected on days 3-5, when TNMO became more than in groups 1 and 2 by 12-13% ($p<0.05$, respectively). On days 7.9-14, the circadian rhythm mesor index TNMO was higher in children of the 3rd group than in the 2nd group by 11-17-27% ($p<0.05$, respectively). An increase in TNMO on day 27 by 19% ($p<0.05$) relative to the level of the indicator on day 1 indicates an unstable state of increased myocardial energy demand even in the later stages of the acute period of SCTBI (tab. 2). Under these conditions, there are obvious indications for metabolic maintenance and stress-limiting therapy with the maintenance of effective coronary blood flow, which depends on the amplitude of daily fluctuations in cardiac output and stabilization of blood pressure.

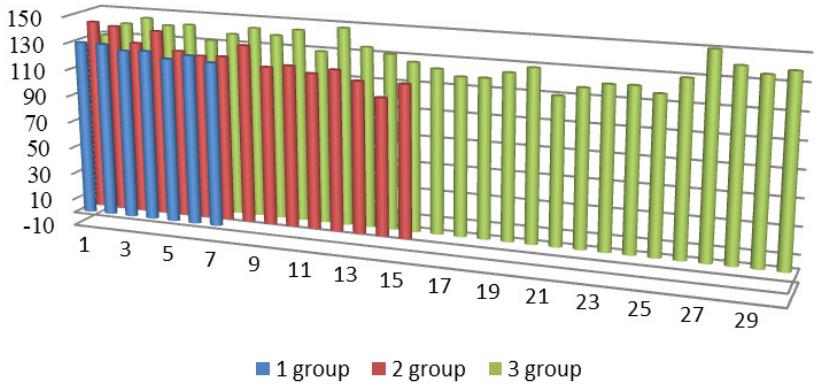

Figure 1. *Dynamics of the mesor of the circadian rhythm TNMO in the acute period of SCTBI in children under 3 years of age*

The most significant fluctuations in TNMO occurred in waves in group 3 with a period of fluctuations of 6, 5, 6, 5,5,6 days (fig. 1).

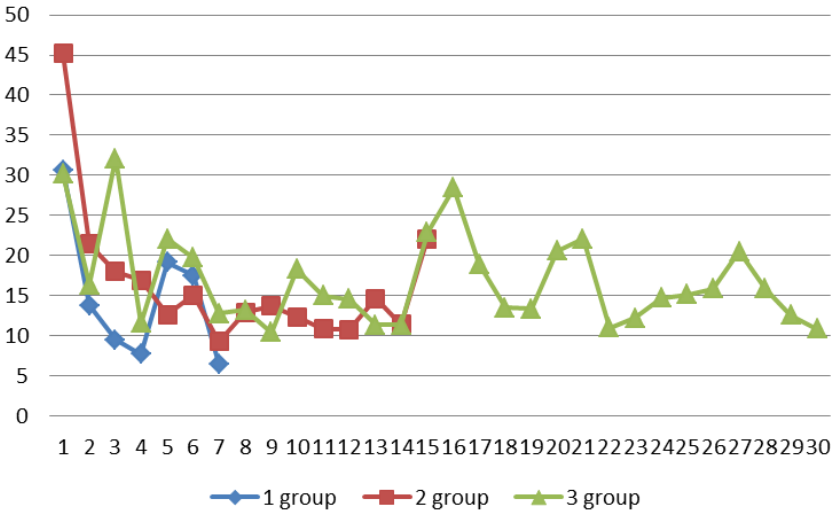

Figure 2. *TNMO circadian rhythm amplitude with SCTBI up to 3 years*

The highest amplitude of the circadian rhythm TNMO was detected on the 1st day in children of the 2nd group, in the following days it decreased to 15-10%. In group 1, the amplitude changes represented a two-phase wave with an oscillation period of 7 days. Relatively more distinct changes in the amplitude of the circadian rhythm TNMO were observed in the 3rd group, making biphasic curves with a wavelength of 3, 3, 5, 6, 5, 6 days. The revealed features of the deformation of the TNMO circa-week biorhythms most likely represent one of the many ways of adaptive restructuring of the functional activity of the heart with the participation of the biorhythmological characteristics of the cellular metabolism of the heart muscle, heart rate regulation centers and other structures involved in ensuring adequate restructuring of blood circulation in the acute period of SCTBI in infants (fig. 2).

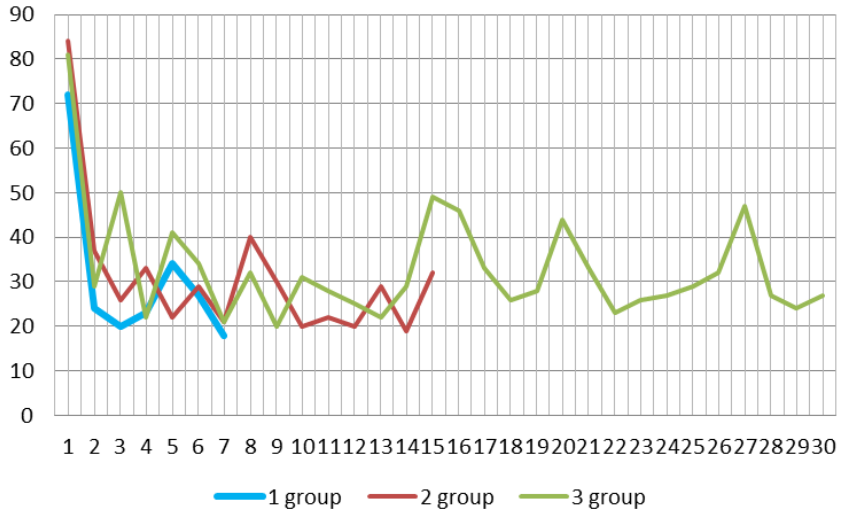

Figure 3. *Daily range of TNMO fluctuations up to 3 years*

Fluctuations in the daily range of changes in myocardial oxygen demand turned out to be the largest on day 1, maintaining a wave-like pattern of changes throughout the entire observation in all groups, regardless of the severity of the injury (fig. 3). More clearly visible 4-5-6 day periods of fluctuations in the 3rd group.

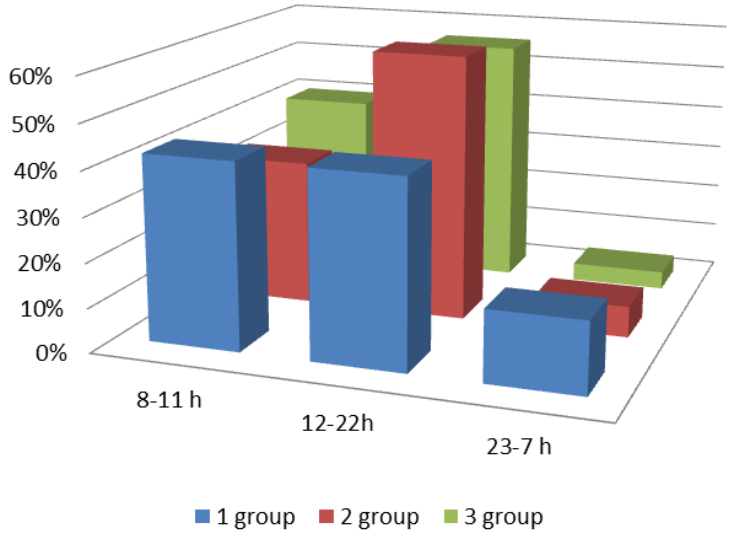

Figure 4. *Duration of TNMO acrophase shifts in the acute period of SCTBI up to 3 years*

The predominance of the duration of a moderate shift in the peak of the acrophase of the circadian rhythm TNMO during the daytime in groups 2 and 3 was noted (fig. 4).

Table 3.
Correlation links of TNMO

	Group 1	**Group 2**	**Group 3**
TNMO/GPVR	-0.6	-0.5	0.0
TNMO/CO	0.8	0.2	0.4
TNMO/SV	0.2	0.4	-0.2
TNMO/Temperature	0.9	0.7	0.5
TNMO/MBP	-0.6	0.1	0.8
TNMO/SBP	-0.5	0.2	0.8
TNMO/DBP	-0.5	0.0	0.7
TNMO/PBP	-0.2	0.6	0.3

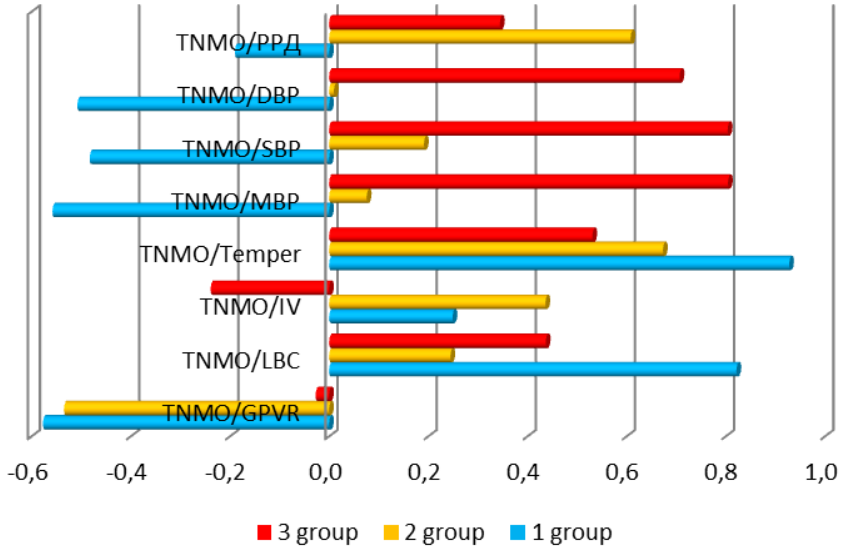

Figure 5. *Correlation links of TNMO*

In groups 1 and 2, a direct strong relationship was found between TNMO and changes in body temperature (0.9; 0.7, respectively), accompanied by a hyperdynamic type of hemodynamic restructuring (0.8). That is, an increase in TNMO was caused by a hyperthermic reaction, with a compensatory increase in CO in group 1, while in children of group 3, the direct relationship between TNMO and body temperature decreased to 0.5. Distinctive features in group 3 were a direct strong correlation between TNMO and SBP (0.8), DBP (0.7) and MBP (0.8), while in children of group 1 these dependencies were negative. That is, in group 1, there was a tendency to increase myocardial oxygen demand with a trend towards a decrease in GPVR (-0.6), a decrease in SBP (0.5), DBP (0.5) and MBP (0.6). The findings confirmed the compensatory orientation of the increase in the level of MBP, SBP, DBP in children of the 1st group (tab. 3). In injured infants of group 3, a more significant increase in SBP, DBP, MBP, which was already significantly increased, caused a significantly significant increase in TNMO, increasing the propensity to aggravate hypoxia, an energy-deficient state of the myocardium. In this regard, the expediency of a more effective stress-protective therapy aimed at the prevention of acute heart failure associated with myocardial hypoxia by the introduction of energy substrates, the prevention of acute mitochondrial myocardial insufficiency in children of the 3rd group in the acute period of SCTBI was indicated.

Conclusion

The mesor of the circadian rhythm TNMO on day 1 was increased by an average of 34% in all injured children under the age of 3 years. An increase in TNMO was caused by a hyperthermic reaction, with a compensatory increase in CO in group 1, while in children of group 3, the direct relationship between TNMO and body temperature decreased to 0.5. The most significant fluctuations in TNMO occurred in waves in group 3 with an oscillation period of 6, 5, 6, 5, 5, 6 days. In injured infants of the 3rd group, a more significant increase in SBP, DBP, MBP, which was already significantly increased, caused a significantly significant increase in TNMO, increasing the risk of worsening hypoxia, an energy-deficient state of the myocardium. A more effective stress-protective therapy aimed at the prevention of acute heart failure associated with myocardial hypoxia by the introduction of energy substrates, the prevention of acute mitochondrial myocardial insufficiency in children of the 3rd group in the acute period of SCTBI is advisable.

References

1. *http://www.grandars.ru/college/medicina/arterialnoe-davlenie.html,*
2. *http://giperton.com/srednee-davlenie.html,*
3. *http://cardiograf.com/napor/vidy/srednee-arterialnoe-davlenie.html*
4. *https://bolitsosud.ru/davlenie/srednee-arterialnoe-davlenie-znachenie.html*
5. *https://www.stud24.ru/medicine/cherepnomozgovaya-travma-u-detej/143013-419898-page1.html*

DOI 10.34660/INF.2022.70.65.277

高血压合并肥胖患者的血管壁
VASCULAR WALL IN PATIENTS WITH ARTERIAL HYPERTENSION IN COMBINATION WITH OBESITY

Yushchuk Elena Nikolaevna
Doctor of Medical Sciences, Full Professor
Sadulaeva Irina Akhmedkhanovna
Candidate of Medical Sciences, Full Professor
Sapunova Daria Alexandrovna
Candidate of Medical Sciences, Associate Professor
A.I. Yevdokimov Moscow State University of Medicine and Dentistry

抽象的。 腹部肥胖和动脉高血压常合并，显着增加心血管疾病的风险。 动脉僵硬度是决定心血管风险的一个重要因素。 本文在“血管年龄”概念的背景下，对确定血管老化和动脉僵硬度在动脉高血压和肥胖患者中的作用做出了自己的研究结果和初步尝试。

关键词：动脉高血压，肥胖，动脉僵硬度，血管老化

Abstract. *Abdominal obesity and arterial hypertension are often combined, which significantly increases the risk of cardiovascular disasters. Arterial stiffness is an integral factor determining cardiovascular risks. The article makes own results and a preliminary attempt to analyze the literature on determining the role of vascular aging and arterial stiffness in patients with arterial hypertension and obesity in the context of the concept of "vascular age".*

Keywords: *arterial hypertension, obesity, arterial stiffness, vascular aging*

Introduction

The idea of the connection of excess adipose tissue with cardiovascular diseases was formed more than 50 years ago. Overweight is observed in 40-75% of patients with arterial hypertension according to the Framingham study. On average, blood pressure rises 6/4 mmHg with an increase in adipose tissue mass by 10%. J.J. Toto-Moukouo et al. the effect of obesity on the elastic properties of the vascular wall was first noted in 1986. The researchers compared two groups of patients who suffered from hypertension for a long time, who had normal and overweight. As a result of the work, the authors concluded that regardless of gender, age and blood pressure level, the pulse wave velocity in the vessels of the upper extremi-

ties was significantly higher in obese patients.

Arterial stiffness is an integral factor determining cardiovascular risks. Vessels are one of the main target organs that are affected by various diseases and conditions: diabetes mellitus, hypothyroidism, hypertension, autoimmune diseases, atherosclerosis, aging, etc. Consequently, determining the stiffness of the vascular wall, the criteria for the development of cardiovascular complications are fixed, which determine mortality from cardiovascular diseases (1).

Vascular aging involves a number of successive changes in the mechanical and structural properties of the arterial wall, the consequence is the destruction and fragmentation of elastin fibers, which are replaced in a higher ratio by collagen, which forms a structure with increased rigidity, which is commonly called "physiological arterial rigidity". The growing interest in arterial stiffness (arteriosclerosis) led to the formation of the concept of early vascular aging (early vascular aging – EVA) in 2008 by Nilsson et al. (2).

In 2019, leading experts in the field of vascular stiffness research confirmed the position that arterial stiffness is the best indicator of the combined effect of known and unknown risk factors for arterial wall damage, and suggested expressing very high and very low arterial stiffness in terms of EVA and SUPERNOVA. In patients with EVA syndrome, the ability to repair vascular damage in response to aggressors such as mechanical and metabolic/oxidative/chemical stress is impaired. With the SUPERNOVA phenotype ("supernormal" vascular aging), patients have extremely low vascular stiffness rates for their age and gender. It can be assumed that for some reason, in the SUPERNOVA phenomenon, exposure to cardiovascular risk factors does not lead to subclinical organ damage and cardiovascular complications (3).

Arterial wall stiffness is determined by the CAVI index (Cardio-Ankle Vascular Index). CAVI correlates with the classical indicator of aortic stiffness – pulse wave velocity, allows you to assess the degree of atherosclerosis, the age of the vessels relative to the sex and age of the patient. CAVI – an indicator of the stiffness of the vascular system as a whole – does not depend on the patient's blood pressure level at the time of the study.

Thus, it is of interest to study changes in the vascular wall in patients with arterial hypertension in combination with obesity, while taking into account modern concepts of vascular aging, which coincides with the scientific and practical topics of the Department of Clinical Functional Diagnostics of the Faculty of Medicine.

Materials and methods

At the clinical base of the Moscow State Medical and Dental University named after A.I. Evdokimov, 60 patients with a previously established diagnosis of arterial hypertension were included in a single study. Clinical examination of patients included clarification of complaints, detailed collection of anamnesis of arterial

hypertension and identification of risk factors for cardiovascular diseases; clinical examination, which included measurement of blood pressure (BP), height (cm), weight (kg), calculation of body mass index (BMI) [body weight (kg)/height (m^2)], measurement of waist volume and hip volume (cm), calculation of the ratio of waist volume to hip volume (Waist/Hip Ratio), measurement of blood pressure (systolic – SBP, diastolic – DBP). The patients underwent a biochemical study of the blood lipidogram. Vascular stiffness was determined on the VaSera VS-1500N device (Fukuda Denshi, Japan) using the arterial wall stiffness index – cardio-ankle vascular index (CAVI) - cardio-ankle vascular index. This technique allows us to identify a group of people with early aging (remodeling) of blood vessels, with preclinical development of atherosclerosis of various localizations. As a result of the study, two CAVI indicators are determined: R-CAVI is the CAVI between the aortic valve and the arteries of the right lower leg, calculated by recording a phonocardiogram and determining the II heart tone and using plethysmography, which registers pulse waves on the right shoulder and right lower leg using cuffs; L-CAVI is the CAVI between the aortic valve and the arteries of the left shin, calculated by recording a phonocardiogram and determining the II heart tone and using plethysmography, which registers pulse waves on the right shoulder and left shin using cuffs. Descriptive statistics including the number of observations in each group, mean (M), standard deviation (SD) and percentages were given for all indicators depending on the nature of the data. All statistical tests were performed for a two-way level of statistical significance ($p<0.05$.

To date, 60 respondents have been examined, where the group of patients with arterial hypertension and overweight was 35 people, and the control group included 25 examined.

Table 1 presents the data of 35 patients in the group with arterial hypertension and overweight, where the average age was 46.40 ±10.16 years.

Table 1

The main indicators of respondents with arterial hypertension and obesity (n=35)

Indicator	Result
BMI (kg/m^2)	29,56±5,75
SBP (mmHg)	134,48±15,22
DBP (mmHg)	84,45±10,18
Waist volume (cm)	77,40±11,28
Waist/Hip Ratio	0,88±0,09
Total cholesterol (mmol/l)	5,59±1,18
Low-density lipoprotein cholesterol (mmol/l)	3,49±1,21

R-CAVI	7,05±0,83
L-CAVI	7,06±0,79

We determined reliable direct correlations between R-CAVI and L-CAVI with age (0.568 and 0.508, respectively), as well as with the Waist/Hip Ratio (0.433 and 0.377, respectively) in the group of respondents with hypertension and obesity.

In the studied group of patients, it is noted that the vascular age according to the study on the VaSera VS-1500N device coincides with the passport age in 9 respondents, less than the passport age in 17 and more than the passport age in 9 respondents.

Table 2 shows the data of 25 respondents of the control group, where the average age was 38.84±8.81 years.

Table 2.

The main indicators of the respondents of the control group (n=25)

Indicator	Result
BMI (kg/m^2)	22,14±2,27
SBP (mmHg)	117,44±12,31
DBP (mmHg)	74,12±7,38
Waist volume (cm)	77,40±11,28
Waist/Hip Ratio	0,79±0,07
Total cholesterol (mmol/l)	4,59±0,92
Low-density lipoprotein cholesterol (mmol/l)	2,56±0,89
R-CAVI	6,94±0,98
L-CAVI	6,90±0,98

Reliable direct correlations between L-CAVI and R-CAVI were determined with an age index (0.71 in both cases) in the respondents of the control group.

In the examined control group, by analogy with the group of patients with arterial hypertension and obesity, a tendency to three subgroups in terms of vascular age was determined: it coincided with the passport age in 8 respondents, was less than the passport age in 7 respondents and exceeded the passport age in 10 respondents.

Discussion

At present, a preliminary assessment of clinical, anamnestic and instrumental data on the surveyed respondents has been carried out, interim results have been presented, which may make adjustments to the design of the study and expand the studied aspects.

The examined group of patients with arterial hypertension and overweight in general showed higher indicators of anthropometric and laboratory data than the respondents from the comparison group. Since the recruitment of both groups has not yet been completed, the final in-depth statistical calculations have been postponed until the end of the study. In the analysis, the studied group with arterial hypertension and obesity demonstrated a reliable direct correlation with the Waist/Hip Ratio, characterizing visceral obesity, which is currently recognized by clinicians as more prognostically significant than the BMI indicator as a risk factor for cardiovascular diseases. At the same time, the respondents of the control group did not show such a trend, which in the future is worthy of additional study. The independent role of obesity in the development of vascular changes was demonstrated by J. Orr et al. The study included young healthy men who were measured the stiffness of the vascular wall against the background of a high-calorie diet, leading to an increase in body weight by an average of 5 kg for 6-8 weeks. More pronounced vascular changes were associated with the presence of visceral obesity, determined by computed tomography and an increase in waist circumference. Researchers have proved that moderate weight gain induced by a high-calorie diet, even in healthy individuals, can lead to an increase in arterial stiffness. The preliminary results obtained by us are consistent with the literature data, while due to the incompleteness of our study, it is premature to draw final conclusions.

In our study, according to preliminary calculations, both in the group of patients with arterial hypertension and overweight, and in the control group, a similar trend was noted in the distribution of respondents into three subgroups according to vascular age. According to the theory of protective mechanisms leading to SUPERNOVA, it is likely that such subjects may have only a fraction of the known risk factors, and they are underestimated or less known. For example, in the ESSE-RF study, the determining factors that were associated with the phenotype of "supernormal" vascular aging were normal blood pressure, normal body weight, lower blood glucose and optimal lipid profile. Stratification of the sample into age groups made it possible to identify age-related features of the influence of risk factors. Younger patients with the SUPERNOVA phenomenon had a lower BMI, but other traditional risk factors did not have a significant effect, it is possible that the cumulative effect of their influence is manifested only at an older age. There are also known data from a study of cardiovascular risk in young people in Finland, which showed that metabolic syndrome in childhood and adolescence (at the age of 9-18 years) predicts the level of arterial stiffness in adulthood (pulse wave velocity measurements were carried out after 21 years at the age of 30-39 years) (4). Consequently, world practice the study of arterial stiffness and, as a consequence, the issue of vascular age, everywhere faces the urgency of regularly expanding the list of factors affecting the functional state of the artery wall. We

have previously raised the issue of the SUPERNOVA phenomenon in a sample of women of reproductive age with phenotypic signs of undifferentiated connective tissue dysplasia, where we discussed the theory of a violation of the ratio of type I and type III collagens with an increase in the proportion of immature collagen in tissues and organs, which probably leads to qualitative changes in the arterial wall, followed by the formation of aneurysms and malformations (5).

Conclusion

1. The study of the concepts of "vascular aging" will allow the clinician to assess the impact of risk factors on the arterial wall and develop tactics of therapeutic intervention.

2. For a comprehensive assessment of vascular age, it is important to take into account social aspects (trajectories from childhood to adulthood), professional status, social deprivation, etc.

References

1. Podzolkov V.I., Tarzimanova A.I., Bragina A.E., Osadchiy K.K., Gataulin R.G., Oganesyan K.A., Lobova N.V., Jafarova Z.B. Changes in Arterial Wall Stiffness in Patients with Obesity and Paroxysmal Form of Atrial Fibrillation. Rational Pharmacotherapy in Cardiology 2020;16(4):516-521. DOI:10.20996/1819-6446-2020-08-05

2. Burko N.V., Avdeeva I.V., Oleynikov V.E., Boytsov S.A. The Concept of Early Vascular Aging. Rational Pharmacotherapy in Cardiology 2019;15(5):742-749. DOI:10.20996/1819-6446-2019-15-5-742-749

3. Rotar OP, Tolkunova KM. EVA and SUPERNOVA concepts of vascular aging: ongoing research on damaging and protective risk factors. Arterial'naya Gipertenziya = Arterial Hypertension. 2020;26(2):133–145. doi:10.18705/1607-419X-2020-26-2-133-145

4. Tolkunova KM, Rotar OP, Erina AM, Boiarinova AM, Alieva AS, Moguchaia EV, Kolesova EP, Solntsev VN, Konradi AO. Supernormal vascular aging — prevalence and determinants at population level (the ESSE-RF data). Arterial'naya Gipertenziya = Arterial Hypertension. 2020;26(2):170–183. doi:10.18705/1607-419X-2020-26-2-170-183

5. Sapunova DA. Undifferentiated connective tissue dysplasia in the context of arterial stiffness - Science and innovations 2021: development directions and priorities. Proceedings of the International Conference. Melbourne, 2021. C. 130-134. DOI 10.34660/INF.2021.84.85.022

DOI 10.34660/INF.2022.48.99.278

缺血性脑卒中患者脑水肿登记方法的优先级

PRIORITY OF METHODS FOR REGISTRATION OF CEREBRAL EDEMA IN PATIENTS WITH ISCHEMIC STROKE

Slepushkin Vitaly Dmitrievich
Doctor of Medical Sciences, Head of Department
Khasueva Albina Umarovna
Postgraduate
North Ossetian State Medical Academy

抽象的。 在对 163 名确诊缺血性卒中患者的动态观察中发现，从发作后的最初几个小时内评估是否存在脑水肿的优先方法是颅内压的侵入性测量和非侵入性方法 - 脑 大脑的血氧饱和度。 脑部 CT 和 MRI 成像在中风发作 12 小时后有效。

关键词：缺血性脑卒中 脑水肿 评估方法

Abstract. *During the dynamic observation of 163 patients with verified ischemic stroke, it was found that the priority methods for assessing the presence of cerebral edema from the first hours after the onset of the episode are invasive measurement of intracranial pressure and a non-invasive method - cerebral oximetry of the brain. CT and MRI imaging of the brain is effective after 12 hours from a stroke episode.*

Keywords*: ischemic stroke, cerebral edema, assessment methods*

The main pathogenetic component of stroke, which forms a neurological deficit in patients, is cerebral edema. Therefore, early diagnosis of the degree of cerebral edema is necessary, as well as constant monitoring of the degree of edema in order to determine the effectiveness of the therapy and, possibly, to identify the prognosis of the course of the disease [Kuznetsov A.N., Vinogradov O.I., 2014; Stakhovskaya L.V., Kotova S.V., 2018].

Purpose of the study: to identify methods for early detection of cerebral edema in patients with ischemic stroke.

Material and research methods

The present study included 163 patients aged 30 to 60 years with severe ischemic stroke: more than 24 points on the NIHSS scale. The patients included 73 men and 90 women. The diagnosis of "ischemic stroke" on the first day from the

onset of the disease was established on the basis of the clinical picture and was confirmed by computed tomography and magnetic resonance imaging. Patients were treated in the intensive care unit of the vascular center. All patients underwent the most unified intensive care based on the European recommendations of 2008 (ESO 2008), as well as standards and clinical recommendations of the Ministry of Health of the Russian Federation [Alferova V.V. et al., 2017].

The following methods of examination of patients were compared:

- Computed tomography (CT)
- Magnetic resonance imaging (MRI)
- Measurement of intracranial pressure (ICP) by placing a subdural sensor
- Determination of blood plasma osmolarity by cryoscopic method
- Measurement of cerebral oxygenation by cerebral oximetry using a cerebral oximeter.

Conducted a sample of research methods that were conducted in patients 6, 12, 18 and 24 hours after the onset of a stroke episode.

The obtained research materials were statistically processed using the methods of parametric and non-parametric analysis. Accumulation, correction, systematization of initial information and visualization of the obtained results were carried out in Microsoft Office Excell 2016 spreadsheets. Statistical analysis was carried out using the program STATISTICA 6.5 (developer StatScoft.Inc).

When processing the obtained results of computer visualization of cerebral edema, the statistical method of a four-field table of conjugate frequencies was used.

Results and discussion

Computer methods of visualization of cerebral edema gave the following dynamic picture (table 1).

Table 1.

The percentage of detection of signs of cerebral edema

Imaging method	**6 hours**	**12 hours**	**18 hours**	**24 hours**
CT	-	14%	58%	95%
MRI	-	18%	73% *	97%

Note: *-P<0.05 in relation to CT examination

6 hours after the onset of an ischemic episode, computerized brain imaging methods do not describe the signs of cerebral edema, but only give the size of the ischemic focus. After 12 hours, both methods in approximately equal proportions reveal signs of cerebral edema. After 18 hours, magnetic resonance imaging was able to visualize signs of edema to a greater extent (CI -13; AR -29; P<0.05). A day later, both methods make it possible to equally assess the presence of edema in almost all patients with ischemic stroke.

Comparative sensitivity of invasive methods for assessing cerebral edema: ICP measurement, determination of blood plasma osmolarity and non-invasive method: brain oximetry, is shown in table 2.

Table 2.

Comparison of the sensitivity of invasive and non-invasive methods for assessing cerebral edema

Methods	Limits of normal values Averages	6 hours	12 hours	18 hours	24 hours
ICP MmHg.	5-12 8.4±1.2	20.2± 2.4*	28.3± 3.1**	30.8± 3.0**	38.6± 3.4**
Osmolarity of blood plasma Mosm/l	295-300 297.3±3.0	306.6± 28.1	342.6± 14.3**	348.5± 15.6**	346.9± 18.3**
Cerebral oximetry %	65-75 67.4±3.2	79.4± 3.0*	84.4± 2.1**	88.9± 2.4**	89.9± 2.5**

Note: *-P<0.05; **-P<0.01 in relation to the mean value of normal values

An invasive method for determining intracranial pressure from the first hours gives positive values indicating the development of cerebral edema. Another invasive method - a blood test by sampling from a vein and subsequent determination of plasma osmolarity - indirectly indicates signs of edema in the form of hyperosmolar syndrome [Ershov V.I. et al., 2017].

A non-invasive method - assessment of the degree of oxygenation of the brain by cerebral oximetry - allows us to talk about hypoxic cerebral edema already from the first hours after the onset of an episode of ischemic stroke.

If computer-assisted brain imaging methods according to clinical recommendations are carried out at weekly intervals, then ICP measurement is carried out for an indefinite time as the subdural sensor is located and functioning. Determining the osmolarity of blood plasma requires blood sampling, which is hardly applicable under normal conditions more than once a day. The method of cerebral oximetry is non-invasive and can be used in real time for an indefinitely long period, which makes it possible to evaluate the effectiveness of ongoing intensive therapy aimed at reducing the degree of cerebral edema, and can also serve as a prognostic criterion.

References

1. Alferova V.V., Belkin A.A., Voznyuk I.A., Gerasimenko M.Yu. Clinical recommendations for the management of patients with ischemic stroke and transient ischemic attacks. Moscow. 2017: 92 P.

2. Ershov V.I., Aizhanova A.A., Chirkov A.N. Clinical and prognostic aspects of water and electrolyte homeostasis disorders in the acute period of ischemic stroke. Bulletin of Intensive Care. 2017; 4:53-57

3. Kuznetsov A.N., Vinogradov O.I. Ischemic stroke. Diagnostics. Treatment. Prevention. Moscow. 2014: 131 P.

4. Stakhovskaya L.V., Kotova S.V. Stroke. Guide for doctors. 2nd edition. Medical information agency. 2018: 487 P.

DOI 10.34660/INF.2022.51.84.279

三岁以下儿童严重合并颅脑损伤急性期的昼夜节律指数
CIRCADIAN INDEX IN THE ACUTE PERIOD OF SEVERE CONCOMITANT TRAUMATIC BRAIN INJURY IN CHILDREN UNDER THE AGE OF THREE YEARS

Muhitdinova Hura Nuritdinovna
Doctor of Medical Sciences, Full Professor
Center for the Development of Professional Qualifications of Medical Workers

抽象的。 在所有组的第一天，都显示出心率增加的趋势。 第3组患者第9、12、13、14天昼夜节律中值指标HR高于第2组。 波长不稳定，在第 3 组儿童中最为明显。 患者病情越严重，昼夜节律幅度越显着，发生心动过速综合征的趋势持续的时间越长。 在所有组的儿童中发现心肌需氧量对节律频率的直接依赖性。 第 1 组和第 2 组儿童以形成高动力型血流动力学的趋势为主。昼夜节律倒转时间最长，第 3 组持续 4 天，第 2 组持续 1 天，第 1 组未发现倒转 .

关键词：昼夜节律指数，严重合并颅脑损伤，儿童期。

Abstract. *On the first day in all groups, a tendency to increased heart rate was revealed. The circadian rhythm mesor indicator HR in patients of group 3 was higher than in group 2 on days 9, 12, 13, and 14. The change in the mesor of the circadian rhythm HR during the acute period of SCTBI was a wavy curve with an unstable wavelength, most pronounced in children of the 3rd group. The more severe the condition of the patients, the more significant was the amplitude of the circadian rhythm, the longer the tendency to develop tachycardia syndrome persisted. A direct dependence of myocardial oxygen demand on the rhythm frequency was found in children of all groups. The predominant tendency to form a hyperdynamic type of hemodynamics was found in children of groups 1 and 2. The inversion of the circadian rhythm was the longest in group 3 for 4 days, in group 2 for 1 day, in group 1 no inversion was found.*

Keywords: *circadian index, severe concomitant traumatic brain injury, childhood.*

Relevance

One of the leading extracranial factors that aggravate the consequences of SCTBI is unstable hemodynamics, which may be the result of autonomic regula-

tion disorders, inflammatory response, increased intracranial pressure (ICP) and other mechanisms, as a rule, observed in concomitant trauma. The circadian index (CI) of the heart rate of a healthy person is an important parameter in the study of the heart and blood vessels, usually in the range of 1.2-1.4. If this figure is less than 1.2, then they speak of a visible rigidity of the circadian rhythm, and this is a consequence of damage to the intracardiac nervous apparatus. In clinical practice, a reduced circadian index leads to the development of arrhythmias, cardiomyopathies, coronary heart disease and can become one of the causes of sudden death syndrome [2,3]. However, there is not enough information in the literature on the characteristics of disorders of hemodynamic parameters, the circulatory system as a whole, and the circadian index in the acute period of SCTBI in infants [1–4].

Purpose of the work

To study and evaluate the effect of severe concomitant trauma on the circadian index in the acute period of severe concomitant traumatic brain injury in children under the age of three years.

Material and research methods

A detailed analysis of reliably significant deviations, intergroup differences in the studied hemodynamic parameters was carried out. The results are obtained by monitoring with hourly recording of body temperature, heart rate (HR), systolic blood pressure (SBP), diastolic blood pressure (DBP), mean blood pressure (MBP), pulse blood pressure (PBP), cardiac output (CO), circadian index (CI).

The research data were processed by the method of variation statistics using the Excel program by calculating the arithmetic mean values (M) and the errors of the means (m). To assess the significance of differences between the two values, Student's parametric test (t) was used. The relationship between the dynamics of the studied indicators was determined by the method of pair correlations. The critical level of significance in this case was taken equal to 0.05.

Of the 18 children (Table 1) diagnosed with severe concomitant traumatic brain injury (SCTBI) admitted to the Republican Center for Emergency Medical Care in infancy, 7 patients were intensively treated in the ICU for 5.9 ± 1.3 days, 6 patients for 14±1.7 days, 7 children for 31.2±5.3 days, which served as the basis for creating randomized groups according to the severity of the condition. The difference is significant ($p<0.05$).

Table 1.

Characteristics of SCTBI patients admitted before the age of 3 years

Groups	Num. of days in ICU	Num. of patients	Gender male	Age	RTA	Catatrau ma	Traum. shock of the 2 degree	Operated on admission	Number of days in hospital
1	5.9±1.3	7	4.	20.8±7.8	71% (5)	29% (2)	71% (5)	71% (5)	15.2±7
2	14±1.7	6	4	23.1±4.7	50% (3)	50% (3)	83% (5)	66% (4)	20±4
3	31.2±5.3	5	3	18.2±4.6	80% (4)	20% (1)	100% (5)	100% (5)	37.4±5.3

In group 1, the frequency of closed traumatic brain injury (CTBI) (71%), concussion (28%) prevailed, the number of operations on the first day after injury was 71%. In the 2nd more severe group, the number of open traumatic brain injury (OTBI) prevailed - 66%, the frequency of severe brain contusion (SBC) - 50%, fracture of the parietotemporal bone with the transition to the base of the skull 48%, severe traumatic shock was observed in all patients. In the most severe group 3, 100% of the severity of the condition at admission was due to CTBI, SBC, subarachnoid hemorrhage (SAH), traumatic shock. In group 1, out of 5.9±1.3 days spent in the ICU, only 1 patient out of 7 was on mechanical ventilation for 3 days in CMV mode, followed by extubation upon restoration of spontaneous breathing. In groups 2 and 3, all patients were transferred to mechanical ventilation upon admission according to indications. Subsequently, out of 14.6 ± 1.7 days spent in the ICU, the average rate of mechanical ventilation in CMV mode in group 2 was carried out for 6.8 ± 2.2 days, SIMV 1.75±0.8, CPAP in 1 patient - 1 day, the duration of spontaneous breathing was 7±1.6 days. In group 3, mechanical ventilation in the CMV mode was performed for three patients for 17±3 days, SIMV 9.5±4.6 days, CPAP 2.5±1.5 days, spontaneous breathing 34±9.5 days.

Results and its discussion

The phase structure of the HR circadian rhythm in the acute period of SCTBI in infancy was studied and assessed. Table 2 shows changes in the circadian rhythm mesor index HR depending on the severity of the injury by groups.

Table 2.

Dynamics of the mesor of the circadian rhythm HR in SCTBI up to 3 years

Days	Group 1	Group 2	Group 3
1	132±17	143±16	125±14
2	138±10	139±12	138±12
3	125±12	125±10	138±11
4	124±11	131±10	137±12
5	122±10	118±10	137±10
6	121±9	115±10*	133±10
7	121±9	116±10*	136±11
8		116±10*	136±11
9		112±9*	135±10‴
10		119±9	131±10
11		113±10*	129±11
12		115±9*	136±11‴
13		111±10*	133±11‴
14		103±8*	127±10‴
15		111±9*	125±12
16			121±12
17			120±10
18			119±10
19			121±10
20			124±11
21			109±10
22			116±10
23			120±11
24			123±10
25			117±10
26			125±11
27			137±11
28			126±10
29			129±10
30			134±10

*-significant relative to the indicator on the first day

‴ - significantly relative to the indicator in group 2.

As presented in table 2 data, on the first day in all groups revealed a tendency to increased heart rate. On the following days, in groups 1 and 3, there was no significantly significant decrease in the circadian rhythm mesor HR, while in group 2 a significantly significant decrease in the circadian rhythm mesor HR was found on days 6-9, 11-15 on average by 18% and by 20% ($p<0.05$, respectively). In group 3, in the absence of deviations from the indicator on day 1, there was a permanently significant difference from the indicator in group 2. That is, the HR mesor indicator of the circadian rhythm of patients in group 3 turned out to be greater than in group 2 on days 9, 12, 13, 14 by 20%, 17%, 19%, 23% ($p<0.05$, respectively). Thus, the most pronounced tendency to tachycardia, observed mainly in children of the 3rd group, was due to the severity of the condition due to trauma. We tend to attribute the tendency to tachycardia in children of the 1st group due to the relatively less significant stress-limiting therapy, the restriction of sedative, hypnotic drugs in connection with the management of patients mainly with the preservation of spontaneous breathing without respiratory support of mechanical ventilation.

In earlier studies with isolated STBI, we revealed a decrease in the HR mesor at the age of up to 3 years in group 1 on day 3, in group 2 on day 14, in group 3 during 30 days of the acute period there was a persistent increase in the mesor of the circadian rhythm HR with the highest values for 3-7 days.

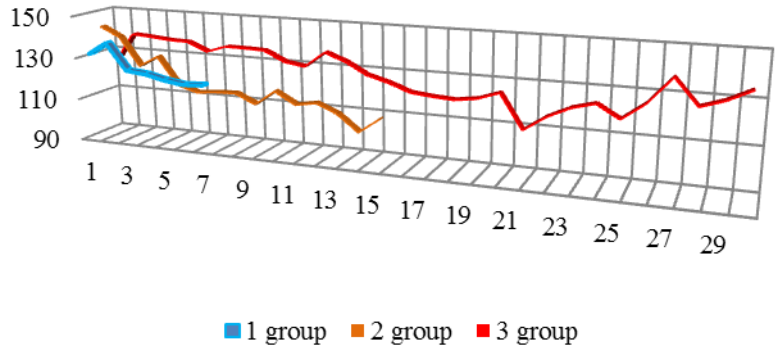

Figure 1. *Dynamics of the mesor of the circadian rhythm HR*

The change in the mesor of the circadian rhythm HR during the acute period of SCTBI was a wavy curve with an unstable wavelength, the most pronounced in children of the 3rd group (fig. 1).

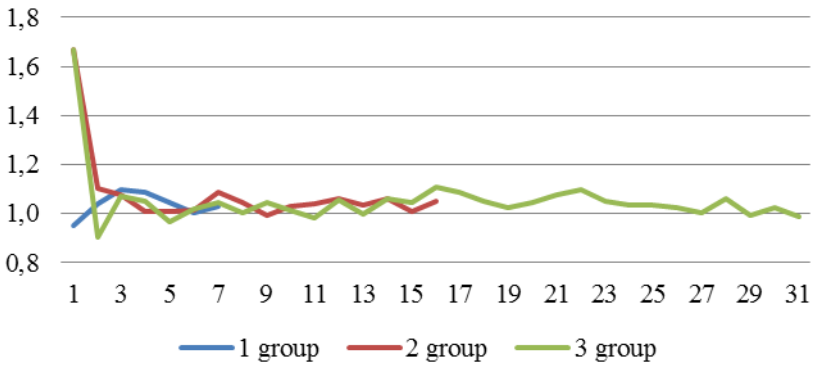

Figure 2. *Circadian index at SCTBI in infancy in children*

As it was revealed earlier, the CI indicator in the acute period of isolated STBI was characterized by heart rhythm rigidity in all children, the most pronounced in group 3, reflecting a persistent reaction of the sympathoadrenal system. In severe concomitant TBI, the most pronounced rigidity of the heart rate was noted on the 2nd day, further remaining within 1-1.1 in both groups 2 and 1 (fig. 2.). The latter confirms the need for further study and development of methods to neutralize the damaging effect of the adaptive-trophic effects of the sympathetic division of the autonomic nervous system on the heart in severe traumatic brain injuries in children.

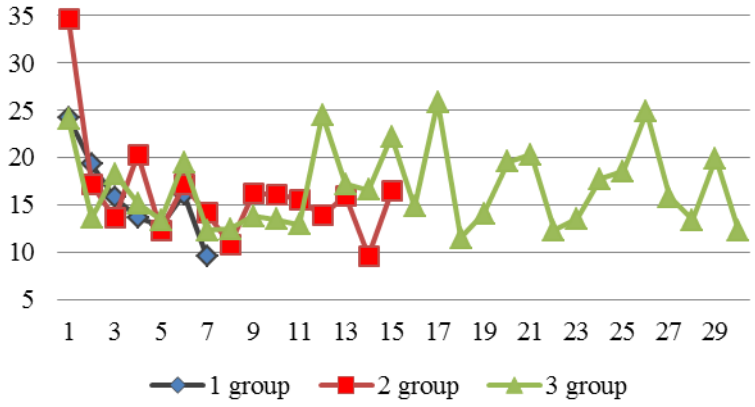

Figure 3. *Dynamics of the amplitude of diurnal fluctuations in HR*

The amplitude of the circadian rhythm in the acute period of traumatic illness caused by SCTBI changed in waves from 24 beats per minute on day 1 to 10 on day 7 in group 1, 35 beats per minute on day 1 and 10 beats per minute on days 8 and 14, from 25 beats per minute at 1, 12, 15, 17, 21, 26 days up to 12 beats per minute at 18, 22, 30 days. That is, the more severe the condition of the patients, the more significant was the amplitude of the circadian rhythm, the longer the tendency to develop tachycardia syndrome persisted (fig. 3).

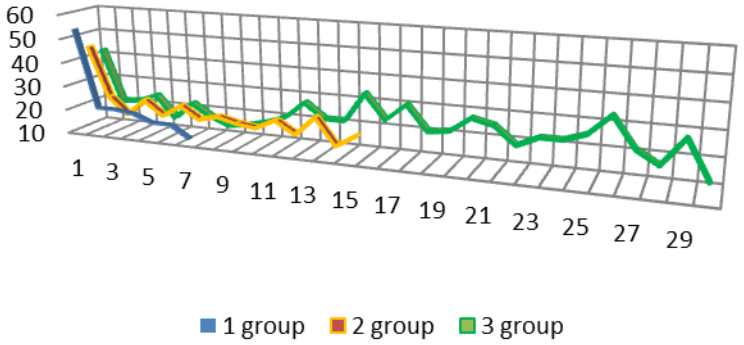

Figure 4. *Maximum daily changes in HR*

The identified features are confirmed (fig. 4) by the most prolonged and pronounced tendency to significant daily changes in HR in group 3 on day 25.29.

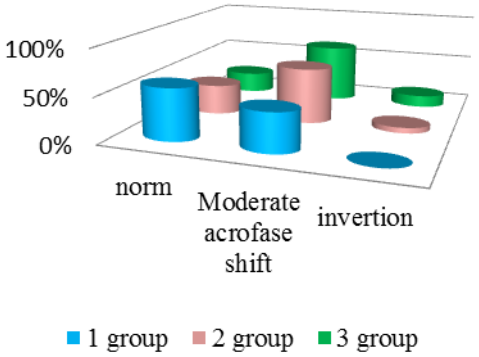

Figure 5. *Duration of shift of the acrophase of the circadian rhythm HR in SCTBI up to 3 years*

Accordingly, in the less severe group 1, the normal position of the peak of the acrophase of the circadian rhythm HR at 8-11 hours prevailed during 57% of the duration of intensive care in the ICU. The inversion of the circadian rhythm was the longest in group 3 for 4 days, in group 2 for 1 day, in group 1 no inversion was found. The longest time was observed a moderate shift in the peak of the acrophase of the circadian rhythm HR amounting to 3 days in group 1, 19 days in group 2-9, and 19 days in group 3 (fig. 5).

Table 3.

Correlations between circadian rhythm mesor HR and hemodynamic parameters

	Group 1	**Group 2**	**Group 3**
HR/AVT	**0.4**	**1.0**	**0.7**
HR/MVP	**0.8**	**0.9**	**0.9**
HR/GPVR	**-0.8**	**-0.8**	**-0.2**
HR/CO	**0.9**	**0.5**	**0.5**
HR/SV	**0.0**	**0.7**	**-0.2**
HR/temperature	**0.9**	**0.6**	**0.8**
HR/MBP	**-0.9**	**-0.3**	**0.5**
HR/SBP	**-0.9**	**-0.2**	**0.5**
HR/DBP	**-0.7**	**-0.4**	**0.5**
HR/PBP	**-0.6**	**0.7**	**0.1**

Direct strong correlation was observed in patients 2 (1) and 3 groups (0.7) tab.3.

A direct dependence of myocardial oxygen demand on the rhythm frequency was found in children of all groups. The predominant tendency to form a hyperdynamic type of hemodynamics was found in children of groups 1 and 2, which characterized a relatively more adequate compensatory response of the cardiovascular system in children of groups 1 and 2.

The most active participation of the heart rate in the compensatory response in group 1 was confirmed by a strong direct correlation between HR and CO (0.9). An interesting fact is that in group 2 a direct relationship between HR and SV (0.7) was revealed. A strong direct dependence of HR on body temperature changes was found in groups 1 (0.9) and 3 (0.8), weaker (0.6) in group 2. A strong inverse correlation between HR and MBP (-0.9), DBP (-0.7) in injured children of the 1st group may be an early indication of the beginning depletion of the adaptive value of the maximum functional activity of the sinus node in conditions of spontaneous external respiration in the preclinical stage (fig. 6).

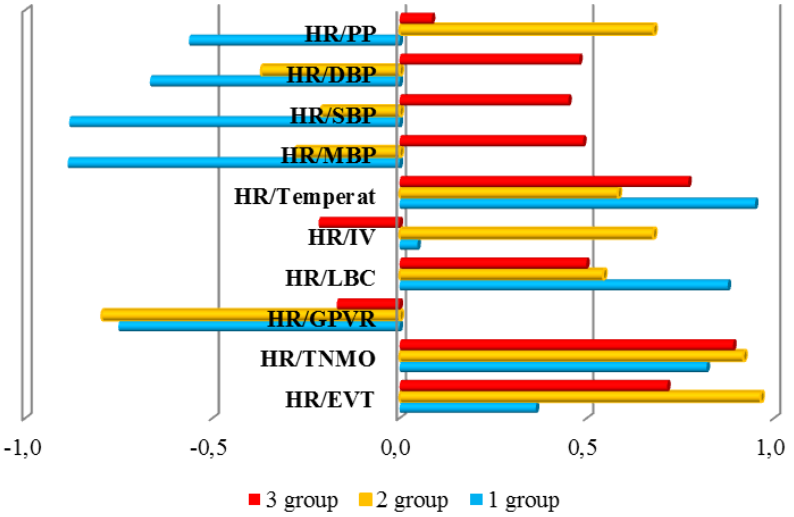

Figure 6. *Correlation relations of HR*

Conclusion

On the first day in all groups, a tendency to increased heart rate was revealed. The HR mesor indicator of the circadian rhythm in patients of group 3 was higher than in group 2 on days 9, 12, 13, and 14. The change in the mesor of the circadian rhythm HR during the acute period of SCTBI was a wavy curve with an unstable wavelength, most pronounced in children of the 3rd group. The more severe the condition of the patients, the more significant was the amplitude of the circadian rhythm, the longer the tendency to develop tachycardia syndrome persisted. A direct dependence of myocardial oxygen demand on the rhythm frequency was found in children of all groups. The predominant tendency to form a hyperdynamic type of hemodynamics was found in children of groups 1 and 2. The inversion of the circadian rhythm was the longest in group 3 for 4 days, in group 2 for 1 day, in group 1 no inversion was found.

References

1. Pogodina A.V. Abstract: Characteristics of the circadian heart rhythm in children and adolescents with vasovagal syncope. Irkutsk, 2004

2. Shkolnikova M.A., Kovaleva I.A., Leontyeva I.V.M. Syncope in children. Ed. "Megapolis" LLC Publishing House, 2016—460 P. URL: http://www.cardio-rus.ru/selected.php

3.https://vbgi.ru/cough/sochetannaya-cherepno-mozgovaya-travma-sochetannaya-cherepno-mozgovaya-i/

4. https://golovaibolit.ru/chmt/chmt-u-detej

DOI 10.34660/INF.2022.29.32.280

儿童半椎体摘除术围手术期失血量:（独立院内回顾性对照经验）
PERIOPERATIVE BLOOD LOSS DURING EXTIRPATION OF HEMIVERTEBRAE IN CHILDREN: (EXPERIENCE OF INDEPENDENT INTRA-HOSPITAL RETROSPECTIVE CONTROL)

Pulkina Olga Nikolaevna
Candidate of Medical Sciences, Anesthesiologist Resuscitator, Head of Department
St. Petersburg Children's Infectious Diseases Hospital, St. Petersburg
Mushin Alexandr Yurievich
Full Professor, Candidate of Medical Sciences, Head Research Officer
St. Petersburg Research Institute of Phthisiopulmonology
Head of the Clinic for Pediatric Surgery and Orthopedics;
Head of the Center for Spine Pathology, SPbRIP

抽象的。 回顾性研究了 50 名 1 至 13 岁患者在单节段半椎体摘除同时后路器械固定量的住院记录。 围手术期失血量与循环血容量（CBV）相关。 术中失血量从 3% 到 29% 不等，大多数（40 人）不超过 CBV 的 15%； 17 名患者接受了新鲜冷冻血浆 (FFP) 输血和补充血浆凝血因子，而回顾性研究仅在 2 名患者中证实需要使用新鲜冰冻血浆 (FFP)。

结论。 现代的半椎骨摘除技术和儿童先天性脊柱侧凸的器械矫正可以最大限度地减少术中失血，并且在大多数情况下不需要使用血液制品。

关键词：先天性脊柱侧弯，半椎骨，失血，脊柱手术中的输血。

Abstract. *The inpatient documentation of 50 patients sequentially operated on at the age of 1 to 13 years in the amount of monosegmental hemivertebra extirpation with simultaneous posterior instrumental fixation was retrospectively studied. Perioperative blood loss was assessed in relation to circulating blood volume (CBV). Intraoperative blood loss ranged from 3% to 29%, in the majority (40 people) not exceeding 15% of the CBV; blood transfusions and replenishment of plasma coagulation factors with fresh frozen plasma (FFP) were performed in 17 patients, while retrospectively the need for its use was proven only in 2.*

Conclusions. *The modern technique of extirpation of the hemivertebrae with instrumental correction of congenital scoliosis in children allows minimizing intraoperative blood loss and in most cases does not require the use of blood products.*

Keywords: *Congenital scoliosis, hemivertebrae, blood loss, blood transfusions during operations on the spine.*

Relevance

Among the operations used in pediatric vertebrology, hemivertebra extirpation with posterior instrumental fixation (PIF) in the treatment of congenital scoliosis remains one of the most standardized. One of the predicted problems of this operation is the operational blood loss, primarily from the epidural vessels and the central artery of the vertebral body [1,2]. Modern surgical technique allows minimizing the level of intraoperative blood loss and reducing the use of blood products [11,12]. Today, everyone knows the possible risks and complications from the use of blood products, including an increase in the length of stay in the hospital with an increase in the financial costs of treating the patient as a whole. Removal of the hemivertebra through combined approaches is considered traditional [1,2], which directs the anesthetist to prepare for planned blood transfusion due to the planned significant blood loss [3, 4]. According to the literature data, the use of perioperative epidural analgesia and proper positioning of the patient [2,3], the use of tranexamic acid [5-9] and preoperative hemodilution [6,10] are considered to be factors that reduce blood loss during such operations, although, in our opinion, the main component, allowing to reduce blood loss during such operations is, first of all, the use of modern technologies of surgical intervention, including the implementation of the full volume of intervention from one access [6,11,12]. Retrospective studies evaluating the amount of blood loss during extirpation of the hemivertebrae in children overwhelmingly characterize it in absolute mean values [12], which is convenient for comparison, but hardly correct given the variability in circulating blood volume (CBV) in children of different ages (from 1 years to 13 years). This fact prompted us to conduct our own retrospective study, one of the unexpected results of which was an assessment of the validity of her replacement therapy.

Purpose of the study

Assess the amount of perioperative blood loss during a standard surgical intervention - hemivertebra extirpation with posterior instrumental fixation.

Design: retrospective observational study**.**

Criteria for inclusion in the study:

surgical treatment in the amount of a single-level two-stage simultaneous extirpation of a hemivertebra with posterior instrumental fixation [2];

use of standard surgical instruments during extirpation, including high-speed burr;

age of children from 1 year to 13 years;

unified surgical team;

3-year period of material analysis - from 06.09.2013 to 06.06.2016.

Criteria for exclusion from the study:

children under 1 year old and over 13 years old;

use of instruments for minimally invasive operations;

children with initial preoperative anemia (hemoglobin level below 100 g/l).

NB! In order to exclude subjectivity in the analysis of the results, the collection of retrospective information and its processing were carried out by a doctor who was ***not*** *directly involved in the anesthetic management and perioperative management of patients.*

Material and methods: a retrospective analysis of 50 case histories of children who were sequentially operated in the specified period was carried out. The main anthropometric data of patients and their distribution by sex and age are presented in Table 1.

Table №1.

Basic anthropometric data and distribution by sex and age (M± SD)

Index	Meaning
Body weight (kg)	19,5 ± 10 (min 9; max 50)
Body length (cm)	104 ± 23 (min 79 ; max 170)
Age (years)	6,2 ± 4,9 (min 1; max 13)
M : F	32 : 18

In 33 children, the hemivertebrae were localized in the thoracic region (Th4÷Th12), in 17 children, in the lumbar region (L1÷L5). The physical condition of the patients at the time of surgery according to the criteria of the ASA (American Society of Anesthesiologists) corresponded to class 3. In all cases, the removal of the body of the hemivertebra was performed through a lateral (extrapleural or extraperitoneal) approach; removal of the arc and instrumental fixation - from the back. Removal of bone structures was carried out using a high-speed drill and Kerrison cutters. Postoperative drains were installed to the area of the anterior reconstruction in 22 patients; the dorsal access zone was always sutured without drains.

All patients underwent the same type of anesthetic management:

premedication - 30 minutes before surgery (diazepam 0.5 mg/kg, atropine 0.01 mg/kg);

induction into anesthesia - sevoflurane 8-6-4 vol%, fentanyl 2 μg/kg, intubation after the introduction of arduan 0.1 mg/kg; ALV in VCV mode, maintenance of anesthesia: sevoflurane + fentanyl.

At the stage of induction into anesthesia, the method of hypervolemic hemodilution was used to reduce intraoperative blood loss. During the main stage of

the operation, infusion therapy was carried out in a volume of 5–8 ml/kg/hour. Balanced crystalloid solutions and colloidal plasma substitutes were used as infusion media. Non-invasive monitoring of hemodynamics (BP, HR), blood oxygen saturation (SpO_2) and sleep depth (BIS VISTA) was performed intraoperatively.

After awakening and extubation in the operating room, the patient was transferred to the intensive care unit. Replenishment of CBV in the postoperative period was carried out with crystalloid and colloid solutions of plasma-substituting action, in accordance with clinical recommendations - in the mode of physiological need plus pathological losses.

Blood loss was recorded by the gravimetric method with recalculation for circulating blood volume (CBV) and the allocation of 3 degrees of its severity: degree 1 - up to 15% CBV, degree 2 - from 15 to 25%, degree 3 - over 25% [2, 3, 4]. The volume of operative blood loss (from the incision to suturing the wound) and postoperative - by drainage from the end of the operation to its removal were separately assessed.

All studied features are included in the database. Estimation of descriptive statistics parameters was carried out using the Statistica 10.0 package. Assessment of the normality of the distribution - using the Shapiro-Wilk test. Scores are presented as Me+SD (mean + standard deviation).

Results and discussion

The mean operation time (Me+SD) was 210 ± 86 min, which is in line with the figures mentioned in other publications on this pathology [12]. The mean hemoglobin level in children before surgery (Me+SD) was Hb = 126 ± 9 g/l (min 107 g/l; max 141 g/l), at discharge Hb = 101 ± 2 g/l (min 83; max 123).

The retrospectively assessed situation of replenishment of surgical blood loss was as follows:

intraoperative CBV replenishment was performed with crystalloid solutions and plasma substitutes, while in 15 patients hemostatic drugs and blood products were not used during the intervention;

as antifibrinolytic drugs in 18 patients, tranexamic acid (TA) was used, recommended to prevent the ***risk*** of massive bleeding [5–9];

10 patients underwent a transfusion of fresh frozen plasma (FFP), 7 - red blood cells;

The ***retrospectively*** estimated total volume of **surgical** blood loss ranged from **3** to **29%** of CBV with the following distribution by severity: (table №2):

Table 2.

Distribution of patients according to the degree of intraoperative blood loss

Number of patients	The degree of surgical blood loss (calculation by CBV)		
	I degree (up to 15%)	II degree (from 15 to 25%)	III degree (over 25%)
Absolute	40	8	2
Relative (%)	80	16	4

Table 3 shows the structure of blood loss and the hemostatic and blood products used in this case, distributed taking into account the actual blood loss.

Table 3.

Number of patients in whom TA and blood products were used with varying degrees of blood loss

Blood loss in % CBV	Tranexamic acid		FFP		Erythrocyte mass	
	Abs.	%	Abs.	%	Abs.	%
up to 15%	14	28	5	10		
from 15 to 25%	3	6	4	8	6	12
above 25%	1	2	1	2	1	2
Total	**18**	**36**	**10**	**20**	**7**	**14**

Abs. – absolute number of observations; % - percentage of the total number of operations

The average value of **postoperative** blood loss through drainage was 26.0 ± 16.0:, while in 11 of 22 children, in whom the operation ended with the establishment of drainage to the reconstruction zone, they did not need to stay for more than one day (an indication for the removal of drains was considered daily loss in volume, less than 50 mm) (tab. 4).

Table 4.

The amount of postoperative blood loss and used hemostatic drugs

	Volume of blood loss after surgery (in ml)(n=22)		
	10 – 50 ml	**50-100 ml**	**>100 ml**
Number of patients	**11**	**6**	**5**
Used hemostatic agents / (number of observations)	FFP / (3)	FFP / (3), er. weight (1)	FFP / (5)

In **5** children, the volume of postoperative blood loss exceeded 100 ml, which, however, did not exceed 15% of CBV in all cases. The maximum values (200.0 and 180.0 ml, respectively) were observed in adolescents aged 13 and 12 years. The use of FFP in all cases was a continuation of intraoperative transfusion.

Discussion

According to modern recommendations [6, 10, 13, 14], CBV replenishment in case of I degree of blood loss is carried out only with crystalloid solutions; at II degree - crystalloids and colloidal solutions are used in a volume ratio of 2: 1; indications for transfusion of erythrocyte-containing components are acute anemia due to the loss of 25-30% CBV, accompanied by a decrease in hemoglobin below 70-80 g/l and hematocrit below 25% with the occurrence of hemodynamic disorders. Indications for FFP transfusion are acute DIC, acute ***massive*** blood loss (more than 30% CBV), and coagulopathy due to deficiency of plasma physiological anticoagulants. In other cases, before transfusing FFP, it is necessary to make sure that there is a deficiency of plasma factors, and in their absence, to replenish CBV with plasma-substituting solutions [6, 13, 14]. Comparing these recommendations with our results, we can draw the following conclusions:

the use of TA (n = 18) was sufficient in **14** children, whose blood loss ultimately corresponded to grade I and did not require the use of other hemostatic drugs or blood products; in other cases (4) FFP was additionally used;

among patients in whom FFP was used as the main drug (n = 10), only in 1 case the volume of blood loss was 29% of CBV. In 9 patients, it was possible to do without its introduction, since their blood loss corresponded to 1 and 2 degrees of severity;

among 7 patients who received red blood cell transfusion, **6** cases were classified as blood loss II (min 17%: max 23% CBV) and one was classified as III (29% CBV).

In other words, analyzing the results of ***real*** intraoperative blood loss with a ***retrospectively*** assessed validity of the hemostatic drugs used, we can conclude that their selection is more based on an empirical approach than on an analysis of objective indicators:

in 47 (94%) cases, surgical blood loss did not require the use of blood substitutes;

only in 3 cases (6%), the use of FFP or erythrocyte mass was really required during the operation;

out of 17 cases in which these drugs were used during operations, their use was actually required in two cases.

Judging by the analysis of **postoperative** blood loss, none of the patients had the need to use blood products at this stage.

Conclusion

Modern trends in the development of surgery and anesthesiology are aimed at the introduction of technologies for accelerated recovery surgery, among which the reduction of the invasiveness of interventions and intraoperative blood loss, and therefore the need for replacement (hemo-) transfusion, is one of the first places. To make a decision on its implementation, a comprehensive assessment of the situation is required, including the use of laboratory and instrumental monitoring, and assessment of tissue oxygenation indicators [6, 15, 16]. However, as the study showed, in real conditions, doctors often individualize management tactics and continue to rely on their own clinical experience, expanding the indications for FFP and red blood cell transfusions.

Conclusions

The results of our study allow us to make sure once again that modern operations to remove a hemivertebra in children in the vast majority of cases are not accompanied by large perioperative blood loss: an intervention performed according to the standard technique, even without the use of modern ultrasonic bone instruments [11] in most cases (96 %) is accompanied by blood loss of I and II severity, which does not require the use of blood products.

On the other hand, it should be recommended to draw up a clinical protocol for intraoperative laboratory and instrumental support of highly traumatic operations in children, which will exclude unreasonable perioperative use of blood products.

Separately, we would like to note that it is an independent audit - the collection and analysis of all the data obtained was carried out by a doctor who ***did not*** take part in the treatment process - that seems to be the most objective today for a retrospective assessment of such clinical indicators as perioperative blood loss.

The authors declare no conflict of interest.

The study did not have financial support.

References

1. Mixailovskij M.V., Hanaev A.L. Vrozhdyonny`e anomalii vne apikal`noj zony`: diagnoz i principy` lecheniya. // Xirurgiya pozvonochnika 2009;№3. S.46 - 50.

2. Ul`rih E`.V. Anomalii pozvonochnika u detej. Rukovodstvo dlya vrachej // SPb. 1995. 335 s.

3. Lebedeva M.N., Saura N.V., Ivanova E.Yu. Krovosberezhenie v xirurgii skolioza // Vestn. intensivnoj terapii. 2007; №5:S. 166-

4. Bird S., McGill N. Blood conservation and pain control in scoliosis corrective surgery: an online survey of UK practice // Paediatr. Anaesth. 2011; Vol. 21: P. 50-53.167.

5. Lebedeva M.N., Saura N.V., Ivanova E.Yu. Primenenie traneksamovoj kisloty` v programme krovesberezheniya pri xirurgicheskix lechenie skolioza // Sb. materialov konf. "Sovremenny`e aspekty` anesteziologii i intensivnoj terapii". - Novosibirsk, 2009;S.79-81.

6. Petrova M.V., Bolixova N.A. Sovremenny`e principy` beskrovnoj xirurgii pri planovy`x operaciyax v onkologii. Literaturny`j obzor, http://vestnic.mcrr/ruvestnic/v10/papers/petrova_v10.htm.

7. Henry D.A., Carless P.A., Moxey A.J. et al. Anti-fibrinolytic use for minimizing perioperative allogenic blood transfusion // Cochrane Database Syst. Rev. 2011; №3. - CD001886.

8. Neilipovitz D.T. Tranexamic acid for major spinal surgery // Eur. Spine J. 2004; P.62-65.

9. Kim E.J., Kim Y.O., Shim K.W. et al. Effect of tranexamic acid based on its population Pharmacokinetics in pediatric patients undergoing distraction osteogenesis for craniosynostosis: rotational thromboelastometry (ROTEM) analysis. // International J. of medical sciences. 2018; №15.(8).P788-795. doi:10.7150.

10.Bulanov A.Yu., Gorodeczkij V.M., Shulutko E.M. Protokol terapii ostroj krovopoteri: osnovny`e polozheniya. // Vestnik intensivnoj terapii 2005; №5.S193-195.

11.Mushkin A.Yu., Naumov D.G., Umyonushkina E.Yu. E`kstirpaciya grudny`x i poyasnichny`x pozvonkov u detej : kak texnika operacii vliyaet na eyo travmatichnost`? (predvaritel`ny`e rezul`taty` i obzor literatury`). // Travmatologiya i ortopediya Rossii.2018;T24(1):S.83-90. DOI: 10.21823/2311-2905-2018-24-3.

12.Ryabykh S.O., Filatov E.Yu., Savin D.N. Rezul`taty`e`kstirpacii polupozvonkov kombinirovanny`m, dorsal`ny`m i pedikulyarny`m dostupom. Sistematicheskij obzor. // Xir. poz-ka. 2017; T14(1):S.14-23.

13. Klinicheskie rekomendacii po okazaniyu medicinskoj pomoshhi postradavshim s ostroj krovopoterej v chrezvy`chajny`x situaciyax. 2013; M. 30s. rezhim dostupa www.vcmk.ru/docs/prof -com/krovopoterya.pdf.

14. Prikaz ot 2 aprelya 2013 g. N 183n Obutverzhdenii pravil ispol'zovaniia donorskoi krovi i (ili) ego komponentov. Zaregistrirovano v Minyuste Rossii 12 avgusta 2013; g. N 29362.

15. Aleksandrovich YU.S., Parshin E.V. i dr. Kislorodnyj status novorozhdennyh pri kriticheskih sostoyaniyah. // Obshchaya reanimatologiya. 2016; №12:S.32-41.

16. Hursin V.V. Transfuzionnaya terapiya pri ostroj massivnoj krovopotere. Metodicheskie rekomendacii. Almaty, 2012; 47S.

DOI 10.34660/INF.2022.11.48.281

奥马珠单抗在严重伴随过敏病理中的疗效和安全性
EFFICACY AND SAFETY OF OMALIZUMAB APPLICATION IN SEVERE CONCOMITANT ALLERGIC PATHOLOGY

Ereshko Oksana Aleksandrovna
Candidate of Medical Sciences, Senior Research Officer
National Medical Research Center for Children's Health
Murashkin Nikolay Nikolaevich
Doctor of Medical Sciences, Head of Division
National Medical Research Center for Children's Health
Vyazankina Svetlana Svyatoslavovna
Ordinator
National Medical Research Center for Children's Health
Pertskheliya Natali Beslanovna
Student
Lomonosov Moscow State University

抽象的。根据一项荟萃分析，儿童人群中慢性自发性荨麻疹 (CSU) 的患病率为 1.4% [1]。由于罕见，儿童和青少年CSU的治疗经验不足[2,3]。主要问题是对传统治疗方法有抵抗力的疾病形式，以及需要多学科方法的诊断困难成为背景[1,4]。

临床上，CSU 表现为持续超过 6 周的瘙痒性水疱和/或血管性水肿 [5]。该病的长期持续病程、使人衰弱的瘙痒和外观缺陷对儿童及其家人的生活质量产生了明显的负面影响，30% 的患者伴有精神障碍，包括抑郁症和躯体形式障碍 [6]。

治疗儿童慢性荨麻疹的主要原则是消除可能的原因/触发因素、及时的药物治疗、耐受诱导、患者及其父母对病情的自我监测 [3,5]。

现代 CSU 药物治疗算法采用逐步方法 [3,5]。在第一阶段，第二代非镇静 H1 抗组胺药 (AHD2) 以标准剂量开处方。如果AHD2的标准剂量在2-4周或更早的时间内无效，在对疾病症状不耐受的情况下，根据孩子的体重和年龄增加其剂量（根据国内建议的两倍和四根据国外的时间）-治疗的第二阶段[3、5]。然而，在 40% 的患者中，增加剂量只会减少瘙痒，但不会减少皮肤荨麻疹的数量和严重程度 [7]。对双剂量 AHD2 治疗无效的 CSU 儿童的管理是最具挑战性的 [3, 8, 9]。在这种情况下，建议使用第三和第四阶段治疗的药物（奥马珠单抗和环孢素 A）[3, 5]。奥马珠单抗是治疗严重慢性荨麻疹的首选药物，如果没有效果，建议在进入第四阶段之前的 6 个月内使用，或者如果症状无法忍受，则更早使用。环孢素 A 在儿科实践中已显示出治疗严重形式的 CSU 的功效 [10]。推荐使用这种药物来治疗奥

马珠单抗或缺乏奥马珠单抗，并且需要定期监测肾功能、血压、血液浓度以防止副作用。抗组胺药的剂量加倍和环孢素 A 的指定由医疗机构的医疗委员会决定，并在 14 岁后由父母或患者签署知情同意书 [3,5]。

随着慢性荨麻疹的恶化，在治疗的任何阶段，都可以用全身性糖皮质激素药物（sGCS）进行短期治疗 - 3至7天。 [3,5]。然而，由于长期使用GCS，患者经常出现严重的副作用，并且由于疾病的持续复发过程而无法取消它们。

由于儿童慢性荨麻疹的患病率低，这种疾病常常被医生低估，并导致严重的器质性疾病和残疾。

自适应症注册以来，我们中心已为 3 名 CSU 患者开具了奥马珠单抗处方：2 名男孩和 1 名女孩，年龄分别为 12 至 16 岁。临床表现的持续时间从七个月到两年半不等。所有青少年都有严重的 CSU。第一阶段和第二阶段的治疗效果不存在。一名患者持续接受 sGCS 治疗。

关键词：慢性特发性荨麻疹，支气管哮喘，血管性水肿，基因工程治疗，奥马珠单抗。

Abstract. *According to a meta-analysis, the prevalence of chronic spontaneous urticaria (CSU) in the pediatric population is 1.4% [1]. Due to the rare occurrence, experience in the treatment of CSU in children and adolescents is insufficient [2,3]. The main problem is presented by forms of the disease resistant to traditional methods of therapy, and diagnostic difficulties that require a multidisciplinary approach come to the background [1,4].*

Clinically, CSU is manifested by the development of pruritic blisters and/or angioedema lasting more than 6 weeks [5]. The long, persistent course of the disease, debilitating itching and cosmetic defects have a pronounced negative impact on the quality of life of children and their families, and 30% of patients have concomitant mental disorders, including depression and somatoform disorders [6].

The main principles of managing children with chronic urticaria are the elimination of possible causes/triggers, timely pharmacotherapy, tolerance induction, self-monitoring of the condition by patients and their parents [3,5].

The modern CSU pharmacotherapy algorithm assumes a stepwise approach [3,5]. At the first stage, non-sedating H1 antihistamine drugs of the second generation (AHD2) are prescribed in a standard dose. If the standard dosage of AHD2 is ineffective for 2-4 weeks or earlier, in case of intolerance to the symptoms of the disease, their dose is increased depending on the body weight and age of the child (two times according to domestic recommendations and four times according to foreign ones) - the second stage of therapy [3, 5]. However, in 40% of patients, increasing the dose only reduces itching, but not the number and severity of urticaria on the skin [7]. The management of children with CSU refractory to double-dose AHD2 therapy is the most challenging [3, 8, 9]. In such cases, the use of drugs of the third and fourth stages of therapy (omalizumab and cyclosporine A) is recommended [3, 5]. Omalizumab is the drug of choice in the treatment of

severe forms of chronic urticaria and is recommended for use within 6 months before moving to the fourth stage if there is no effect, or earlier if the symptoms are intolerable. Cyclosporine A has shown efficacy in the treatment of severe forms of CSU in pediatric practice [10]. The appointment of this drug is recommended for torpidity to omalizumab or its absence and requires regular monitoring of kidney function, blood pressure, blood concentrations to prevent side effects. Doubling the dose of antihistamines and the appointment of cyclosporine A is carried out by decision of the medical commission of a medical organization with a signed informed consent by the parent or patient after reaching the age of 14 years [3,5].

With exacerbation of chronic urticaria, at any stage of treatment, it is possible to conduct a short course of therapy with systemic glucocorticosteroid drugs (sGCS) - three to seven days. [3,5]. However, patients often present with severe side effects due to long-term use of GCS and the impossibility of canceling them due to the continuously relapsing course of the disease.

Due to the low prevalence of chronic urticaria among children, the disease is often underestimated by doctors and leads to serious organic disorders and disability.

Since the registration of indications, omalizumab has been prescribed at our center to three patients with CSU: 2 boys and 1 girl aged 12 to 16 years. The duration of clinical manifestations varied from seven months to two and a half years. All adolescents had severe CSU. The effect of the therapy of the first and second stages was absent. One patient received sGCS treatment on an ongoing basis.

Keywords: *chronic idiopathic urticaria, bronchial asthma, angioedema, genetic engineering therapy, omalizumab.*

Clinical case

Girl K., 16 years old, from the Khanty-Mansiysk Autonomous Okrug, was admitted to the Department of Dermatology on 11.05.2021 with a group of laser surgery with complaints of widespread itchy rashes on the skin of the type of blisters, swelling of the face, hands and lower extremities, episodes of shortness of breath during physical exertion and emotional stress. In addition, episodically disturbed by pain in the elbow joints and abdomen, twitching of the upper limbs.

From the anamnesis: a child from the 1st pregnancy, which proceeded physiologically, the 1st independent birth in time. At birth, body weight - 2800 g, length - 50 cm. APGAR score 8/9 points. Heredity for allergic diseases is not burdened. Home conditions are satisfactory, the elimination regime is observed. Until adolescence, she grew and developed without features.

At the age of 14, after a series of acute respiratory viral infections, recurrent episodes of bronchial obstruction appeared. An allergist at the place of residence

conducted an allergy examination, according to which a moderate sensitization to mold allergens was revealed, specific IgE to house dust mites were not detected. The diagnosis was made: Atopic bronchial asthma, without specifying the severity and degree of control. In basic therapy, she received inhaled glucocorticosteroids (IGCS) - 500 mcg/day through a nebulizer, asthma control remained incomplete. Further, the combined drug formoterol/budesonide (4.5/80 mcg, 1 ing. 2 times a day) was prescribed. During treatment, there was a temporary improvement, then the attacks resumed. From the age of 16, the volume of daily basic therapy was increased to high doses of fluticasone propionate (FP): formoterol/budesonide (4.5/160, 1 ing. 2 times a day). Against this background, attacks of shortness of breath disturbed 1-2 times a month, and also at night, dyspnea persisted during physical exertion.

At the age of 15, the debut of the skin process in the form of urticaria, swelling of the face, hands and lower extremities. Against the background of taking cetirizine at an age dosage, the condition was stopped within a day. Three days later, edema and urticarial rashes of various localization reappeared. No association with food intake or other trigger factors has been established. Cetirizine was returned to therapy, however, against the background of treatment, rashes appeared daily in the amount of >50 elements, edema of the previous localization was also disturbing. The girl was repeatedly hospitalized in hospitals at the place of residence, the dosage of cetirizine was increased to 20 mg/day, for the relief of exacerbations, short courses of sGCS were carried out - with a temporary positive effect. Subsequently, due to frequent relapses of the disease, the dosage of cetirizine was increased to 40 mg/day, prednisolone 40 mg/day per os was prescribed for a long period (more than a month), however, the symptoms of the disease persisted, the condition remained unstable.

Episodes of urticarial rashes and edema were accompanied by severe pain in the abdomen. There were also pains in the elbow joints and twitching of the upper extremities.

When examining the girl at the time of hospitalization, the skin is moderately dry, widespread urticarial rashes are noted, in some places confluent, with severe itching. Pastosity of the face, hands and lower extremities (fig. 1,2,3,4). Urticaria Activity Score for 7 days (UAS7) [5] - 35 points, corresponds to the severe course of the disease. On auscultation of the lungs, breathing is hard, evenly carried out in all departments, rales are not heard. With forced expiration coughs. Asthma control test (AST-test) [11] - 20 points, corresponds to partial control. Moderate pain when moving in the elbow joints. Single twitching of the muscles of the shoulder girdle and arms by the type of myoclonic paroxysm.

Indicators of clinical and biochemical blood tests within the reference values. C-reactive protein - 1.02 mg/l (normal 0-5). When conducting an immunological

blood test, total IgE - 80.03 IU / ml (normal <200); IgG -5.57 mg/ml (5.3-16.5), IgA - 0.42 mg/ml (0.8-4.0), IgM -2.04 mg/ml (0.5-2.0).

For differential diagnosis with hereditary angineurotic edema, the levels of C3, C4 complement components and C1 esterase inhibitor were analyzed. The absence of deviations from the reference values and a characteristic clinical picture made it possible to exclude this pathology.

The laboratory examination also made it possible to exclude the presence of parasitic infections, rheumatological pathology, pathology of the thyroid gland and celiac disease.

When examined on the ImmunoCap analyzer, specific IgE to allergens of milk, egg white, gluten and wheat were not detected.

Assessment of the function of external respiration revealed moderate violations of the patency of the peripheral bronchi. FVC and FEV1 are normal. After a test with a bronchodilator, reversibility was 19% (510 ml). When checking the inhalation technique, shortcomings were identified, and training was provided. Montelukast 10 mg 1 time per night was added to the basic therapy.

According to the ultrasound examination of the abdominal cavity, signs of secondary changes in the pancreas were found. Gastroduodenitis. She was consulted by a gastroenterologist, fibrogastroduodenoscopy was prescribed, the identified changes correspond to the course of chronic gastroduodenitis, the urease test for H. pylori is negative. Recommendations for treatment are given.

She was consulted by a geneticist, to rule out autoinflammatory syndrome, a study of target regions of 83 genes was prescribed - no mutations were found.

Given the presence of neurological symptoms, she was consulted by a neurologist, and an examination was scheduled. According to video-EEG monitoring, a photoparoxysmal response was registered against the background of photostimulation, Waltz IV. Magnetic resonance imaging of the brain showed no organic pathology. Recommended observance of the regime of the day and rest, observation in dynamics.

Due to the long-term continuous recurrent course of urticaria, the presence of angioedema and concomitant severe partially controlled bronchial asthma, as well as resistance to ongoing therapy, including sGCS, after signing the informed consent of the parents, therapy with the immunobiological genetically engineered drug omalizumab was initiated at the standard recommended dose of 300 mg subcutaneously every 4 weeks [3,5]. There were no adverse reactions to the administration of the drug. Prednisolone 40 mg/day and cetirizine 20 mg/day also remained in therapy.

According to the teenager and the data of medical documentation, 2 weeks after discharge from the hospital, a sharp decrease in urticarial rashes, the disappearance of angioedema was noted. Under the supervision of an endocrinologist

at the place of residence, the dose of sGCS was gradually reduced, followed by withdrawal, and the dose of AHD2 was also reduced to 10 mg/day. After three injections of omalizumab, a pronounced clinical improvement was observed, single urticaria appeared 1-2 times a month. After 4 months of biological therapy, urticaria symptoms regressed (UAS7 - 0) (Fig. 5.6,7,8), pain in the abdomen and elbow joints stopped, the frequency and severity of neurological symptoms decreased, and there were no episodes of bronchial obstruction. When assessing the condition after 6 months of biological therapy, no exacerbations of urticaria were noted, the condition remained stable.

Discussion

The presented clinical case demonstrates the importance of using a multidisciplinary approach, the interaction and succession of doctors of various specialties in the management of patients with severe forms of the disease. The high efficacy and safety of the use of the immunobiological drug omalizumab in the treatment of chronic spontaneous urticaria accompanied by angioedema and severe, partially controlled course of bronchial asthma in a 16-year-old adolescent was also shown.

The efficacy and safety of the use of biological therapy in allergology has been proven earlier in the treatment of severe forms of atopic bronchial asthma [12,13]. The appointment of omalizumab for CSU has officially become possible since 2014. To date, the European consensus document for the classification, diagnosis and treatment of urticaria (EAACI/GA(2)LEN/EDF/WAO) lists omalizumab as the only biologic drug approved for use in AHD2 resistance [3].

Following the completion of phase III clinical studies of ASTERIA I and II, as well as GLACIAL, omalizumab was approved by the US Food and Drug Administration and the European Medicines Agency for the treatment of CSU in children aged 12 years and older, and registered in Russia [14, 15, 16]. In 2015, the results of a meta-analysis of 7 randomized, double-blind, placebo-controlled studies evaluating the efficacy and safety of omalizumab were published in 1312 patients with CSU. Meta-analysis data provided evidence of the high efficacy and safety of omalizumab at a dose of 300 mg every 4 weeks, regardless of body weight and total IgE levels [17].

The frequency of assessing the patient's condition during therapy with omalizumab is every 3 months. The optimal duration of treatment has not been established, the recommended course of omalizumab for CSU is 6 months. Rapid discontinuation of the drug can provoke relapse [5]. In our patient, an incomplete response to therapy was noted as early as 2 weeks after the first injection, remission was achieved after 4 months of treatment, however, given the severity of the initial lesions (high initial score on the UAS7 scale - 35), the presence of angioedema and comorbid background, the girl was recommended long-term treatment with a genetically engineered drug.

Conclusion

Chronic spontaneous urticaria is an urgent medical and social problem. Due to the lack of standardized pediatric phenotyping tests and established age limits for the use of symptom-relieving drugs, the management of children with CSU is challenging. Omalizumab is the only biological drug with high safety and efficacy approved for use in CSU in patients over 12 years of age.

References

1. *Fricke J, Ávila G, Keller T, et al. Prevalence of chronic urticaria in children and adults across the globe: Systematic review with metaanalysis. Allergy. 2020;75(2):423–432. doi: 10.1111/all.14037.*
2. *Ulrich W. Anti-IgE for chronic urticaria — are children little adults after all? Pediatr Allergy Immunol. 2015:26(6):488–489. doi: 10.1111/pai.12424.*
3. *Zuberbier T, Aberer W, Asero R, et al. The EAACI/GA(2)LEN/ EDF/WAO Guideline for the Definition, Classification, Diagnosis and Management of Urticaria. The 2017 Revision and Update. Allergy. 2018. doi: 10.1111/all.13397.*
4. *Greaves M. Chronic urticaria. J Allergy Clin Immunol. 2000;105(4):664–672. doi: 10.1067/ mai.2000.105706.*
5. *Allergology and clinical immunology. Clinical recommendations. Ed. by R.M. Khaitov, N.I. Ilyina. Moscow: GEOTARMedia; 2019. 352 p. (Series "Clinical recommendations"). (In Russ).*
6. *Gonçalo M, Gimenéz-Arnau A, Al-Ahmad M, et al. The global burden of chronic urticaria for the patient and society. Br J Dermatol. 2021;184(2):226–236. doi: 10.1111/bjd.19561*
7. *Guillén-Aguinaga S, Jáuregui Presa I, Aguinaga-Ontoso E, et al. Updosing nonsedating antihistamines in patients with chronic spontaneous urticaria: a systematic review and meta-analysis. Br J Dermatol. 2016;175(6):1153–1165. doi: 10.1111/bjd.14768.*
8. *Greenberger PA. Chronic urticaria: new management options. World Allergy Organ J. 2014;7(1):31. doi: 10.1186/1939-4551-7-31.*
9. *Neverman L, Weinberger M. Treatment of chronic urticaria in children with antihistamines and cyclosporine. J Allergy Clin Immunol Pract. 2014;2(4):434–438. doi: 10.1016/j.jaip.2014.04.011.*
10. *Doshi DR, Weinberger MM. Experience with cyclosporine in children with chronic idiopathic urticaria. Pediatr Dermatol. 2009;26(4):409–413. doi: 10.1111/j.1525-1470.2009.00869.x.*

11.Nathan RA, Sorkness CA, Kosinski M, Schatz M, Li JT, Marcus P, Murray JJ, Pendergraft TB. Development of the asthma control test: a survey for assessing asthma control. J Allergy Clin Immunol. 2004 Jan;113(1):59-65. doi: 10.1016/j.jaci.2003.09.008.

12.Schmetzer O., Lakin E., Topal F.A., et al. IL-24 is a common and specific autoantigen of IgE in patients with chronic spontaneous urticaria // J Allergy Clin Immunol. 2018. Vol. 142, N 3. P. 876–882. doi: 10.1016/j.jaci.2017.10.035

13.Lanier B, Bridges T, Kulus M, et al. Omalizumab for the treatment of exacerbations in children with inadequately controlled allergic (IgE-mediated) asthma. J Allergy Clin Immunol. 2009;124(6):1210– 1216. doi: 10.1016/j.jaci.2009.09.021.

14.Saini SS, Bindslev-Jensen C, Maurer M, et al. Effi cacy and safety of omalizumab in patients with chronic idiopathic/ spontaneous urticaria who remain symptomatic on H1 antihistamines: a randomized, placebo-controlled study. J Invest Dermatol. 2015;135(1):67–75. doi: 10.1038/jid.2014.306.

15.Maurer M, Rosén K, Hsieh HJ, et al. Omalizumab for the treatment of chronic idiopathic or spontaneous urticaria. N Engl J Med. 2013;368(10):924–935. doi: 10.1056/NEJMoa1215372.

16.Kaplan A, Ledford D, Ashby M, et al. Omalizumab in patients with symptomatic chronic idiopathic/spontaneous urticaria despite standard combination therapy. J Allergy Clin Immunol. 2013;132(1):101–109. doi: 10.1016/j.jaci.2013.05.013.

17.Zhao Z.T., Ji C.M., Yu W.J., et al. Omalizumab for the treatment of chronic spontaneous urticaria: A meta-analysis of randomized clinical trials // J Allergy Clin Immunol. 2016. Vol. 137, N 6. P. 1742–1750.e4. doi: 10.1016/j.jaci.2015.12.1342.

Figure 1 ***Figure 2*** ***Figure 3*** ***Figure 4***

Figure 1, 2, 3, 4. *The state of the skin process before the start of anti-IgE therapy with omalizumab.*




Figure 5 ***Figure 6*** ***Figure 7*** ***Figure 8***

Figure 5, 6, 7, 8 Skin condition 4 months after the start of anti-IgE therapy with omalizumb

DOI 10.34660/INF.2022.89.15.282

治疗严重特应性疾病患者的新可能性

NEW POSSIBILITIES OF THERAPY FOR PATIENTS WITH SEVERE ATOPIC DISEASES

Galimova Albina Albertovna
Research Assistant, Allergist-Immunologist
Makarova Svetlana Gennadievna
Doctor of Medical Sciences, Head of the Center for Preventive Pediatrics
Vyazankina Svetlana Svyatoslavovna
Resident
National Medical Research "Center for Children's Health"

抽象的。特应性疾病的增加是影响发达国家和发展中国家人民的主要公共卫生问题[1]。

尽管这些疾病，如特应性皮炎 (AtD)、支气管哮喘 (BA)、食物过敏 (FA) 等，是影响不同靶器官的异质性疾病，但具有共同的过敏性炎症基本机制 [2]。中度至重度特应性合并症患者的管理，如 BP、BA、嗜酸性食管炎 (EoE) 对医生来说是一个相当大的挑战，而儿科患者的治疗选择通常有限。全身性免疫抑制治疗长期治疗有副作用，部分患者对这种治疗仍有抵抗力。在这些情况下，生物制剂代表了一种创新的治疗方法 [3,4]。

在世界儿科实践中，描述了 1 例患有支气管哮喘并伴有过敏性病变的患者，在使用 dupilumab 治疗期间，他的所有特应性疾病（BA、AtD、EoE、花粉热、慢性鼻窦炎）均实现了客观改善。 5]。

我们中心成功地对严重的 AtD、BA 进行了靶向治疗，但该病例的独特之处在于它结合了超过 3 种相互加重的伴随病症。

关键词：特应性皮炎，支气管哮喘，嗜酸性食管炎，靶向治疗，dupilumab

Abstract. *The rise in atopic diseases is a major public health problem affecting people in developed and developing countries [1].*

Despite the fact that these diseases, such as atopic dermatitis (AtD), bronchial asthma (BA), food allergy (FA) and others, are heterogeneous disorders that affect different target organs, but have common fundamental mechanisms of allergic inflammation [2]. The management of patients with moderate to severe atopic comorbidities such as BP, BA, eosinophilic esophagitis (EoE) is quite a challenge

for physicians, and therapeutic options are often limited for pediatric patients. Systemic immunosuppressive therapy has side effects with long-term treatment, and some patients remain resistant to such treatment. In these cases, biologics represent an innovative therapeutic approach [3,4].

In the world pediatric practice, one case of a patient with bronchial asthma and concomitant allergic pathology was described, who achieved an objective improvement in all of his atopic diseases (BA, AtD, EoE, hay fever, chronic sinusitis) during treatment with dupilumab [5].

Our Center successfully conducts targeted therapy for severe AtD, BA, but this case is unique in that it combines more than 3 concomitant conditions that aggravate each other.

Keywords: *atopic dermatitis, bronchial asthma, eosinophilic esophagitis, targeted therapy, dupilumab*

A 6-year-old boy was admitted to the clinic with complaints of widespread skin rashes accompanied by severe itching. In addition, the patient suffered from partially controlled bronchial asthma for a long time, the manifestations of rhinitis, conjunctivitis were also disturbed during the year with worsening in the spring, there was a lack of body weight and episodes of difficulty swallowing, vomiting, and belching.

Heredity for allergic diseases is burdened: in the mother - BA, AtD; older brother has FA, allergic rhinitis. Perinatal history without features. Breastfeeding was up to 1.5 years, complementary foods were introduced from 6 months.

From the anamnesis it is known that from the first month of life the child was disturbed by manifestations of FA in the form of skin rashes. According to the results of an allergological examination, sensitization to cow's milk protein (CMP) was revealed. At the age of 1.5, the child, at the initiative of the parents, was transferred to the diet with a mixture based on goat's milk, against this background, there was a deterioration in the skin process with the addition of gastrointestinal symptoms (bloating, abdominal pain, constipation, streaks of blood in the stool). At 2 years 6 months. was switched to a mixture based on partially hydrolyzed milk protein, there was no clinical improvement. A re-examination revealed an expansion of the spectrum of food sensitization.

From the age of 3 years, the course of AtD was of a severe continuous-recurrent nature, external anti-inflammatory therapy was carried out with a short-term effect. Simultaneously with the deterioration of the skin pathological process, abdominal pain intensified, belching appeared, vomiting occasionally occurred, blood streaks in the stool. According to primary esophagogastroduodenoscopy (EGDS) at the age of 3 years, catarrhal reflux esophagitis, erosive bulbitis, superficial antral gastritis were detected, for which the boy was observed by a gastroen-

terologist. However, there was an increase in the severity of FA symptoms: with the use of dairy products and eggs - vomiting, belching; buckwheat and rice - suffocation; apples - rhinoconjunctival syndrome. The child was repeatedly consulted by a nutritionist, a dairy-free gluten-free hypoallergenic diet was prescribed, the diet was corrected, against which some positive dynamics were noted, as well as a temporary decrease in abdominal pain and normalization of the stool, but the diet was not strictly observed.

At the age of 4, the boy was diagnosed with Bronchial asthma, which worsened against the background of acute respiratory infections, physical activity, during the period of active dusting of trees, and was stopped by inhalation of short-acting bronchodilators (SABA) and inhaled corticosteroids. In the same period, the manifestations of rhinoconjunctival syndrome were added during the year, with an increase mainly in the spring. Household and pollen sensitization was revealed. However, due to persistent episodes of bronchial obstruction and weekly need for SABA, obstructive changes in spirometry, at the age of 5, the basic therapy was replaced with a combined drug (salmeterol + fluticasone propionate) at a dose of 25/250 mcg, 1 inhalation 2 times a day. Against this background, the frequency of seizures decreased to 3-4 times a month. After the correction of the basic therapy, episodes of dysphagia, increased belching, vomiting, and underweight, despite adherence to targeted diet therapy, began to be noted.

When examining a boy at the time of hospitalization in the clinic (at the age of 6), protein-energy deficiency was noted. A laboratory examination revealed moderate eosinophilia - 0.96×109/l (14%), a pronounced increase in the level of total IgE - 5285 IU/ml. According to the results of ultrasound examination of the abdominal organs - signs of an increase in the gallbladder, secondary changes in the pancreas, hepatosplenomegaly, changes in the liver parenchyma, mesadenitis. Considering the persistent complaints from the gastrointestinal tract, EGDS was performed with a biopsy, endoscopic signs of EoE were detected (EREFS - 5 points), the histological picture corresponds to the manifestations of EoE (eosinophils up to 37-50 in the field of view at x400 magnification). Based on the available data, a diagnosis of EoE was established.

As part of the complex therapy for the treatment of atopic dermatitis, bronchial asthma, EoE oral viscous budesonide (OVB) therapy was prescribed: budesonide suspension, antacid, proton pump inhibitors, as well as continued compliance with a dairy-free and gluten-free diet with the exception of eggs, an amino acid mixture was introduced into the diet.

To assess the results of EoE therapy, EGDS was repeated after 3 months with a biopsy, slightly pronounced endoscopic signs of EoE were recorded (EREFS - 1-2 points). The morphological picture of the biopsy corresponds to the manifestation of EoE with positive dynamics (eosinophils up to 25-36 in the field of view at

x400 magnification).

Based on the therapy, a positive dynamics of z-score indicators (WAZ -0.43; HAZ -0.32; BAZ -0.37) can be noted, as well as a decrease in abdominal pain and normalization of stool, relief of symptoms of dysphagia, vomiting. However, due to the severity of a common skin pathological process that is resistant to the ongoing treatment with topical corticosteroids, local immunosuppressants, the presence of concomitant allergic diseases, and the absence of contraindications, the child is additionally indicated for therapy with a genetically engineered biological drug, dupilumab, which was initiated in February 2021.

Against the background of the ongoing complex therapy, after 12 months, there is a positive trend in the skin process, it was possible to achieve longer remissions of AtD, the frequency of exacerbations of BA decreased, which made it possible to reduce the dose of basic therapy, and the volume and need for symptomatic therapy decreased. EoE symptoms completely stopped without targeted basic therapy (endoscopic and morphological picture corresponded to the absence of signs of eosinophilic inflammation). It was also possible to introduce dairy products and eggs into the diet as part of baking.

Atopic diseases result from Th2, an inflammatory response triggered by a wide range of allergens, which leads to various immune responses culminating in the production of immunoglobulin E. Two key cytokines, interleukin 4 (IL-4) and 13 (IL-13), play a decisive role in the pathogenesis of atopic dermatitis and other allergic diseases, including asthma, FA, AR, EoE. Through understanding the pathophysiology of allergy, it has become clear that the atopic march is a stereotypical progression of conditions that share common genetic and environmental predisposing factors, as well as general immunological features of a Th2-type inflammatory response that results in specific IgE production, granulocyte activation, and other features such as mucus production and edema. Classically, the march begins with BP and progresses to IgE-mediated FA, BA, and AR [6]. There is also evidence to suggest that EoE may be one of the steps in the atopic march [2]. The described pathogenetic mechanism is confirmed by the frequency of detection of concomitant allergic diseases in patients with EoE.

According to a study involving 449 patients with EoE, among which approximately 3/4 patients had at least one disease (BA, AtD or AR), 1/2 had two atopic diseases, and 1/4 of the patients had all three variants of this pathology [8]. In addition, EoE shares genetic features with all other manifestations of the march, including polymorphisms in thymic stromal lymphopoietin (TSLP) and signal transducer and transcription activator 6 (STAT6) [9,10]. These findings may suggest that EoE is a late manifestation of the allergic march.

The given clinical example of a pediatric patient is unique in the variety and

severity of the manifestations of the atopic march, as well as in the pronounced positive dynamics of the state with a comprehensive approach to the treatment of allergic diseases, including the appointment of targeted therapy.

Dupilumab, a human monoclonal antibody that simultaneously inhibits IL-4 and IL-13 receptors, has demonstrated significant clinical efficacy in AtD and BA [11]. The fact that these diseases often occur as comorbidities and respond to the same therapy confirms that the cytokines IL-4 and IL-13 play a central role in regulating the pathogenesis of these atopic diseases. Although dupilumab is not approved for the treatment of EoE, a phase 2 study in adults is currently underway and has shown a reduction in both symptoms of dysphagia and intraepithelial eosinophils [12].

This case emphasizes the importance of pathogenetic therapy prescribed for a child with comorbid atopic pathology.

References

1. Arias Á, Lucendo AJ. Incidence and prevalence of eosinophilic oesophagitis increase continuously in adults and children in Central Spain: a 12-year population-based study. Dig Liver Dis 2019; 51: 55–62

2. Hill DA, Spergel JM. The atopic march: critical evidence and clinical relevance. Ann Allergy Asthma Immunol. 2018 Feb;120(2):131–7.

3. Benzecry V, Pravettoni V, Segatto G, Marzano AV, Ferrucci S. Type 2 Inflammation: Atopic Dermatitis, Asthma, and Hypereosinophilia Successfully Treated With Dupilumab. J Investig Allergol Clin Immunol. 2021 Jun 22;31(3):261-263. doi: 10.18176/jiaci.0614.

4. Licari A, Manti S, Castagnoli R, Parisi GF, Salpietro C, Leonardi S, Marseglia GL. Targeted Therapy for Severe Asthma in Children and Adolescents: Current and Future Perspectives. Paediatr Drugs. 2019 Aug;21(4):215-237. doi: 10.1007/s40272-019-00345-7. PMID: 31325115.

5. Bawany F, Franco AI, Beck LA. Dupilumab: One therapy to treat multiple atopic diseases. JAAD Case Rep. 2020 Sep 9;6(11):1150-1152. doi: 10.1016/j.jdcr.2020.08.036. PMID: 33134458; PMCID: PMC7591322

6. Hill DA, Spergel JM. The atopic march: Critical evidence and clinical relevance. Ann Allergy Asthma Immunol. 2018 Feb;120(2):131–7

*7. Hill DA, Grundmeier RW, Ramos M, Spergel JM. Eosinophilic Esophagitis Is a Late Manifestation of the Allergic March. J Allergy Clin Immunol Pract. 2018 Sep-Oct;6(5):*1528-1533

8. Mohammad AA, Wu SZ, Ibrahim O, Bena J, Rizk M, Piliang M, et al. Prevalence of atopic comorbidities in eosinophilic esophagitis: A case-control study of 449 patients. J Am Acad Dermatol. 2017 Mar;76(3):559–60.

9. Marenholz I, Esparza-Gordillo J, Ruschendorf F, Bauerfeind A, Strachan DP, Spycher BD, et al. Meta-analysis identifies seven susceptibility loci involved in the atopic march. Nat Commun. 2015 Nov 6;6:8804

10.Hirota T, Nakayama T, Sato S, Yanagida N, Matsui T, Sugiura S, et al. Association study of childhood food allergy with GWAS-discovered loci of atopic dermatitis and eosinophilic esophagitis. J Allergy Clin Immunol. 2017 Jun 16

11.Harb H, Chatila TA. Mechanisms of Dupilumab. Clin Exp Allergy. 2020 Jan;50(1):5-14. doi: 10.1111/cea.13491. Epub 2019 Sep 30. PMID: 31505066; PMCID: PMC6930967.

12.Hirano I., Dellon E.S., Hamilton J.D. Efficacy of dupilumab in a phase 2 randomized trial of adults with active eosinophilic esophagitis. Gastroenterology. 2020;158(1):111–122.e10.

DOI 10.34660/INF.2022.89.82.283

食物过敏和严重特应性皮炎儿童的生长和营养状况

GROWTH AND NUTRITIONAL STATUS IN CHILDREN WITH FOOD ALLERGY AND SEVERE ATOPIC DERMATITIS

Emeliashenkov E. Evgeniy
postgraduate

Makarova G. Svetlana
Doctor of Medical Sciences, Head of the Center for Preventive Pediatrics, Full Professor

Ereshko A. Oksana
Candidate of Medical Sciences, allergist, junior researcher

Murashkin N. Nikolay
Doctor of Medical Sciences, Head of department
National Medical Research Center for Children's Health

抽象的：

相关性：食物过敏原可能是特应性皮炎恶化的关键诱因，尤其是在儿童早期。今天，食物过敏治疗的主要方法是饮食消除。饮食不均衡会导致各种营养素缺乏，对身体发育产生不利影响，并可能加重特应性皮炎的病程。

目的：研究各种因素对重度特应性皮炎和食物过敏患儿生长和营养状况的影响。

方法：这项回顾性研究包括 210 名 0-17 岁、中位年龄 97 个月 (51;123) 的患有严重特应性皮炎和食物过敏的儿童。我们分析了发病史和人体测量指标；对所有儿童进行了全血细胞计数、总和特异性 IgE 检测、血清维生素 D 水平评估。

结果：162名儿童（77.1%）BAZ正常，8名（3.8%）消瘦，2名（1%）严重消瘦。 27名（12.9%）儿童超重，11 名（5.2%）儿童肥胖。 HAZ与儿童年龄呈显着正相关（r=0.32，p=0.02），HAZ、BAZ与排除食物组数呈负相关（r=-1.32，p=0.029）和（r =-1.43，p=0.015），分别。排除牛奶及其制品的儿童的 HAZ (p=0.019) 和 BAZ (p=0.022) 显着低于接受该食物组的儿童。 49 名（23.75%）儿童血清维生素 D 不足，94 名（45.0%）儿童缺乏。 BAZ 与血清维生素 D 水平呈显着正相关（r=0.38，p=0.01），血红蛋白水平与排除食物组数呈负相关（r=-0.12，p=0.045）。

结论：消除饮食的处方和成分必须严格合理。营养师必须定期咨询有生长障碍风险的儿童，以了解适当的消除饮食成分以及维生素和矿物质补充剂的处方。排除了几个食物组的儿童必须由儿科医生和营养师特别仔细地监测和咨询。炎症过程的严重程度、饮食成分和身体发育等因素之间的因果关系需要进一步研究。

关键词：儿童，特应性皮炎，消除饮食，食物过敏，人体测量指标，俄罗斯联邦

Abstract:

Relevance: *Food allergens can be critical triggers for atopic dermatitis exacerbation, especially in early childhood. Today the main method of food allergy treatment is dietary elimination. Prescription of an insufficiently balanced diet can lead to a deficiency of various nutrients, which adversely affects physical development and may aggravate the course of atopic dermatitis.*

Goal: To study the influence of various factors on growth and nutritional status of children with severe atopic dermatitis and food allergies.

Methods: *This retrospective study included 210 children with age of 0-17 years, a median age 97 months (51;123) with severe atopic dermatitis and food allergies. We analyzed the morbidity history and anthropometric indices; the complete blood count, total and specific IgE tests, serum vitamin D levels evaluation were performed for all children.*

Results: *162 children (77.1%) had normal BAZ, 8 (3.8%) had wasting, 2 (1%) - severe wasting. 27 (12.9%) children were overweight and 11 (5.2%) were obese. There was a statistically significant positive correlation between HAZ and age of children (r=0.32, p=0.02), a negative correlation between HAZ, BAZ and the number of excluded food groups (r=-1.32, p=0.029) and (r=-1.43, p=0.015), respectively. HAZ (p=0.019) and BAZ (p=0.022) in children with excluded cow's milk and its products were significantly lower than in children who received this food group. 49 (23.75%) children had serum vitamin D insufficiency and 94 (45.0%) - deficiency. There was a statistically significant positive correlation between BAZ and serum vitamin D levels (r=0.38, p=0.01) and a negative correlation was indicated between hemoglobin levels and the number of excluded food groups (r=-0.12, p=0.045).*

Conclusions: *The prescription and composition of the elimination diet must be strictly justified. Children at risk of growth impairment must be consulted by a nutritionist regularly for adequate elimination diet composition and prescription of vitamins and minerals supplementation. Children with several food groups excluded must be monitored and consulted by pediatricians and nutritionists especially carefully. Causal relationships between factors such as the severity of the inflammatory process, the composition of the diet and physical development require further study.*

Keywords: *children, atopic dermatitis, elimination diet, food allergy, anthropometric indices, Russian Federation*

Introduction

Food allergens can be critical triggers for atopic dermatitis (AD) exacerbation, especially in early childhood. Today the main method of food allergy (FA)

treatment is dietary elimination. Therefore, prescription and duration of the elimination diet must be strictly justified. Moreover, such diets must meet a child's nutritional needs for their current age (1).

Cow's Milk Protein (CMP) is one of the most significant food allergens in childhood. According to various studies, the frequency of the tolerance formation to CMP differs significantly (2-4). In patients with IgE-mediated, cows' milk protein allergy (CMA) tolerance to milk proteins may develop later in life. Up to 57% of patients with IgE-mediated CMA develop tolerance by 4-5 years (2). The drawback of the current food allergy treatment is that prolonged elimination diet may be associated with high nutritional risks. In fact, today an increasing number of clinical studies have indicated growth impairment in children with FA (5,6). Based on the analysis of the results of 6 studies, it was concluded that children with multiple food allergies have a higher risk of impaired growth and may have a higher risk of inadequate nutrient intake than children without food allergies (7).

The recent analysis of more than 20 different studies regarding the growth of children with FA, conducted by Meyer et al. (2018), showed that these patients had lower growth indices compared to general population and control groups (8). Severity of the impairment had an inverse correlation with the number of eliminated food groups.

Another recent study involved 12 allergy centers and 430 patients (9). This survey showed that 6% of patients with FA were underweight, 9% were stunted and 8% were overweight. It also showed that cow's milk elimination resulted in lower weight-for-height Z-scores in comparison with Z-scores of the children with other foods elimination. Patients with non-IgE and mixed IgE and non-IgE mediated allergies had lower height-for-age Z-scores than patients with IgE-mediated CMA.

Furthermore, the role of the different factors, including elimination diet itself, is also a highly debatable topic. At the same time, there were no recent studies looking at this problem in Russian Federation. Thus, for the current study, the most problematic group of patients with severe AD and FA was chosen in order to assess the role of different factors that affect nutrition status of the patients.

Methods and Materials

The retrospective study included 210 children treated in Dermatology with the Laser Surgery department in the National Medical Research Center of Children's Health from January 2018 to February 2022.

Inclusion criteria were age of 0-17 years; confirmed severe atopic dermatitis (SCORAD index more than 50) and FA verified during the hospitalization or no more than six months before it. Children with non-allergic comorbidities that significantly impact nutritional status and feeding behavior were excluded from the study.

Growth indices were assessed with WHO AnthroPlus (20). Weight-for-age (WAZ), height-for-age (HAZ) and BMI-for-age (BAZ) z-scores were used to assess nutritional status. According to the national guidelines Z-scores from -1 to +1 were considered as normal. Children with HAZ <-2SD were considered stunted. Children with HAZ>+2SD were considered to have high height. Children with BAZ>+1SD were considered overweight and obese with BAZ>+2SD. BAZ from -2 to -3 was classified as wasting, from -3 and lower as severe wasting (10).

The Complete Blood Count was performed using Sysmex XN-1000 Hematology Analyzer (Sysmex Co., Japan). Total IgE level was evaluated with Cobas E411 Analyzer (Roche Diagnostics, Switzerland). Specific IgE levels were evaluated with ImmunoCAP 250 Analyzer (UniCAPSystem, ThermoFisherScientific) using indirect immunofluorescence technique. The ImmunoCAP 250 Analyzer limit of quantitation is 0.01 kU/L. Levels of serum vitamin D (25[OH]D) were evaluated. Serum 25[OH]D level was evaluated with Access 2 Immunoassay System Analyzer (Beckman Coulter LLC, USA). Level of 25[OH]D was considered insufficient in range of 20-29 ng/ml and deficient if was lower than 20 ng/ml.

The data was analyzed with IBM SPSS Statistics 26 (IBM SPSS Statistics for Windows, Version 26.0. Armonk, NY:IBM Corp.). The obtained data was tested for normality with the Shapiro-Wilk test. The majority of the samples came from a non-normal distribution. The median, 25-th and 75-th percentiles were calculated. Spearman's rank correlation coefficient were implemented. Correlation of r = 0-0.299 was considered weak, correlation of r = 0.3-0.699 - moderate, correlation of r = 0.7-1.0 - strong. For sets of categorical data comparison Pearson's chi-squared test and Fisher's exact test were implemented. The results were considered statistically significant with $p<0.05$.

Results

210 children were involved in the study, 107 of them were males (51.0%). The median age of children was 97 months (8 years 1 month). Cases of atopic diseases in family members were reported in 150 (71.4%) children. The median age at first reported atopic dermatitis symptoms was 3 months. All children had a history of an adverse reaction to different food groups. IgE-mediated FA was proved in 126 (60%) patients.

52 children had only AD as an allergy disease (24.8%). 67 children (31.9%) had a single atopic comorbidity: allergic rhinitis was in 10% of children, angioedema - in 3.8%, gastrointestinal symptoms of FA - in 8.6%. Two or more atopic comorbidities were diagnosed in 91 children (43.3%).

Before the admission to the clinic, hypoallergenic diets with the exclusion of particular food products were prescribed to most of the children, cow’s milk and products elimination was recommended to 48.4% of the patients. 86 of 97 (88.7%) children with verified CMA had 8 or more excluded food groups. Other common

eliminated food groups were hen's eggs fish, seafood, tree nuts and peanuts (fig. 1).

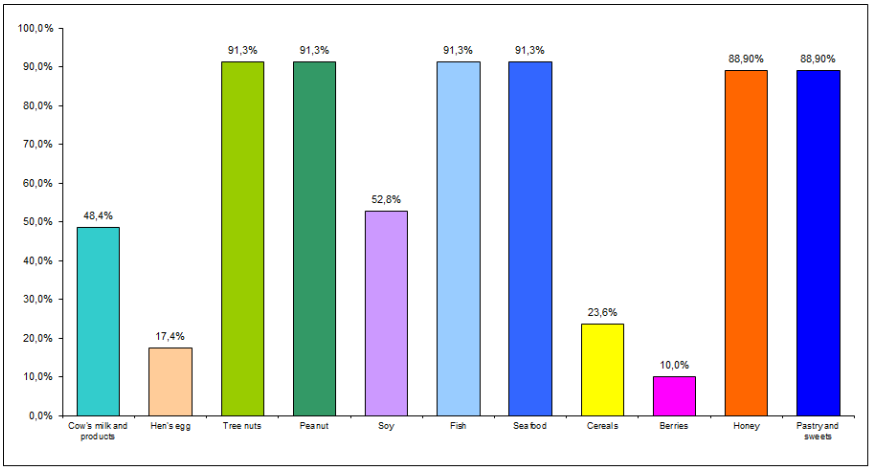

Figure 1. Frequency of exclusion of various food groups

199 children (94.7%) had a normal HAZ. 7 children (3.4%) had a HAZ > +2. 4 (1.9%) children were considered stunted, all of them were confirmed to have CMA. 8 (3.8%) patients had wasting and 2 (1%) had severe wasting. 27 (12.9%) children were overweight and 11 (5.2%) were obese (fig. 2).

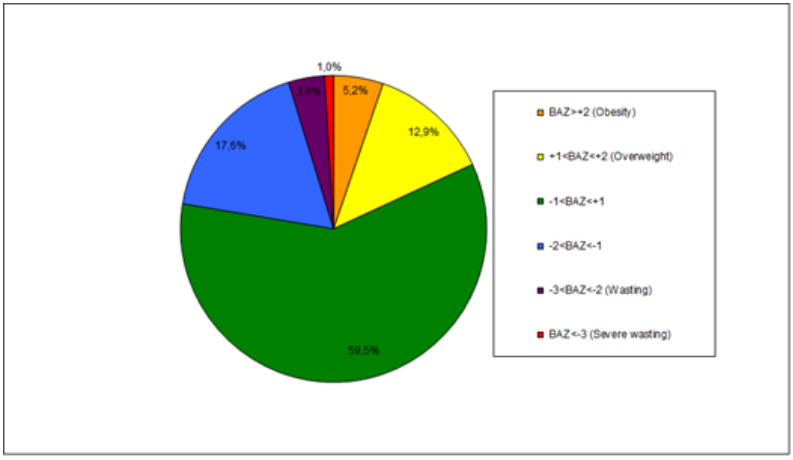

Figure 2. BAZ scores analysis

7 (70%) children with BAZ <-2 had 8 or more food groups excluded from the diet. 7 (87.5%) children with wasting and all children with severe wasting had IgE-mediated FA.

There was a statistically significant positive correlation between HAZ and age of children (r=0.32, p=0.02), a negative correlation between HAZ, BAZ and the number of excluded food groups (r=-1.32, p=0.029) and (r=-1.43, p=0.015), respectively (fig. 3). There was no correlation between HAZ, BAZ scores and adherence to the diet. There were no statistically significant differences between BAZ scores of children with and without dietitian consultation (p=0.45).

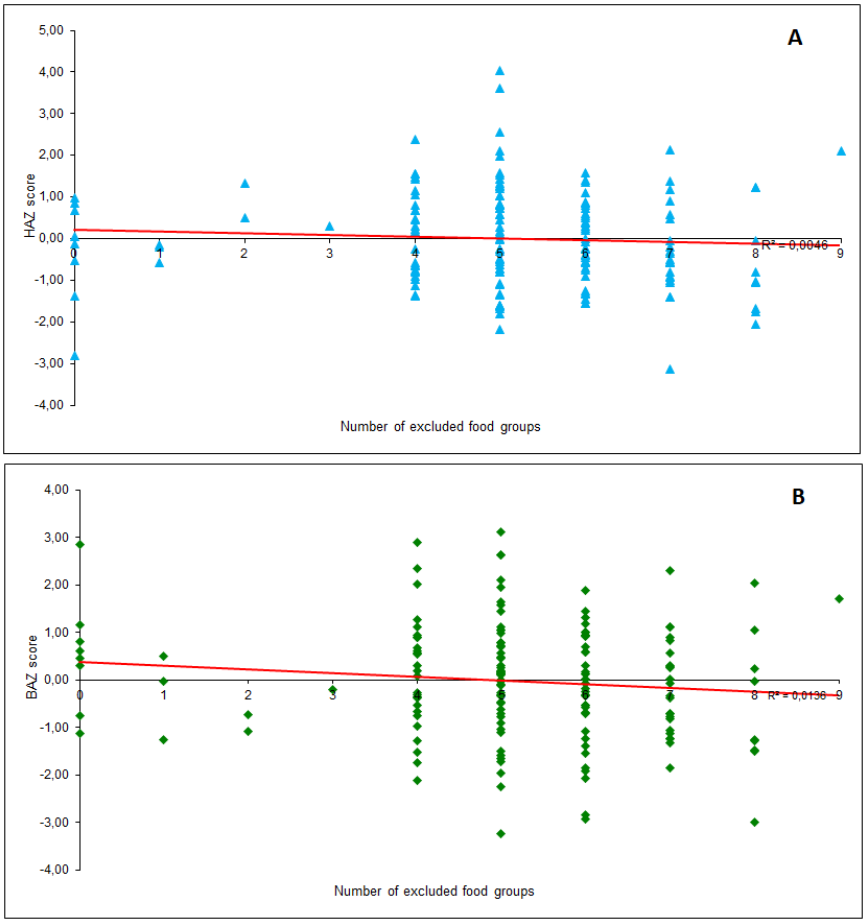

Figure 3. Correlation between HAZ (A), BAZ (B) and number of excluded food groups

Anemia was verified in 10 of 210 (4.8%) cases. 9 of 10 children with anemia had increased level of specific IgE and IgE-mediated FA. Total IgE levels were increased in 151 (71.9%) children. 49 (23.75%) children had serum vitamin D insufficiency and 94 (45.0%) - deficiency. A positive correlation was observed between BAZ scores and serum 25[OH]D levels (r=0.38, p=0.01). A negative correlation was indicated between hemoglobin levels and the number of excluded food groups (r=-0.12, p=0.045). No correlation between the number of excluded food groups and serum 25[OH]D levels (r=0.014) was found, as well as between BAZ scores and levels of hemoglobin (p=0.15) or total IgE (p=0.79). There was no correlation between BAZ scores of children with IgE and non-IgE mediated FA (p=0.53).

Discussion

In total antropometric indices of the patients with the severe AD and FA were lower than of the healthy children in Russian Federation. In the national cross-sectional study involving 2540 healthy children BMI from -1 to +1 had 60.6% of the 11 years old boys. In this group 5.4% of the boys had BMI less than -1, 15.5% were overweight and 18.6% were obese. For the 11 years old girls these numbers were 66%, 10.5%, 14.3% and 9.2%. In the group of 15 - years old children 63.6% of boys had BMI from -1 to +1, 8.5% had BMI less than -1, 11.5% were overweight and 10% were obese. For the girls these numbers were 67.1%, 8.9%, 18.6% and 3.6% (12). Although our study focused more on undernutrition and its potential consequences, the high numbers of overweight and obese children in the results attracted our attention as well. Surprisingly, frequency of the overweight and obesity is comparable with the results of the populational surveys. A significant number of children with severe AD and following the elimination diet had BAZ scores over +1. It is highly possible that this nutritional status deviation occurred due to imbalanced diet composition.

In the current study, we found a significant positive correlation between HAZ and age of children (r=0.32, p=0.02), a negative correlation between HAZ, BAZ and the number of excluded food groups (r=-1.32, p=0.029) and (r=-1.43, p=0.015), respectively. Furthermore, a negative correlation was indicated between hemoglobin levels and the number of excluded food groups (r=-0.12, p=0.045). Therefore, children with multiple food allergies require closer pediatrician attention and dietologist consultation.

Positive correlation was observed between BAZ scores and serum 25[OH]D levels (r=0.38, p=0.01). Moreover, 23.75% of children had serum vitamin D insufficiency and 45.0% had deficiency. According to the research results children with low level of 25[OH]D also had a higher predisposition for AD (13), while low level of 25[OH]D was associated with higher IgE levels and higher SCORAD indices (14). Lower 25[OH]D intake was also more common for children with

multiple food allergies than for those who were mono-allergic (15).

In addition, atopic comorbidities had no impact on nutritional status. These results are consistent with Boaventura et al. (2019) research (16).

There were no differences between BAZ scores in the children consulted and not consulted by dietitian before hospitalization. No difference in nutritional status of children with or without strict diet indicates the necessity of additional prospective research. We assume that the issue how the diet meets the nutritional requirements of a child are of great importance.

Overall, it is recommended to consult with dietitian/nutritionist for accurate diet correction and vitamin and mineral supplementation if there is a risk of child's growth impairment. It is important to start treatment of children with lowered growth indices as early as possible. For children at age 1 this means the right choosing of infant formula (17). In older patients diet correction is important as well.

References

1. Muraro A, Werfel T, Hoffmann-Sommergruber K, Roberts G, Beyer K, Bindslev-Jensen C, Cardona V, Dubois A, duToit G, Eigenmann P, Fernandez Rivas M, Halken S, Hickstein L, Høst A, Knol E, Lack G, Marchisotto MJ, Niggemann B, Nwaru BI, Papadopoulos NG, Poulsen LK, Santos AF, Skypala I, Schoepfer A, Van Ree R, Venter C, Worm M, Vlieg-Boerstra B, Panesar S, de Silva D, Soares-Weiser K, Sheikh A, Ballmer-Weber BK, Nilsson C, de Jong NW, Akdis CA; EAACI Food Allergy and Anaphylaxis Guidelines Group. EAACI food allergy and anaphylaxis guidelines: diagnosis and management of food allergy. Allergy. 2014 Aug;69(8):1008-25. doi: 10.1111/all.12429. Epub 2014 Jun 9. PMID: 24909706.

2. S.G. Makarova, A.A. Galimova, A.P. Fisenko, O.A. Ereshko, I.V. Zubkova, M.A. Snovskaya, T.R. Chumbadze, D.S. Yasakov, I.G. Gordeeva, O.V. Kozhevnikova. Markers of cow's milk allergy persistence: results of a 5-year follow-up. Pediatria named after G.N. Speransky2020; 99 (2): 88–95 DOI: 10.24110/0031-403X-2020-99-2-88-95

3. Savilahti EM, Savilahti E. Development of natural tolerance and induced desensitization in cow's milk allergy. Pediatr Allergy Immunol. 2013 Mar;24(2):114-21. doi: 10.1111/pai.12004

4. Schoemaker AA, Sprikkelman AB, Grimshaw KE, et al. Incidence and natural history of challenge-proven cow's milk allergy in European children--EuroPrevall birth cohort. Allergy. 2015;70(8):963-972. doi:10.1111/all.12630

5. Pavić I, Kolaček S: Growth of Children with Food Allergy. Horm Res Paediatr 2017;88:91-100. doi: 10.1159/000462973

6. Jhamnani RD, Levin S, Rasooly M, Stone KD, Milner JD, Nelson C, DiMaggio T, Jones N, Guerrerio AL, Frischmeyer-Guerrerio PA. Impact of food allergy on the growth of children with moderate-severe atopic dermatitis. J Allergy Clin Immunol. 2018 Apr;141(4):1526-1529.e4. doi: 10.1016/j.jaci.2017.11.056

7. Sova C, Feuling MB, Baumler M, Gleason L, Tam JS, Zafra H, Goday PS. Systematic review of nutrient intake and growth in children with multiple IgE-mediated food allergies. NutrClinPract. 2013 Dec;28(6):669-75. doi: 10.1177/0884533613505870

8. Meyer R, Wright K, Vieira MC, Chong KW, Chatchatee P, Vlieg-Boerstra BJ, Groetch M, Dominguez-Ortega G, Heath S, Lang A, Archibald-Durham L, Rao R, De Boer R, Assa'ad A, Trewella E, Venter C. International survey on growth indices and impacting factors in children with food allergies. J Hum Nutr Diet. 2019 Apr;32(2):175-184. doi: 10.1111/jhn.12610. Epub 2018 Nov 9. PMID: 30412327

9.Oren E, Banerji A, Camargo CA Jr. Vitamin D and atopic disorders in an obese population screened for vitamin D deficiency. J Allergy Clin Immunol. 2008 Feb;121(2):533-4. doi: 10.1016/j.jaci.2007.11.005

10. Training Course on Child Growth Assessment, WHO Child Growth Standards. C: Interpreting Growth Indicators, p 14.

https://www.who.int/childgrowth/training/module_c_interpreting_indicators.pdf

11. WHO AnthroPlus Software. https://www.who.int/tools/growth-reference-data-for-5to19-years/application-tools

12. Namazova-Baranova L.S., Yeletskaya K.A., Kaytukova E.V., Makarova S.G. Evaluation of the Physical Development of Children of Secondary School Age: an Analysis of the Results of a Cross-Sectional Study. Pediatric pharmacology. 2018;15(4):333-342.https://doi.org/10.15690/pf.v15i4.1948

13. Di Filippo P, Scaparrotta A, Rapino D, Cingolani A, Attanasi M, Petrosino MI, Chuang K, Di Pillo S, Chiarelli F. Vitamin D supplementation modulates the immune system and improves atopic dermatitis in children. Int Arch Allergy Immunol. 2015;166(2):91-6. doi: 10.1159/000371350

14. Wang SS, Hon KL, Kong AP, Pong HN, Wong GW, Leung TF. Vitamin D deficiency is associated with diagnosis and severity of childhood atopic dermatitis. Pediatr Allergy Immunol. 2014 Feb;25(1):30-5. doi: 10.1111/pai.12167

15. Baek JH, Shin YH, Chung IH, Kim HJ, Yoo EG, Yoon JW, Jee HM, Chang YE, Han MY. The link between serum vitamin D level, sensitization to food allergens, and the severity of atopic dermatitis in infancy. J Pediatr. 2014 Oct;165(4):849-54.e1. doi: 10.1016/j.jpeds.2014.06.058

16. Boaventura RM, Mendonça RB, Fonseca FA, Mallozi M, Souza FS, Sarni ROS. Nutritional status and food intake of children with cow's milk allergy. AllergolImmunopathol (Madr). 2019;47(6):544-550. doi:10.1016/j.aller.2019.03.003

17. Vanderhoof J, Moore N, de Boissieu D. Evaluation of an Amino Acid-Based Formula in Infants Not Responding to Extensively Hydrolyzed Protein Formula. J PediatrGastroenterolNutr. 2016 Nov;63(5):531-533. doi: 10.1097/MPG.0000000000001374].

DOI 10.34660/INF.2022.71.38.284

土壤氮和肥料在提高伏尔加河上游地区土壤轮作生产力中的作用
THE ROLE OF SOIL NITROGEN AND FERTILIZERS IN INCREASING THE PRODUCTIVITY OF CROP ROTATIONS ON THE SOILS OF THE UPPER VOLGA REGION

Okorkov Vladimir Vasilyevich
Doctor of Agricultural Sciences, Head Research Officer
Upper Volga Federal Agrarian Research Center

抽象的。在对 Vladimir opolye 灰色森林土壤的长期研究和伏尔加河上游地区黑灰-灰化土壤的短期试验的基础上，研究了肥料对土壤中硝酸盐和铵氮储量的含量和动态的影响。 .在以高阳离子交换容量 (CEC) 为特征的灰色森林土壤中，矿质肥料氮和牛粪对作物生产力的决定性作用通过早期 0-40 cm 土壤层中的硝酸盐和铵态氮的储量表现出来。作物植被的阶段。在这些土壤上，氮对作物营养的决定性作用属于硝酸盐氮。这是由于土壤向液相的 $N\text{-}NH_4$ 转变程度较低。在 7 轮作的第 3 轮和第 4 轮中，它分别在 1.4% 到 3.4% 和 0.6% 到 2.4% 之间变化。在CEC高的黑灰土上，鸡粪的后效不超过2.7%，作物产量还取决于0-40 cm土层N-NO3的储量。交换量和物理粘土的含量分别从 2.0 到 14.6 meq/100 g 土壤和 1.4 到 22.5% 不等，土壤向液相的 $N\text{-}NH_4$ 转变程度从 7.0 到 22、4%、随着阳离子交换容量和物理粘土含量的降低而增加。在这种情况下，要诊断土壤含氮量的有效性，应采用传统方法，即土壤中硝酸盐和铵态氮之和的含量。

关键词：伏尔加河上游地区的灰色森林和灰泥土，有机和矿物肥料，轮作和作物的生产力，硝酸盐和铵态氮。

Abstract. *Based on long-term studies on gray forest soils of the Vladimir opolye and short-term experiments on soddy-podzolic soils of the Upper Volga region, the effect of fertilizers on the content and dynamics of nitrate and ammonium nitrogen reserves in the soil was studied. On gray forest soils characterized by a high cation exchange capacity (CEC), the decisive role of mineral fertilizer nitrogen and cattle manure on crop productivity was manifested through the reserves of nitrate and ammonium nitrogen in the soil layer of 0–40 cm in the early stages of crop vegetation. On these soils, the decisive role in the nutrition of crops with nitrogen belongs to nitrate nitrogen. This is due to the low degree of* $N\text{-}NH_4$ *transition of the soil into the liquid phase. In the 3rd and 4th rotations of the 7-field crop rotation, it varied from 1.4 to 3.4 and from 0.6 to 2.4%, respectively. On soddy-podzolic soils with high CEC, it did not exceed 2.7% by the aftereffect of chicken manure,*

the crop yield was also determined by the reserves of N-NO_3 in the soil layer of 0-40 cm. On sandy and sandy loam sod-podzolic soils of Meschera, in which the capacity of cation exchange and the content of physical clay varied, from 2.0 to 14.6 meq/100 g of soil and from 1.4 to 22.5%, respectively, the degree of transition of N-NH_4 soil to the liquid phase ranged from 7.0 to 22.4%, increasing with a decrease in the capacity of cationic exchange and physical clay content. In this case, to diagnose the availability of soils with nitrogen, the traditional approach should be used, that is, the content of the sum of nitrate and ammonium nitrogen in the soil.

Keywords: *gray forest and soddy-podzolic soils of the Upper Volga region, organic and mineral fertilizers, productivity of crop rotations and crops, nitrate and ammonium nitrogen.*

On soddy-podzolic [1-3] and gray forest soils of the Vladimir opole [4], the decisive role of nitrogen fertilizers in increasing the productivity of cultivated field crops in various crop rotations was revealed. However, in some years, more favorable in terms of moisture, on light soddy-podzolic soils with the use of complete mineral fertilizer, a higher yield of field crops is observed than on the more fertile gray forest soils of Opole. According to the ideas developed in [5–6], this is due to differences in the nutrition of plants with mobile forms of nitrogen, which are formed during the transformation of organic and nitrogen mineral fertilizers, depending on the physicochemical properties of the soil (cation exchange capacity, mineralogical and granulometric composition). The studies were carried out on the soils of the Upper Volga region.

The Upper Volga region is an integral part of the Central Economic Region of Russia. It contains more than 30% of arable land. Its area is 4402.6 thousand ha, hayfields - 1445, pastures - 1354.2 thousand ha [1]. The region is dominated by soddy-podzolic soils.

The soddy-podzolic soils of the Upper Volga region have a highly variable acidity (pH_{KCl} 4.0–6.0), and the subsurface horizons have a high content of exchangeable aluminum. The degree of saturation with bases is 43-75%, the humus content varies within 0.8-1.8%. They are insufficiently provided with mobile compounds of nitrogen and phosphorus, exchangeable potassium and available forms of microelements.

According to the degree of podzolization, strongly podzolic soils predominate (42%). The basis of increasing their fertility is chemical reclamation and the use of fertilizers. The granulometric composition is represented by medium (30%) and light (25%) loams, as well as sandy loams (34%), which are convenient for processing. The remaining areas are approximately half occupied by sandy and heavy loamy soils.

Among the typical podzolic soils in the Upper Volga region, there are islands of dark-colored soils, similar in their characteristics to zonal gray forest soils, the so-called "opoly" soils. They occupy an area of 830 thousand hectares, including 305 thousand hectares of arable land (6.9% of the region). This unique natural formation makes up a significant part of the arable land (33%) of the Vladimir Oblast [4,7]. In recent years, they receive more than 70% of gross agricultural output. They occur as individual inclusions in the Ivanovo and Yaroslavl Oblasts [1].

Plowed gray forest soils have a significant cultivated horizon (25-30 cm), a higher humus content (2.3-4.5%), lower acidity (pH_{KCl} 5.2-6.5). They are often rich in carbonates and are characterized by a high degree of saturation with bases (75-95%), and are also better supplied with nitrogen and ash elements [7]. Throughout the soil profile, they lack exchangeable aluminum in amounts toxic to the root systems of cultivated crops [8, 9]. Due to the peculiarities of the mineralogical composition [4] and the higher content of humus (compared to soddy-podzolic soils), gray forest soils have an absorption capacity of 15–33 meq/100 g of soil. On these soils, detailed studies have been carried out on the effect of the content and reserves of ammonium and nitrate forms of nitrogen in the soil on the productivity of cultivated crops.

Stationary experiment was established in 1991-1993. In the 1st and 2nd rotations, the alternation of crops is as follows: 1) busy fallow (vetch-oat mixture); 2) winter rye; 3) potatoes; 4) oats with overseeding of grasses; 5) herbs of the 1st year of use; 6) grasses of the 2nd year of use: 7) winter rye (spring wheat); 8) barley [4].

In the busy steam of the 1st rotation, liming was carried out according to the total hydrolytic acidity. Against this background, we studied the effect of various doses of cattle bedding manure (0, 40, 60, and 80 t/ha) applied under winter rye after harvesting the occupied fallow, and mineral fertilizers, their combination on the agrochemical and physicochemical properties of gray forest soils. In the 2nd to 4th rotation, studies were carried out on the aftereffect of liming.

In an 8-field crop rotation (1st and 2nd rotations), P40K40 and N40P40K40 (single dose of NPK) fertilizers were applied for cereals, annual and perennial grasses, and P60K80 and N60P60K80 (single dose) for potatoes, double doses of NPK. Under the herbs of the 1st year of use, N40P80K80 was used as a double dose of NPK in all rotations.

In the 7-field crop rotation of the 3rd and 4th rotations, tilled crops were excluded, P40K40 and N40P40K40 (single dose), N80P80K80 (double dose) were applied for cereals and grasses of the 2nd year of use.

An analysis of data on the productivity of crops in 8- and 7-field crop rotations (tab. 1) showed that liming had little effect on this parameter on weakly acidic gray forest soils. This is explained by the absence of exchangeable aluminum in the control over the entire meter layer of these soils in amounts toxic to the root

systems of cultivated crops. It ensured their spread to deeper moist soil layers when the upper ones dried up.

Table 1.

Influence of fertilizer systems on the average productivity of crops in 8- and 7-field crop rotations on gray forest soils of the Vladimir opolye, c/ha g.u.

Option	1st rotation of 8-field crop rotation, 1991-2000	2nd rotation of 8-field crop rotation, 1999-2008	3rd rotation of 7-field crop rotation, 2007-2015	4th rotation of the 7-field crop rotation, 2014-2020 (field 1)
1.Control	29,0	32,9	30,8	34,6
2.Liming background	29,3	30,9	30,2	34,8
3.Background + PK	31,4	33,8	33,5	37,4
4.Background + NPK	36,4	39,6	39,7	43,1
5.Background + 2 NPK	40,0	41,6	42,6	45,3
6.Background + manure 40 t/ha (M40)	31,8	34,9	33,8	39,1
7.Background + manure 60 t/ha	34,1	35,8	35,0	39,9
8. Background + manure 80 t/ha	33,5	35,8	35,3	40,6
9.Background + M40 + PK	32,4	36,0	35,6	39,9
10.Background + M40 + NPK	38,8	40,7	40,9	45,1
11. Background + M40 + 2NPK	42,2	42,2	43,0	47,0
12. Background + M60 + PK	33,4	36,4	36,3	40,6
13. Background + M60 + NPK	39,0	42,0	41,0	46,5
14. Background + M60 + 2NPK	41,3	42,0	44,0	46,7
15. Background + M80 + PK	34,0	37,8	37,1	42,0
16. Background + M80 + NPK	40,3	41,9	41,4	46,7
17. Background + M80 + 2NPK	41,5	43,3	45,5	47,7
HCP_{05}, c/ha g.u.	2,8	4,3	3,4	2,9

The average annual productivity of an 8-field grain-grass-row crop rotation by 89.1-94.7% and a 7-field grain-grass crop rotation by 92-93% was determined by the use of nitrogen mineral fertilizers and cattle manure (tab. 2). Participation in the dependencies of phosphorus-potassium fertilizers increased the tightness of the relationship by 4.3-7.4%.

Since the decisive influence on the productivity of crop rotations on gray forest soils of the Upper Volga region was exerted by the use of nitrogen, mineral fertilizers and manure, in tab. 3 shows the average annual dynamics of nitrate and ammonium nitrogen under crops of a 7-field crop rotation.

By the 1st observation period, the applied nitrogen mineral fertilizers were transformed into nitrates, nitrogen from soil organic matter (humus, plant residues) and organic fertilizers into ammonia and nitrate forms. Therefore, the stocks of the latter during this period were usually maximum. By the middle of the growing season, the reserves of $N\text{-}NO_3$ decreased due to intensive absorption by plants, by the harvesting of crops they slightly increased, and in dry years they could decrease.

Table 2.

Mathematical dependencies on the effect of fertilizers on the average productivity of crop rotations, c/ha g.u. (against the background of liming)

Rotation, years of study	Relationship equation, n = 16	R^2
1-st, 1991-2000	$У = 31,0 + 0,313\ x_1 + 0,114\ x_2$	0,947
	$У = 30,7 + 0,313\ x_1 + 0,184\ x_2 – 0,0009x_2^2$	0,971
2-nd, 1999-2008	$У = 33,6 + 0,324\ x_1 + 0,0895\ x_2$	0,891
	$У=32,5+0,324\ x_1+0,173x_2+0,041x_3-0,0014x_2^2$	0,965
	$У = 33,4 + 0,324\ x_1 + 0,175\ x_2 – 0,0011\ x_2^2$	0,939
3-rd, 2007-2015	$У = 33,1 + 0,256\ x_1 + 0,122\ x_2$	0,929
	$У=31,9+0,256x_1+0,180\ x_2+0,060x_3-0,0014x_2^2$	0,972
4-th, 2014-2020	$У = 37,2 + 0,360x_1 + 0,107x_2$	0,920
	$У = 36,3 + 0,360x_1 + 0,199x_2 + 0,040x_3 – 0,0017x_2^2$	0,974

Notes: У – average per rotation crop rotation productivity, c/ha g.u.; x_1 – annual average dose of manure application in crop rotation, t/ha; x_2 – annual average dose of nitrogen N_{aa}, kg/ha; x_3 – annual average dose of application of PK fertilizers in terms of P_2O_5, kg/ha. In 1 ton of manure, the nitrogen content varied from 4.2 to 4.6 kg.

Table 3.

Influence of fertilizer systems on the dynamics of the average annual reserves of N-NO_3 and N-NH_4 in the soil layer of 0-40 cm under crops of a 7-field crop rotation for 2007-2015, kg/ha

Option	Seedlings or resumption of vegetation (1st term)		Heading and budding (2nd term)		After cleaning		Decrease in stocks in the 2nd term compared to the 1st			
							kg/ha		%	
	N-NO_3	N-NH_4	N-NO_3	N-NH_4	N-NO_3	N-NH_4	ΔN-NO_3	ΔN-NH_4	ΔN-NO_3	ΔN-NH_4
1.Control	42,2	98,1	18,1	84,3	25,6	97,9	24,1	13,8	57	14,1
2.Liming background	42,4	98,2	19,8	84,8	28,7	102	22,8	13,4	54	13,6
3.Background + PK	44,1	96,0	18,9	83,2	28,7	98,9	25,1	12,8	57	13,3
4.Background + NPK	90,0	107,3	28,7	98,9	37,8	104	61,3	8,0	68	7,5
5.Background + 2 NPK	123	118,2	44,8	107	52,3	109	78,2	11,4	64	10,7
6.Background + manure 40 t/ha (M40)	46,5	103,5	20,6	92,2	31,2	98,8	26,0	11,3	56	10,9
7.Background + manure 60 t/ha	50,6	105,9	22,3	91,7	34,1	106	28,3	14,2	56	13,4
8. Background+ manure 80 t/ha	51,3	104,6	19,9	90,6	33,8	98,5	31,5	14,0	61	13,4
9.Background + M40 + PK	47,1	109,0	19,4	95,9	27,8	100	27,7	13,1	59	12,0
10.Background + M40 + NPK	97,5	114,1	33,0	92,1	39,9	104	64,5	20,0	66	17,5
11. Background + M40 + 2NPK	144	122,6	46,9	92,4	57,0	109	97,1	30,2	67	24,6
12. Background + M60 + PK	51,0	110,5	20,8	94,2	33,7	108	30,2	16,3	59	14,8
13. Background + M60 + NPK	101	114,9	35,3	89,8	41,1	111	65,7	25,1	65	21,8
14. Background + M60 + 2NPK	150	136,0	48,3	106	53,9	118	102	30,5	68	22,4

15. Background + M80 + PK	56,8	102,3	23,9	82,1	33,7	112	32,9	20,2	58	19,8
16. Background + M80 + NPK	111	115,9	33,4	93,3	43,7	117	77,6	22,6	70	19,5
17. Background + M80 + 2NPK	160	126,9	50,6	93,8	57,9	113	109	33,1	68	26,1

It can be seen that when using nitrogen mineral fertilizers (ammonium nitrate), the reserves of nitrate nitrogen in the 1st observation period in the soil layer 0-40 cm increased from 42.2 (control) up to 90-160 kg/ha, while the reserves of ammonium nitrogen varied within small limits (98.1 and 96-136 kg/ha, respectively). In the variants fertilized with nitrogen, the absorption of $N\text{-}NO_3$ (decrease in their reserves in the 2nd period compared to the 1st in kg/ha) in the responsible phases was 2.5-3.4 times higher than $N\text{-}NH_4$. Obviously, they played a decisive role in increasing the productivity of crop rotation, since they were completely in the liquid phase. Ammonium ions on soils with a high cation exchange capacity passed into the liquid phase in small amounts. The coefficient of use for the 1st half of the growing season of crops of $N\text{-}NO_3$ reserves in the soil layer of 0-40 cm varied from 54 to 70%, and $N\text{-}NH_4$ reserves - from 7.5 to 26.1%. The sum of reserves of $N\text{-}NO_3$ and $N\text{-}NH_4$ in the liquid phase of the soil during the period of germination or renewal of vegetation of crops was called the mobile fund (MF) of nitrogen [4]. The basis of the mobile nitrogen fund was the reserves of the nitrate form. The MF value of nitrogen is determined by the nitrogen mobilization pool, which is proportional to the average annual dose of applied nitrogen mineral fertilizers and part of the nitrogen supplied with organic fertilizers and due to symbiotic nitrogen fixation. Between the annual average productivity of crop rotation, on the one hand, nitrogen MF and the average annual reserves of $N\text{-}NO_3$ in the soil layer of 0-40 cm in the early period of crop vegetation, on the other hand, a close power-law or hyperbolic relationship was revealed [4,5].

Differences in the use of $N\text{-}NO_3$ and $N\text{-}NH_4$ reserves for the specified period are due to the complete presence of nitrate nitrogen in the liquid phase of the soil, and ammonium - partial. For the 1st-4th rotation, the reserves of $N\text{-}NO_3$ in the soil layer of 0-40 cm in the early period of crop vegetation and their changes by the middle of it were of the same type. However, the reserves of $N\text{-}NH_4$ in the 0-40 cm layer of soil in the 1st observation period, compared with the 1st and 2nd rotations, decreased in the 3rd rotation by 1.58-1.77 times, and in the 4th – 3-4 times (tab. 4).

In the liquid phase (soil:water ratio 1:1) in the 1st and 2nd rotations, the size of the transition of $N\text{-}NH_4$ soil in a layer of 0-20 cm varied from 3.3 to 5.4%, in the 3rd - from 1.4 to 3.5, and in the 4th - from 0.6 to 2.4% (tab. 5). The decrease in both $N\text{-}NH_4$ reserves in the soil (by 3-4 times) and the share of their transition

to the liquid phase in the 4th rotation compared to the 1st and 2nd rotations confirmed the weak role of ammonium nitrogen and the determining role of $N\text{-}NO_3$ in the nutrition of cultivated crops when using scientifically based doses of nitrogen fertilizers (tab. 4 and 5).

The high bond strength of ammonium ions of SAC (with a high cation exchange capacity) led to the decisive role of $N\text{-}NO_3$ reserves on the productivity of cultivated crops and crop rotations, high agronomic efficiency of mineral and organomineral fertilizer systems compared to organic. This was associated with a faster transformation of the nitrogen of the applied mineral fertilizers into the nitrate form in the early periods of crop vegetation than organic nitrogen (tab. 6).

Table 4.

Influence of fertilizer systems on the average annual stocks of $N\text{-}NH_4$ in the soil layer of 0-40 cm by rotation of crop rotations in the early periods of crop vegetation for 1992-2020, kg/ha

Option	Seedlings or resumption of vegetation (1st term)		
	1st and 2nd rotations for 1992-2008	3rd rotation for 2007-2015	4th rotation for 2014-2020
1.Control	178	98,1	42,0
2.Liming background	174	98,2	46,7
3.Background + PK	182	96,0	46,4
4.Background + NPK	185	107	51,1
5.Background + 2 NPK	194	118	54,9
6.Background + manure 40 t/ha (M40)	184	104	44,1
7.Background + manure 60 t/ha	188	106	50,5
8. Background + manure 80 t/ha	189	105	48,8
9.Background + M40 + PK	180	109	48,6
10.Background + M40 + NPK	186	114	52,4
11. Background + M40 + 2NPK	191	123	63,2
12. Background + M60 + PK	190	110	46,2
13. Background + M60 + NPK	187	115	54,3
14. Background + M60 + 2NPK	192	136	64,0
15. Background + M80 + PK	182	102	53,1
16. Background + M80 + NPK	186	116	57,5
17. Background + M80 + 2NPK	201	127	61,7

Table 5.

The share of the transition of soil ammonium nitrogen into the liquid phase in the soil layer of 0-20 cm in the years of research on crop rotations,%

Option	2-nd rotation, 2007	3-rd rotation, 2013-2014	4-th rotation, 2020
1.Control	4,32	2,2	0,71
2.Liming background	5,45	3,2	1,02
3.Background + PK	3,66	2,0	0,94
4.Background + NPK	4,15	2,3	1,41
5.Background + 2 NPK	3,73	3,3	1,84
6.Background + manure 40 t/ha (M40)	4,31	2,2	0,59
7.Background + manure 60 t/ha	3,91	1,7	1,05
8. Background + manure 80 t/ha	4,69	2,4	0,58
9.Background + M40 + PK	4,80	1,6	0,58
10.Background + M40 + NPK	4,64	1,4	1,98
11. Background + M40 + 2NPK	5,03	2,6	1,62
12. Background + M60 + PK	3,28	2,1	1,38
13. Background + M60 + NPK	4,63	2,4	1,28
14. Background + M60 + 2NPK	6,08	3,5	2,20
15. Background + M80 + PK	5,62	1,9	1,76
16. Background + M80 + NPK	4,17	3,4	1,70
17. Background + M80 + 2NPK	5,26	3,3	2,36
Average	4,66	**2,5**	1,35

Table 6.

Mathematical dependences on the relationship of average annual doses of nitrogen applied by organic (x_1, kg/ha) and mineral (x_2, kg/ha) fertilizers with reserves of nitrate nitrogen in the soil layer of 0-40 cm in the early growing season of field crops (y, kg/ha)

Rotation of crop rotations, years of research	**Relationship equation, n = 17**	**R^2**
1-st and 2-nd, 1992-2008	$У = 44,7 + 0,18\ x_1 + 1,26\ x_2$	0,996
	$У = 45,1 + 1,26\ x_2 + 0,0045 x_1^2$	0,997
3-rd, 2007-2015	$У = 38,2 + 0,351\ x_1 + 1,274\ x_2$	0,987
	$У = 41,8 + 0,186 x_1 + 0,981 x_2 + 0,0023 x_3^2 + 0,0063 x_1 x_2$	0,998
4-tf, 2014-2020	$У = 42,4 + 0,39 x_1 + 1,30\ x_2$	0,994
	$У = 42,9 + 0,39\ x_1 + 1,06\ x_2 + 0,0034\ x_2^2$	0,996
	$У = 44,7 + 1,072\ x_2 + 0,0079\ x_1^2 + 0,0033\ x_2^2$	0,996

It has been established that 1 kg of nitrogen of applied organic fertilizers in the soil layer of 0-40 cm in the 1st and 2nd rotations in the early growing season of crops ensured the accumulation of 0.18 kg of nitrate nitrogen, and 1 kg of mineral nitrogen - 1.26 kg. In the 3rd and 4th rotations of crop rotation, the accumulation of nitrate nitrogen from 1 kg of manure nitrogen increased from 0.18 to 0.35 and 0.39 kg, 1 kg of ammonium nitrate nitrogen - from 1.26 to 1.27 and 1.30 kg.

The lower $N\text{-}NO_3$ accumulation in the 1st and 2nd rotations of the crop rotation from 1 kg of nitrogen of organic fertilizers is due to the fact that the content and reserves of $N\text{-}NH_4$ in the soil were higher (174-201 kg/ha) than in 3 th (96-136 kg/ha) and 4th (45-62 kg/ha) rotations (tab. 4). Accordingly, in the 1st and 2nd rotations, the sizes of $N\text{-}NH_4$ transition to the liquid phase were also higher (tab. 5). This led to their active nitrification to the detriment of its flow during the transformation of organic fertilizers. In part, this was facilitated by a change in climatic conditions towards warming.

In the 3rd and 4th rotations on gray forest soils, on average, for a rotation of a 7-field crop rotation in the early period of vegetation of crops in a soil layer of 0-40 cm, when using 1 kg of ammonium nitrate nitrogen, 1.27-1.30 kg of nitrate nitrogen is formed, and 1 kg of nitrogen of organic fertilizers - 0.35 ... 0.39 kg of $N\text{-}NO_3$. Since half of the nitrogen in the ammonium nitrate itself is represented by nitrate, the other half by ammonium nitrogen, the efficiency of manure nitrogen compared to ammonium nitrate nitrogen will be: $\frac{0,35}{0,64} ... \frac{0,39}{0,65}$, or 0.55 ... 0.60.

And on soddy-weakly podzolic light and medium loamy soils of the Yaroslavl Oblast, characterized by hydromicaceous mineralogical composition of silt and high cation exchange capacity of 14-24 meq/100 g of soil, according to the action of chicken manure (CM), the content of ammonium nitrogen in the layer of 0-40 cm increased to 4-6 mg/100 g, and the degree of its transition into the liquid phase - up to 8-22.5%. Already by the aftereffect of CM, these parameters decreased to 1.46–1.76 mg/100 g of soil and to 2.5–2.7%. According to the aftereffect of CM, the yield of cultivated crops was determined by the reserves of nitrate nitrogen in the soil layer of 0–40 cm [10].

On light soddy-podzolic soils of Meshchera, in which the cation exchange capacity and the content of physical clay varied from 2.0 to 14.6 meq/100 g of soil and from 1.4 to 22.5%, respectively, the degree of $N\text{-}NH_4$ transition of soil into the liquid phase increased with a decrease in both parameters ($r^2 = 0.907$), varying from 7.0 to 22.4% [5.11]. Obviously, on such soils, the role of $N\text{-}NH_4$ in the nutrition of cultivated crops increases sharply; when diagnosing soil nitrogen supply, one can use the traditional approach, that is, the content of the sum of nitrate and ammonium nitrogen in the soil.

Thus, on soils with a high cation exchange capacity, in the early periods of vegetation of crops, the nitrogen of the applied mineral fertilizers is much faster transformed into the nitrate form than the nitrogen of the bedding manure. This predetermines a higher productivity of crop rotations with mineral and organomineral fertilizer systems compared to organic. To diagnose the nitrogen nutrition of plants, it is necessary to use the content or reserves of nitrate nitrogen in the early periods of crop vegetation.

References

1. Nenaydenko G.N. Rational use of fertilizers in a market economy. – Ivanovo, 2007. 350 P.

2. Sychev V.G., Shafran S.A. Agrochemical properties of soils and efficiency of mineral fertilizers. - M.: VNIIA, 2013. 296 P.

3. Lukin S.M. Long-term stationary field experiments with organic fertilizers: the significance, results and prospects of research on soddy-podzolic soils / Proceedings of the International Scientific Conference dedicated to the 90th anniversary of the FSBSI "ARRI of Agrochemistry" and the 80th anniversary of the Geographical Network of Experiments with Fertilizers (December 1-2, 2021.). Ed. S.I. Shkurkin. – M.: VNII agrochemistry, 2022. P. 107-116.

4. Okorkov V.V., Fenova O.A., Okorkova L.A. Techniques for the integrated use of chemicals in crop rotation on gray forest soils of the Upper Volga region in agricultural technologies of various intensity. Suzdal, 2017. 176 P.

5. Okorkov V.V., Fenova O.A., Okorkova L.A. Gray forest soils of the Vladimir opolye and the efficiency of using their resource potential. Ivanovo: PresSto, 2021. 188 P.

6. Okorkov V.V. To the question of the equivalence of plant nutrition with nitrate and ammonium nitrogen // Agrochemistry. 2021. № 12. P. 3-14.

7. Farming system of Vladimir Oblast. - Vladimir: Publishing House of the ARAAS NZ RSFSR, 1983. 341 P.

8. Liming of acidic soils / Ed. N.S. Avdonina, A.V. Petersburg, S.G. Shederova. - M.: Kolos, 1976. 304 P.

9. Okorkov V.V. On the theory of chemical melioration of acidic soils // Agrochemistry. № 9. 2019. P. 3-17.

10. Okorkov V.V., Okorkova L.A., Shchukin N.N. Chicken droppings influence on sod-podzolic soil fertility change studying experience // In the scientific collection IOP Conference Series: Earth and Environmental Science. Series «Advances in Science for Agriculture «Achievements of Science for the Agro-Industrial Complex». 2021. P. 012062. Nemchinovka. https//iopscience.iop.org/issue/1755-1315/843/1.

11. Okorkov V.V. Differences in the use of nitrate and ammonium soil nitrogen by plants // Problems and questions of modern science. Peer-reviewed collection of scientific papers. June 2019 № 2(3). Part 1. Ed. Research and Publishing Center of the International United Academy of Sciences (RPC IUAS). 2019. P. 66-76.

DOI 10.34660/INF.2022.71.13.285
UDC 636.32 /.38. 033

卡拉柴羊去势对肉制品定量和定性指标的影响

THE EFFECT OF CASTRATION OF KARACHAI SHEEP ON QUANTITATIVE AND QUALITATIVE INDICATORS OF MEAT PRODUCTS

Gabaev Musa Sultanovich
Candidate of Agricultural Sciences.
Institute of Agriculture
Kabardino-Balkarian Scientific Center of the Russian Academy of Sciences
Nalchik, Russia

抽象的。 在卡巴尔达-巴尔卡尔共和国（KBR）山肉粗毛羊养殖中，对卡拉恰伊公羊去势对肉制品定量和定性指标的影响进行了研究。

获得的结果表明，在公羊去势中，由于性腺激素功能的破坏（停止），新陈代谢水平降低，肌肉和骨骼组织的生长减慢。 各个年龄阶段的去势公羊（valushki）在活重、屠宰产量、一级切割产量、蛋白质质量指标方面均低于公羊。 与此同时，在去势公羊中，脂肪沉积的过程在较早的年龄就可以观察到。

关键词：山羊育种，卡拉柴品种，公羊，去势，肉产量，质量指标。

Abstract. *Studies have been carried out on the effect of castration of Karachay rams on the quantitative and qualitative indicators of meat products in the mountain meat coarse-wool sheep breeding of the Kabardino-Balkarian Republic (KBR).*

The results obtained indicate that in rams-castrates, due to a violation (cessation) of the hormonal function of the gonads, the level of metabolism decreases, and the growth of muscle and bone tissues slows down. Castrated rams (valushki) in all age periods were inferior to rams in terms of live weight, slaughter yield, grade I cut yield, protein quality indicator. Along with this, in castrated rams, the process of fat deposition is observed at an earlier age.

Keywords*: mountain sheep breeding, Karachai breed, rams, castration, meat productivity, quality indicators.*

Introduction

At this stage of development, the breeding of local coarse-haired sheep of the Karachay breed of the meat-wool-milk direction of productivity is the basis of

sheep breeding in the KBR mountain zone [1].

At the same time, one of the important tasks is the development of methods for the effective use of the existing gene pool against the background of the use of reserves of scientifically based organization of production processes, with the effective pasture use of cheap natural phytocenosis of mountain meadows.

Podkorytov A.T., Podkorytov A.A., Podkorytov N.A. (2013) argue that in modern conditions of a market economy, the main task of improving sheep breeding is the development of breeding and technological methods for increasing the genetic potential of meat productivity of sheep, its solution depends on many factors: genotype, methods of selection and breeding work, keeping technology [2].

At present, the most promising solution for increasing the production of lamb, increasing the profitability and competitiveness of sheep breeding in KBR is the organization of intensive rearing and feeding of young animals on natural mountain pastures, followed by sale for slaughter in the year of birth [3].

The use of biological capabilities of Karachai sheep in breeding and breeding work to increase meat productivity in accordance with their productivity in specific economic and climatic conditions of year-round mountain pasture maintenance is the most promising [4].

But along with this, when growing young animals, unacceptable technologies are used, over-repair rams, in the vast majority of farms, are castrated at the age of 2-3 weeks, which negatively affects the breeding process. The selection of a limited number of replacement rams is carried out only by origin, in connection with this, there is a high probability that animals with a high genetic potential for productivity and high adaptability to the harsh conditions of the highlands, not evaluated by their own productivity, will be eliminated from the breeding process, which hinders the selection, effective use of the existing gene pool, leads to a decrease in the realization of the genetic potential of their feeding capacity.

Many years of experience and analysis of scientific research gives grounds to assert that in mountain meat coarse-wool sheep breeding, even with the most careful selection of animals from parents with high productivity, there is no certainty that their offspring will be as highly productive. The level of meat productivity of young sheep is determined by genetic and paratypic factors. In this case, it must be taken into account that the factor of adaptation to the harsh conditions of the mountainous zone, with a sharply rugged relief and high humidity and rockiness, plays a significant role against the background of the preservation and manifestation of genetically incorporated high productive qualities. Along with this, due to the fact that sires come from different parents and have unequal heredity, the offspring of highly productive sires mated with identical queens often differ significantly in their productive qualities.

Purpose of research

To establish the effect of castration of lambs of sheep of the Karachay breed on the dynamics of live weight and quality indicators.

Material and methods of research

The studies were carried out in the breeding reproducer of sheep of the Karachay breed LLC "Dargan" of the Cherek district, the mountainous zone of KBR.

The material for the research was lambs of sheep of the Karachay breed, 3 groups of March lambing were formed, 25 heads each: I - rams, II - valushki (rams were castrated at 2 weeks of age), III - yarovka.

All experimental lambs were kept together until the end of the study, in one flock, before being driven to mountain pastures, the level of feeding and maintenance were identical. On mountain alpine pastures, mother's milk and pasture grass served as the main source of nutrition, additional mineral supplements and table salt were received.

Weaning was carried out at 4 months of age. During the period of weaning and after fattening on mountain pastures at 6 and 8 months of age, a control slaughter was carried out according to the method of VIZh (1978) on three heads typical for each group, with the determination of the varietal composition of carcasses, the chemical composition of the average sample of minced meat, the content of tryptophan and hydroxyproline in longissimus dorsi muscle.

The productivity of experimental animals was determined according to GOST 25955-83, the quality indicators of carcasses - in accordance with the requirements of GOST 7596-81 and RF GOST 32605-2013. Mince chemical composition was determined according to GOST 25011-81, GOST R 53642-2009, GOST R 51479-99, GOST 23042-86. The content of tryptophan and hydroxyproline in the long back muscle was determined on an amino acid analyzer brand AAA 339M (Czech Republic).

Equipment and technical means

Electronic floor scales MIDL MP "Live weight U 12" (1000 VEDA F-1 (200/500; 2000x1200) ("Middle", Russia), platform scales MP 150 VDA F-3 (20/50; 450x600) "Red Army T" ("Middle", Russia).

Statistical processing

The resulting digital material was processed using the methods of variation statistics (Plokhinsky N.A., 1970) on PC according to A.P. Pyzhov (1988), "Microsoft Office" software package, "Excel" program (Microsoft, USA).

Research results

An analysis of the dynamics of the live weight of the experimental young animals showed that sexual dimorphism in sheep is laid in the embryonic period and manifests itself at birth, newborn ewes (III gr.) were inferior in live weight to lambs of groups I and II by 0.3 kg (8.3%) (tab. 1).

Table 1.

The dynamics of the live weight of the experimental young animals, kg.

Age, months	Group					
	I		II		III	
	X ± Sx	Cv	X ± Sx	Cv	X ± Sx	Cv
At birth	3.9±0.29	13.27	3.9±0.35	13.34	3.6±0.11	11.26
2	16.2±0.37	9.78	15.8±0.45	11.14	13.9±0.38	10.07
4	27.8±0.33*	7.35	26.2±0.64	10.39	24.9±0.51	8.98
6	35.9±0.52**	8.18	32.4±0.41	8.82	30.2±0.45	9.54
8	41.6±0.48**	8.92	37.2±0.57	9.11	34.4±0.62	8.79

Note (hereinafter): * – P≤0,05; ** – P≤0,01; *** – P≤0,001.

Differences are shown when comparing group I relative to groups II and III.

In terms of live weight, rams, starting from birth, occupied a leading position. Intergroup differences in live weight of young animals at 2, 4, 6 and 8 months of age showed that the rank of distribution of animals did not change, and intergroup differences in absolute values became more significant. Thus, rams surpassed valushki in the studied trait: at 2 months - by 0.4 kg (2.5%), 4 months - by 1.6 kg (6.1%), 6 months - 3.5 kg (10.8%) and at 8 months - by 4.4 kg (11.8%).

A comparative analysis of the slaughter qualities of experimental animals showed that castration of rams at an early age leads to a slowdown in the intensity of live weight growth, relatively earlier brining and a decrease in carcass weight due to changes in the hormonal status of the body (tab. 2).

Table 2.

The influence of gender and age on the slaughter qualities of young sheep, X ± Sx

Index	Group		
	I	II	III
4 months			
Number of heads, n	3	3	3
Pre-slaughter weight, kg	27.8±0.33	26.2±0.64	24.9±0.51
Carcass weight, kg	13.5±0.35	12.9±0.33	11.7±0.42
Incl. fat tail weight, kg	0.9±0.06	0.7±0.05	0.6±0.05
Weight of internal fat, kg	0.3±0.02	0.3±0.01	0.3±0.01
Slaughter weight, kg	13.8±0.38	12.8±0.34	11.7±0.29
Slaughter yield, %	49.6	49.0	47.1

6 months			
Number of heads, n	3	3	3
Pre-slaughter weight, kg	35.9±0.52	32.4±0.41	30.2±0.45
Carcass weight, kg	17.7±0.39**	15.4±0.44	14.0±0.37
Incl. fat tail weight, kg	1.5±0.06	1.3±0.08	1.2±0.08
Weight of internal fat, kg	0.4±0.05	0.6±0.05	0.7±0.08
Slaughter weight, kg	18.1±0.41**	16.0±0.38	14.7±0.36
Slaughter yield, %	50.5	49.4	48.6
8 months			
Number of heads, n	3	3	3
Pre-slaughter weight, kg	41.6±0.48	37.2±0.57	34.4±0.62
Carcass weight, kg	21.2±0.59***	17.9±0.68	16.5±0.52
Incl. fat tail weight, kg	1.7±0.09	1.5±0.08	1.4±0.08
Weight of internal fat, kg	0.5±0.07	0.9±0.11	0.8±0.11
Slaughter weight, kg	21.7±0.55***	18.8±0.62	17.3±0.49
Slaughter yield, %	52.2	50.6	50.3

So, at the age of 4 months, lambs surpassed valushki both in slaughter weight and in carcass weight by 1.0 and 0.6 kg, at 6 months by 2.1 and 2.3 kg, at 8 months by - 2.9 and 3.3 kg, respectively.

Changes in the hormonal status of the body of rams after castration, delaying the growth of live weight, accelerate the process of fat deposition, so in rams at the age of 6 months, a relatively more intensive growth of adipose tissue was noted. The ratio of the mass of internal fat to the mass of the carcass in valushki was 3.9% at 6 months of age, at 8 months - 5.0%, in rams it was in the range - 2.3-2.4%.

In order to establish the commercial value of carcasses of slaughtered young animals, the varietal composition was studied with the calculation of the specific weight of cuts of the first and second grades. The results showed that with age, as a general pattern for growing young animals associated with the build-up of muscle tissue, the share of cuts of grade I steadily increases in animals of all sex and age groups (tab. 3).

Table 3.

Varietal composition of carcasses of slaughtered young animals (n=3, X ± Sx)

Group	Carcass weight, kg	Including			
		I kind	%	II kind	%
4 months					
I	13,5±0,35	11,0±0,35	81,5	2,5±0,14	18,5
II	12,9±0,33	10,5±0,29	81,4	2,4±0,16	18,6
III	11,7±0,42	9,5±0,38	81,2	2,2±0,12	18,8
6 months					
I	17,7±0,39	14,9±0,31**	84,2	2,8±0,11	15,8
II	15,4±0,44	12,8±0,28	83,1	2,6±0,15	16,9
III	14,0±0,37	11,6±0,29	82,9	2,4±0,13	17,1
8 months					
I	21,2±0,59	18,2±0,48***	85,9	3,0±0,21	14,1
II	17,9±0,68	15,1±0,39	84,4	2,8±0,22	15,6
III	16,5±0,52	13,8±0,51	83,6	2,7±0,15	16,4

The yield of meat of the first grade over a period of 4 to 8 months increased in rams by 7.2 kg (64.5%), in valushki by 4.6 kg (43.8%), in ewes by 4.3 kg (45.3 %). At the same time, the share of cuts of grade I in the carcasses of 8 monthly rams was 85.9% and exceeded the indicators of valushki on this basis by 1.5 abs. perc., yarochek - 2.3 abs. perc.

Analysis of the chemical composition of the average sample of minced meat showed that the meat of young animals, both at 4, 6 and 8 months of age, has some differences. The carcasses of valushki and ewes, with almost the same protein content, were superior in fat content to rams, the difference increased with age (tab. 4).

Table 4.

The chemical composition of the average sample of minced meat, X ± Sx

Index		Group		
		I	II	III
4 months				
Content, %	Moisture	67,59±0,88	66,82±0,37	66,16±0,46
	Fat	14,28±0,31	14,75±0,19	15,15±0,47
	Protein	17,12±0,33	17,40±0,35	17,66±0,22
	Ash	1,01±0,02	1,03±0,02	1,03±0,01

Active acidity, PH		5,78	5,85	5,82
Calorie content of 100 g of pulp, kcal		203	209	213
6 months				
Content, %	Moisture	65,21±0,68	64,78±0,41	64,19±0,76
	Fat	15,81±0,56	17,04±0,39	17,84 ±0,42
	Protein	17,91±0,61	17,13±0,52	16,92±0,24
	Ash	1,07±0,06	1,05±0,05	1,05±0,05
Active acidity, PH		5,93	5,97	6,01
Calorie content of 100 g of pulp, kcal		220	229	235
8 months				
Content, %	Moisture	63,24±0,52	60,16±0,52	59,87±0,46
	Fat	17,23±0,56	20,20±0,45	20,34±0,92
	Protein	18,44±0,61	18,53±0,47	18,68±0,54
	Ash	1,09±0,09	1,11±0,12	1,11±0,14
Active acidity, PH		6,09	6,13	6,12
Calorie content of 100 g of pulp, kcal		236	264	266

In our opinion, the onset of carcass brining in ewes at an earlier age and with a lower body weight compared to rams is associated with their earlier puberty, and in valushkas due to a violation (cessation) of the hormonal function of the gonads. As a result, the level of metabolism decreases, the process of fat deposition increases, and the growth of muscle and bone tissues slows down, which negatively affects the realization of the genetic potential of meat productivity.

Analysis of the chemical composition of the average sample of minced meat shows that the meat of young animals, both at 4 months of age, and at 6 and 8 months of age, has differences. The carcasses of valushki and ewes, with almost the same protein content, were superior in fat content to sheep, the difference increased with age, therefore, the chemical composition and calorie content of the carcass pulp is largely determined by the sex and age of the slaughtered young.

It should be noted that in the carcasses of all the studied groups, the level of dry matter content increases with age, respectively, and calorie content, due to an increase in both adipose and muscle tissue.

At the same time, it was found that both during the period of weaning from mothers at 4 months and at 6 months of age, after feeding on mountain pastures for 2 months, the meat of rams was better in terms of the ratio of protein / fat, protein / moisture and the physiological maturity of the meat.

One of the important indicators characterizing the nutritional value of meat

is the ratio of protein to fat. Not only nutritional value, but also its digestibility, digestibility and energy value depend on the ratio of proteins and fats in meat. The best digestibility is meat, in which the ratio between protein and fat is 1:1.

The results of age-related accumulation of fat show that fat is deposited at relatively early stages of development and in larger quantities in valushkas and ewes. In our opinion, the beginning of carcass brining in ewes at an earlier age and with a lower body weight compared to rams is associated with their earlier puberty, and in valushkas, due to a violation (cessation) of the hormonal function of the sex glands. As a result, the level of metabolism decreases, the process of fat deposition increases, the growth of muscle and bone tissues slows down, which negatively affects the realization of the genetic potential of meat productivity.

Changes in the hormonal status of the body of rams after castration, delaying the growth of live weight, accelerated the process of fat deposition, so in rams at the age of 6 months, a relatively more intensive growth of adipose tissue was noted. The ratio of the mass of internal fat to the mass of the carcass in valushki was 3.9% at 6 months of age, at 8 months - 5.0%, in rams it was in the range - 2.3-2.4%.

The completeness of the protein, determined by the content of the amino acids tryptophan and hydroxyproline, both in the longissimus dorsi muscle and in the pulp of carcasses, all other things being equal, significantly depends on the sex and age of the animals.

The research results indicate certain intergroup differences in the concentration of amino acids in the longest back muscle. In all cases, lambs were characterized by a relatively high content of the essential amino acid tryptophan in muscle tissue, which determined a higher level of protein quality index of meat products (tab. 5).

Table 5.

Protein quality index, $X \pm Sx$

Amino acids, mg %	**Group**		
	I	**II**	**III**
4 months			
Tryptophan	261±3,71	255±3,84	249±4,23
Oxyproline	79,21±0,34	80,22±0,59	80,47±0,45
BKP	3,29	3,18	3,09
6 months			
Tryptophan	276±3,37*	268±3,49	255±4,04
Oxyproline	68,22±0,74	70,91±0,44	70,25±0,52
BKP	4,04	3,78	3,63

8 months			
Tryptophan	296±3,42**	279±3,98	268±2,92
Oxyproline	62,45±0,57	64,53±0,57	64,65±0,48
BKP	4,74	4,32	4,15

With age, an increase in the content of tryptophan and a decrease in the concentration of hydroxyproline in the longissimus muscle of young animals of all groups were observed. At the same time, the content of tryptophan in the muscle tissue of rams exceeded that of rams and ewes, against the background of a lower content of oxyproline, and this trend increased with age. As a result, the protein quality index in rams was 4 months - 3.29, at 6 months - 4.04 and at 8 months 4.74, which exceeded the indicators of valushki and yarochek by: 0.11 and 0.2; 0.26 - 0.77; 0.42 and 0.59 respectively.

In general, ram meat was characterized by an optimal fat and protein content and a higher protein quality index.

Conclusion

Young sheep of the Karachay breed, kept on mountain pastures without additional feeding with concentrated feed, grew and developed normally, showed a fairly high genetic potential of meat productivity. In all periods of growth and development, according to all indicators, the leading position was occupied by rams, valushki - an intermediate position, the minimum level was for ewes.

Castration of rams leads to a sharp change and disruption of physiological functions in the body, makes certain adjustments to the processes of their growth and development. In castrated animals (valushki), due to a violation (cessation) of the hormonal function of the sex glands, the level of metabolism decreases, the growth of muscle and bone tissues slows down, and the process of fat deposition in the body increases.

Conclusions

Castration of rams of the Karachay breed in mountain meat-coarse-wool sheep breeding with grazing in alpine meadows is not advisable, since it prevents the manifestation of the genetically inherent potential of meat productivity, ceteris paribus, feed conversion for the production of meat products is reduced.

In all age periods, lambs surpass both ewes and valushki in terms of meat quality, by the end of feeding on mountain pastures, at 8 months of age, this superiority is enhanced.

The question of the expediency of castration of lambs in each farm must be decided on the basis of specific conditions.

The studies were carried out according to the research plan № 0212-2019-0258 of the animal husbandry laboratory of the IA KBSC RAS.

References

1. Gabaev M.S. Economic efficiency of mountain sheep breeding depending on the live weight of queens // Animal husbandry and fodder production 2021. V. 104 № 1. P. 43-53.

2. Podkorytov A.T., Podkorytov A.A., Podkorytov N.A. Influence of the level of milk productivity of ewes on the intensity of growth of lambs of the Katun type // Bulletin of the Altai State Agrarian University. № 9 (107). 2013. P. 65-67.

3. Gabaev M.S., Berbekova N.V. Milk productivity of ewes of the Karachay breed and its relationship with live weight and vertical zoning of pastures // Genetics and breeding. 2020. № 4. P. 17-21

4. Gabaev M.S., Gukezhev V.M. The effectiveness of the use of queens of different live weights in mountain sheep breeding // International scientific research. 2017. № 2 (31). P. 96-99.

5. GOST 25955-83. Methods for determining the parameters of sheep productivity. M.: Standards Publishing House, 1983. 13 P.

6. Methodology for studying the meat productivity of sheep. Guidelines VIZh. M., 1978. 45 P.

7. OST 25011-81. Meat and meat products. Protein determination methods. Methods of analysis: Coll. of GOSTs. M.: Standartinform, 2010. 12 P.

8. GOST R 53642-2009. Meat and meat products. Methods for determining the mass fraction of total ash. M.: Standartinform. 2010. 11 P.

9. GOST R 51479-99. Meat and meat products. Methods for determining the mass fraction of moisture. Moscow. Standartinform. 2010. 6 P.

10. GOST 23042-86 Meat and meat products. Methods for determining fat. M.: Standartinform. 2010. 6 P.

DOI 10.34660/INF.2022.54.83.286

铸造印度芝麻植物对特征复合体的影响
INFLUENCE OF MINTING INDIAN SESAME PLANTS ON THE COMPLEX OF FEATURES

Kympan Marina Igorevna
Postgraduate
Chavdar Nina Semenovna
Candidate of Agricultural Sciences, Associate Professor
Nevinglovsky Evgeny Anatolievich
Undergraduate
Shevchenko Transnistria State University

抽象的。 文章介绍了追赶印度芝麻品种 Lebed 对发芽能量、发芽率、千粒重和产量的影响结果。

关键词：印度芝麻，追逐，发芽能量，发芽，千粒重，生产力。

Abstract. *The article presents the results of the influence of chasing Indian sesame variety Lebed on germination energy, germination, weight of 1000 seeds, and yield.*

Keywords: *Indian sesame, chasing, germination energy, germination, weight of 1000 seeds, productivity.*

Introduction

Sesame among oil plants is characterized by the highest fat content (48.0 - 63.0%). Sesame seed oil is semi-drying, as are almost all edible oils [1]. Sesame seeds contain many macronutrients. In terms of absolute content, there is a lot of calcium, phosphorus and potassium. But according to the content of silicon in 100 g of seeds, there are more than six daily norms for a person, calcium and magnesium - one each. 100 g of sesame seeds contain four daily norms of copper, a little more than one norm of vanadium, nickel, manganese, one daily norm of iron. 14 vitamins were found in sesame seeds, vitamins of group B are of particular importance: (B_1, B_2, B_3, B_6, B_9) [2].

Breeding sesame varieties adapted to the conditions of cultivation in Transnistria and the development of elements of cultivation technology is relevant.

For the first time in Transnistria, the study of the effect of minting on the sowing qualities and seed yield of the Indian sesame variety Lebed is being studied.

In 2018, the Transnistrian State University named after T.G. Shevchenko received a patent for the Indian Lebed sesame variety with a priority date of December 12, 2017, registered in the State Register of the Ministry of Justice of the Transnistrian Moldavian Republic on January 23, 2018. For further introduction into production, it is necessary to develop a technology for the cultivation of sesame for the conditions of Transnistria.

Purpose of the study:

To study the effect of minting sesame plants of the Lebed variety on the sowing quality of seeds and yield.

Material and methods

The object of the study was the Indian sesame variety "Lebed".

Sesame variety Lebed was created by physical mutagenesis followed by selection of the best line. The duration of the growing season is 130-140 days. Plants of the Lebed variety in the conditions of Transnistria have a height of 165-175 cm, branching - 7-8 shoots of the first order. The height of the first branch is 10-13 cm. The flowers of the Lebed variety are pubescent, light pink. The length of the productive part of the main shoot is 100-115 cm, on which there are from 50 to 76 densely spaced bolls. In total, 250-400 two-carpel four-celled bolls are formed on the plant; when ripe, they crack weakly. The length of the box is 24-25 mm. The mass of seeds from one plant is 25-55 g, on some plants up to 75 g of seeds are formed. The weight of 1000 seeds is 2.7-2.9 g. The seeds are white with a cream shade of an elongated shape.

Research methodology

Sowing scheme (90x20) cm. Row length - 2 meters. The material was seeded on May 12, 2019.

In the experiment, we studied the effect of minting on the sowing qualities of sesame seeds, depending on their location on the plant and yield.

Variants of the studied factors:

Factor	Option
A (minting)	1. No minting
	2. Minting
B (location of seeds on the plant)	1. Upper part of the central shoot
	2. The middle part of the central shoot
	3. The lower part of the central shoot
	4. Side shoots

In the experiment, the productivity was recorded from each plant separately and fractionally:

from the lower, middle, upper parts of the main shoot and side shoots.

Germination energy and germination were determined according to **GOST 12038-84**[3].

The weight of 1000 seeds was determined according to **GOST 12042-80** [4].

Mathematical data processing was carried out by the method of dispersion analysis according to B.A. Dospekhov [5].

Research results

Influence of minting on sowing qualities of sesame seeds

The germination energy of sesame seeds in the experiment was high and varied from 74.9% for the seeds of the lower part of the central shoot to 98.9% for the seeds of the upper part of the central shoot with chasing. In the experiment on the effect of chasing on the germination energy of sesame seeds of the Lebed variety, there are significant differences because:

$F_{fact.}A > F_{theoret.}A$;

$F_{fact.}B > F_{theoret.}B$;

$F_{fact.}AB > F_{theoret.}AB$ (tab.1).

The germination energy of sesame seeds of the Lebed variety in the variant with chasing is significantly higher than in the variant without chasing, the NSR for factor A is 3.79%, and the difference in the variants is (94.2 - 80.0 = 14.2%). This is significantly greater than the NSR value.

The energy of seed germination of the Lebed variety, depending on the location, has significant differences. At NSR_{05} = 6.3%, the energy of seed germination in the middle part of the central shoot was 94.4%, which is significantly higher than in the lower part and from the side shoots. However, the energy of seed germination in the middle and upper parts is the same, because there are no significant differences between them. Taking into account NSR_{05} AB = 10.2% - for comparison of partial averages, the germination energy of sesame seeds of the Lebed variety in the variant with chasing is higher in the upper, lower and side shoots (tab. 1).

Table 1.

Germination energy of seeds of sesame variety Lebed

Minting (factor A)	Location of seeds (factor B)				Average factor A (NSR_{05} = 3.79 %)
	Upper part of the central shoot	The middle part of the central shoot	The lower part of the central shoot	Side shoots	
No minting	77.6	92.3	75.1	74.9	80.0
Minting	98.9	96.5	86.75	94.5	94.2
Average factor B (NSR_{05} = 6.3 %)	88.3	94.4	80.9	84.7	87.1
NSR_{05} AB = 10.2% – to compare private averages					

There is a significant difference in terms of germination of sesame seeds of the Lebed variety, depending on the minting. In the variant of the experiment with chasing, the germination of seeds is significantly higher, with NSR $_{05}$ = 2.97%, the difference is 4.7%. The germination of seeds, depending on their location, is the same in the upper, middle parts of the central shoot and on the lateral ones. Seed germination from the lower part of the central shoot was significantly lower than in all other variants (tab. 2).

Table 2.

Germination of seeds of sesame variety Lebed

Minting (factor A)	Location of seeds (factor B)				Average factor A (NSR$_{05}$ = 2.97 %)
	Upper part of the central shoot	The middle part of the central shoot	The lower part of the central shoot	Side shoots	
No minting	94.1	98.4	82.7	95.9	92.8
Minting	99.8	98.5	92.9	98.6	97.5
Average factor B (NSR$_{05}$ = 4,3 %)	96.95	98.45	87.8	97.25	95.1
NSR$_{05}$ AB = 5.,2% – to compare private averages					

Influence of minting on the weight of 1000 seeds and yield

Analysis of variance of a two-factor experiment on the effect of minting and seed location on the weight of 1000 seeds showed that the actual value of the Fisher criterion in the experiment significantly exceeds the theoretical values of the Fisher criterion for factors A, B and their interaction AB (tab. 3).

Table 3.

Analysis of variance of a two-factor experiment on the effect of minting on the weight of 1000 sesame seeds, depending on their location on the plant

Dispersion	Sum of squares	Degrees of freedom	Medium square	Fisher's criterion	
				Fact.	Theoret.
General	4.5499	63	-	-	-
Repetitions	0.7150	7	-	-	-
Minting (factor A)	1.2386	1	1.2386	45.705	4.035
Location of seeds (factor B)	0.9211	3	0.3070	11.3284	2.795
AB interaction	0.3471	3	0.1157	4.2694	2.795
Residuum (errors)	1.3281	49	0.0271	-	-

Taking into account $NSR_{,5}$ for factor A (chasing) equal to 0.08 g, in the variant with chasing plants, the weight of 1000 seeds of sesame variety Lebed is significantly higher than in the variant without chasing (control) (3.05 g-2.77 g = 0.28 g).

Taking into account $NSR_{0,5}$ for factor B (location of seeds on the plant), equal to 0.06 g, the weight of 1000 sesame seeds in the lower part of the main shoot is significantly higher than in the middle part of the main shoot (3.06 g-2.99 g = 0.07 g), significantly higher than in the upper part (3.06 g - 2.82 g = 0.24 g) and significantly higher than on the side shoots (3.06 g - 2.77 g = 0.29).

In the variant of the experiment without minting, the weight of 1000 seeds of the Lebed variety in the lower part of the central shoot was significantly higher than in the middle and upper parts of the central shoot and side shoots.

In the variant of the experiment with minting, the weight of 1000 seeds of the Lebed variety in the lower part of the central shoot is the same as in the middle part (3.13 g - 3.10 g = 0.03 g); the same as in the upper one (3.13 g - 3.06 g = 0.07 g); significantly higher than on lateral shoots (3.13g-2.90g = 0.23g). The weight of 1000 seeds in the middle part of the central shoot is significantly higher than in the upper one (3.13 g - 3.06 g = 0.07 g).

The highest value of the mass of 1000 seeds of the Lebed variety in the experiment is observed in the lower part of the central shoot of the variant with minted plants (3.13 g). This value is significantly higher than in the upper and middle parts of the central shoot and lateral shoots in the variant without chasing and lateral shoots with chasing, taking into account NSR_{05} AB equal to 0.17 g, for comparison of private averages (tab. 4).

Table 4.

Influence of plant minting and location of seeds on the plant on the mass of 1000 seeds of the Lebed variety

Minting (factor A)	**Location of seeds (factor B)**				**Average factor A (NSR_{05} = 0.08 g)**
	Upper part of the central shoot	**The middle part of the central shoot**	**The lower part of the central shoot**	**Side shoots**	
No minting	2.57	2.85	3.02	2.63	2.77
Minting	3.06	3.13	3.10	2.90	3.05
Average for factor B (NSR_{05} = 0.06 g)	2.82	2.99	3.06	2.77	2.91
NSR_{05} AB = 0.17 g. - for comparison of private averages					

A significant excess of the weight of 1000 seeds in the variant of the experiment with chasing led to an increase in seed yield. Mathematical processing of the experimental data by analysis of variance showed a significant excess in the yield of seeds of the Lebed variety in the variant of the experiment using plant minting.

Table 5.

Influence of plant minting on the yield of Lebed sesame seeds, cen/ha

Agricultural technique	Seed yield, cen/ha
Plants without minting	11.2
Plant minting	14.8
NSR_{095}	0.9

The yield in the variant with chasing was 14.8 cen./ha, which is significantly higher than in the variant without chasing, where the yield was 11.2 cen./ha with NSR_{095}, equal to 0.9 cen./ha (tab. 5).

Conclusions

The minting of plants had a positive effect on:

- germination energy of sesame seeds (exceeding 14.2%);
- seed germination from 92.8% to 97.5% (excess by 4.7%);
- increase in the weight of 1000 seeds from 2.77 g to 3.05 g (excess by 0.28 g);
- a significant increase in the yield of sesame seeds of the Indian variety Lebed from 11.2 cen/ha to 14.8 cen/ha.

References

1. Plant growing: Textbook for students of higher educational institutions / G.S. Posypanov, V.E. Dolgodvorov, G.V. Korenev [et al.]; [ed. G.S. Posypanova]. M.: Kolos, 1997. 448 P.

2. Sesame. Women's product. / Konovalova E.Yu. http://pharmacognosy.com.ua/index.php/vashe-zdorovoye-pitanije/orekhi-i-semena/kunzhut (appeal date 07.12.2020)

3.GOST 12038-84 Seeds of agricultural crops. Germination detection methods

4. GOST 12042-80 Seeds of agricultural crops. Methods for determining the mass of 1000 seeds

5. Dospekhov B.A. Methodology of field testing. – M.: Kolos, 1985. – 416 P.

DOI 10.34660/INF.2022.88.70.287

无需编程即可创建本国语言的知识库
CREATION OF KNOWLEDGE BASES IN NATIONAL LANGUAGES WITHOUT PROGRAMMING

Evgenev Georgy Borisovich
Doctor of Technical Sciences, Full Professor
Bauman Moscow State Technical University
Moscow, Russia

抽象的。 当前，世界正在经历第四次工业革命，即“工业4.0”。 这场革命的目标是创造数字化制造。 然而，在不久的将来，我们正在等待第五次工业革命或工业 5.0。

关键词：工业5.0、数字化制造、智能设计系统

Abstract. *Currently, the world is experiencing the fourth industrial revolution, called "Industry 4.0". The goal of this revolution is to create digital manufacturing. However, in the near future we are waiting for the fifth industrial revolution or Industry 5.0.*

Keywords: *Industry 5.0, digital manufacturing, intelligent design systems*

Introduction

An important direction in the improvement of mechanical engineering is digitalization, which should cover all stages of the product life cycle.

Industry digitalization — this is the concept of a new digital space, a single system into which all systems of design and technological design, planning and production management are integrated, including production machines and CNC robots, life support and enterprise security systems, that is, all electronics of the organization.

At the same time, the concepts of humanization should be applied in digitalization, which means the use of a form as close as possible to natural language for the presentation of initial and resulting information, and computer language codes should be generated automatically. ExPro [1] expert programming system functions exactly in this way. This system is available for the work of expert knowledge carriers and does not require the involvement of programmers. On the basis of ExPro, a system for designing technological processes SprutTP was developed, which is widely used in industry [2].

Theoretical provisions

The knowledge element is a generalized functional block. The most successful and widely used representation of function blocks is the international standard IDEF0. In this standard, the functional block has the design shown in fig. 1.

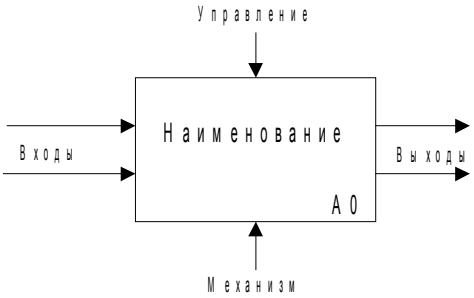

Figure 1. *IDEF0 function block*

Arrows of input data approach the left side of the block, which can be both integer and real numbers, and non-numeric symbolic values. The input data is converted by the block to the output, which is depicted by an arrow extending from the right side. The transformation is carried out using a mechanism (formulas, tables, databases, etc.). The gear pointer (*M*) fits on the underside of the block. The operation of the block is performed under the influence of control information, the arrow of which approaches the upper side of the block. Output and control data, as well as input data, can be both numeric and symbolic.

In the production systems of artificial intelligence, the element of knowledge representation is the rule-production. Such a rule contains a precondition that determines its applicability for a specific state of database variables (if <condition>, then <action>).

Production-rules can also be represented in the form of IDEF0 blocks. In this case, the condition is determined by the control arrow *C* (fig. 1), and the action to transform the input into an output is implemented by the mechanism.

To solve complex problems that require the use of many functional blocks, elementary blocks are combined into a complex function, which is an object method (fig. 2).

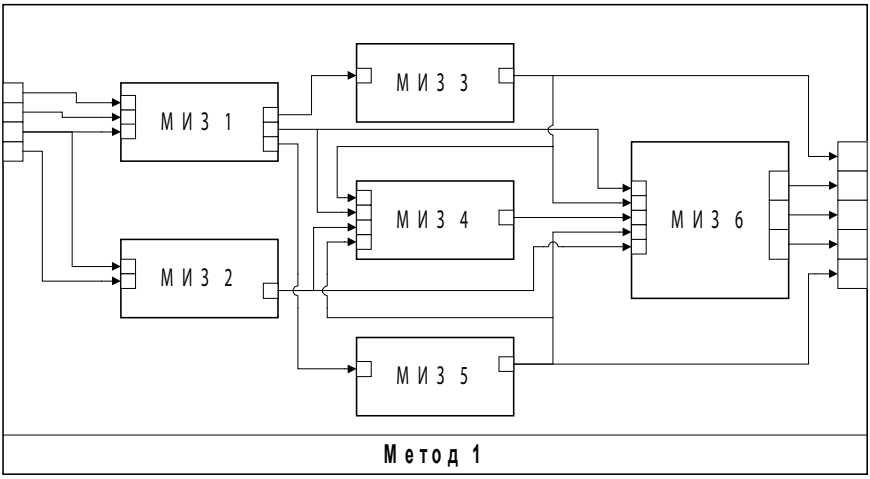

Figure 2. *Object method (complex function)*

Modules of engineering knowledge

The above theoretical schemes must be presented in a form convenient for their definition by a person when entering knowledge into a computer. The simplest form is a table (fig. 3).

Module: <Name>
Denomination: <Function Description>

Parameter denomination	Name	Meaning
Input (I) and control (C)		Condition (C)
Exit (O)	Address	Mechanism (M)

Figure 3. *External representation of the engineering knowledge module*

Such a table contains all the elements of the functional block shown in fig.1. Parameter names must be selected from the system dictionary, as well as their names - identifiers necessary for writing formulas. A condition is a restriction imposed on the input and control parameters and defining the scope of the function implemented by the module.

An unstructured set of engineering knowledge modules in a particular application area is a knowledge base (KB) of this area.

The names and names of the input, control and output variables of the EKM should be selected from the dictionary of the knowledge base (tab. 1).

Table 1.
Dictionary

Denomination	Name	Type
Standard axle diameter, mm	d	R
Axle length standard, mm	L	R
Chamfer width, mm	c	R
Collar diameter, mm	D	R
Bead width, mm	H	R
Fillet radius, mm	r1	R
Shoulder rounding radius, mm	r2	R
Material Grade	Brand	S
Bending moment, N*mm	Mi	R
Permissible bending stress, MPa	Ti	R
Initial axle diameter, mm	do	R
Axle length initial, mm	Lo	R
Axis type	TO	S
Detail number	Nom	I
Estimated axle diameter, mm	dr	R

Mechanisms of engineering knowledge modules (EKM) should provide the implementation of all the functions that are used when writing engineering books.

The simplest function - is the assignment of values to output variables (fig. 4). When specifying restrictions on numeric variables, round and square brackets are used, between which two numbers are written separated by commas: the allowable smallest and largest. When using parentheses, extreme values are excluded from the allowed values, and square brackets - included. When specifying unlimited ranges, one of the extreme values is missing. For example, the range of all positive numbers is given by such a notation (0,).

From the point of view of the IDEF0 structure, the EKM shown in fig. 4 has two control and one output variables. Module mechanisms are triggered when the values of input and control variables become known and they satisfy the specified constraints.

If we consider this EKM as a general product, then it is equivalent to the following sentence: "if the original axle diameter is greater than 0 and less than or equal to 30 mm and the material grade is steel 45 improved, then the allowable bending stress is 0.85 MPa".

Module: M2
Developer: Evgenev G. B.
Denomination: Determination of allowable stress
Source of information: Anuryev V.I. Designer's Handbook, v. 2, tab. 8, p. 21

Denomination	Name	Limitation
Initial axle diameter, mm Material Grade	do Brand	(0, 30] 45 improved
Permissible voltage bending, MPa	Ti	0.85

Figure 4. *Module external representation - assignments*

In engineering books, functional dependencies are often presented as formulas. The external representation of the module - formulas is shown in fig.5.

Module: V13
Developer: Evgenev G. B.
Denomination: Calculation of the nominal amount of deformation
Source of information: Shuvalov S. A. Methodical instructions for the calculation of wave gears on a computer. Publishing house of N.E. Bauman MSTU, 1987

Denomination	Name	Limitation
Reducer type Gear ratio given Number of teeth of the flexible wheel pre	TypeRed uz zf	wave single-crown (0,)
Starting torque increase factor	K1	1.9
Nominal value of radial deformation	NWo	0.84+0.001*uz+1.6*10^(-3)*K1*uz^(1/2)+0.15*10^(-3)*K1*uz
Depth of teeth admissible, mm	hd	4*NWo-(4.6-4*NWo)*zf/10^3-2.45

Figure 5. *External representation of the combined module*

It is possible to use one EKM to assign values to variables and perform calculations using a set of interrelated formulas (fig. 5). In this case, the previous output variables can be used to determine the subsequent output variables.

Using the EKM type of formulas, you can generate text variables, for example, product designations, texts for the content of technological operations and transitions, etc. Figure 6 shows an example of the formation of the content of the machining transition in accordance with the USTD.

With the values of the input variables Per=”Sharpen”, ElObr=”groove”, NoEl=1, DinPer2=”ring”, DinPer4=”final”, the content of the transition will look like this: ”Sharpen ring. groove 1 finally”. The STR function converts data from numeric to string form.

Module: TKP3
Developer: Evgenev G. B.
Denomination: Shaping the transition content
Source of information: USTD

Denomination	Name	Limitation
Cutting transition Item being processed Item number Addit. transition information 2 Addit. transition information 4 Amount of elements	Per ElObr NoEl DinPer2 DinPer4 KolEl	 [1,)
Element number string Transition content	NoElStr SodPer	STR(NoEl:0) Per+” “+ DinPer2+” “+ ElObr+” “+ NoElStr+” “+ DinPer4

Figure 6. *External representation of a module − text variable formation formulas*

Functional dependencies in engineering books are often presented in tabular form. To enter such dependencies into knowledge bases, knowledge modules with mechanisms in the form of tables are used.

An example of such a module for assigning numerical values is shown in fig. 7. The table attached to the module can have a header and a sidebar.

Module: M5
Developer: Evgenev G. B.
Denomination: Standard length assignment
Source of information: Anuryev V.I. Designer's Handbook, v.2, p.8

Denomination	Name	Limitation
Standard axle diameter, mm Axle length initial, mm	d Lo	(0, 22] (25, 30]
Axle length standard, mm	L	Table: TABL1

Table 1

Axis length initial, mm	Standard axle diameter, mm							
	5	6	8	10	12	16,18	20	22
(25, 28]	28	28	28	28	28	28		
(28, 30]	30	30	30	30	30	30	30	

Figure 7. *External representation of the module - tables*

Information about the properties of materials, the parameters of standard and purchased products, as well as production resources (properties of machines, fixtures, tools, etc.) are often stored in databases. During the design process, it is necessary to select information from database tables. For these purposes, EKM selection (selection) from databases is used.

An example of a database selection module is shown in fig. 8. In this module, the axis type is a control variable. It is necessary to select from the database the values of only those variables that define a part of a given type - a smooth axis.

Module: M3
Developer: Evgenev G. B.
Denomination: Assigning standard axle dimensions to smooth
Source of information: Anuryev V.I. Designer's Handbook, v.2, p.7

Denomination	Name	Limitation
Axis type Estimated axle diameter, mm	TO dr	axis smooth (0, 50]
Standard axle diameter, mm Chamfer width, mm	d c	Base: STND Table: Axles Where " d ">=dr

Figure 8. *External representation of the module - selection from the database*

Geometric and complex mathematical calculations cannot be represented in EKM form. To use mathematical knowledge, modules with mechanisms in the form of software modules have been introduced. An example of such a module is shown in fig. 9.

Module: M8
Developer: Evgenev G. B.
Denomination: drawing formation
Source of information: Anuryev V.I. Designer's Handbook, v.2, p.7

Denomination	Name	Limitation
Axis type Standard axle diameter, mm Axle length standard, mm Chamfer width, mm	TO D L c	axis smooth (0 , 50]
Detail drawing	AXLE	AXLES.prt

Figure 9. *External representation of a module - geometric procedures*

(Restriction - program name AXLES.prt; Name - denomination of the graphics base segment)

Methods (complex functions) generated from elementary EKMs can be represented as EKMs and used to solve complex problems.

The system provides for the possibility of organizing cyclic processes. Cycles are generated automatically when one of the method modules appears in the out-

put variables, which performs the function of controlling the repetition of the cycle of the selected variable with the identifier FinCalc.

Conclusion

Methods and means of digitalization of industry have been developed to ensure the creation of intelligent systems for design and technological design, planning and production management.

The concept of humanization has been fully implemented, which ensures the use of a form that is as close as possible to natural language for the presentation of initial and resulting information. In this case, computer language codes are generated automatically.

References

1. Evgenev G.B. Sprut ExPro – a tool for generating multi-agent design systems in mechanical engineering. Part 2. News of higher educational institutions. Engineering. №7, 2017, P.60-70

2. Evgenev G.B. Fundamentals of automation of technological processes and productions: textbook: in 2 v. V.1: Information models. Publishing house of Bauman MSTU, 2015, 441 P. V.2: Design and control methods. Publishing house of Bauman MSTU, 2015, 479 P.

DOI 10.34660/INF.2022.69.63.288

HXD2型电力机车单相牵引变流器的电能可以更好地返回牵引网
THE ELECTRICAL ENERGY OF HXD2 ELECTRIC LOCOMOTIVE SINGLE-PHASE TRACTION CONVERTER CAN BE BETTER RETURNED TO THE TRACTION NETWORK

Zhang Qiyan
Undergraduate
Gao Qi
Undergraduate
Vasiliev Vitaly Alekseevich
Candidate of Technical Sciences, Associate Professor
Vikulov Ilya Pavlovich
Candidate of Technical Sciences, Associate Professor
Emperor Alexander I St. Petersburg State Transport University

抽象的。 本文以HXD2大功率机车牵引交流变流器为研究对象。 通过理论分析和仿真表明，在单相牵引整流器（4QS）中，交流侧电流可以很好地跟随市电电压，保持直流环节电容电压稳定。 验证了所提控制策略的正确性。 当机车从行驶状态转变为制动状态时，可以很好地使单相整流器进入逆变器工作状态，从而使电能更好地返回到牵引网中，牵引效果更好。

关键词：HXD2型电力机车；牵引传动系统；四象限整流器（4QS；功率因数。

Abstract. *In this article, the HXD2 high power locomotive traction AC converter is used as an object of study. Through theoretical analysis and simulation, it is shown that in a single-phase traction rectifier (4QS), the current from the AC side can follow the mains voltage well and keep the DC link capacitor voltage stable. The correctness of the proposed control strategy has been verified. When the locomotive changes from the driving state to the braking state, the single-phase rectifier can be well brought into the inverter working state, so that the electric power can be better returned to the traction network with better traction effect.*

Keywords: *HXD2 electric locomotive; Traction drive system; Four-quadrant rectifier (4QS; Power factor).*

There are different modes of transport in China. In land transport, the main mode of transport is rail transport.

The energy sector in my country is characterized by rich coal reserves, and it is one of the few countries that use coal as the main source of energy. The share of coal in the production and consumption of primary energy in the country has remained above 70% for a long time. It has been scientifically proven that increasing the weight of a train to 20000 tons can significantly increase throughput. № 1 in the world in this regard, a powerful AC freight electric locomotive HXD2 has appeared.

"Express, big load" - is my country's freight development policy. Therefore, it is necessary to comprehensively improve the technical level of railway vehicles and equipment in my country.

A more comprehensive and in-depth study of high power AC drive systems and their control is required. The HXD2 electric locomotive system is developed in cooperation with Dalian Electric Locomotive Co., Ltd and French Alstom. traction converter and traction motor. The schematic diagram and structural composition of the traction electric drive system are shown in figure 1.

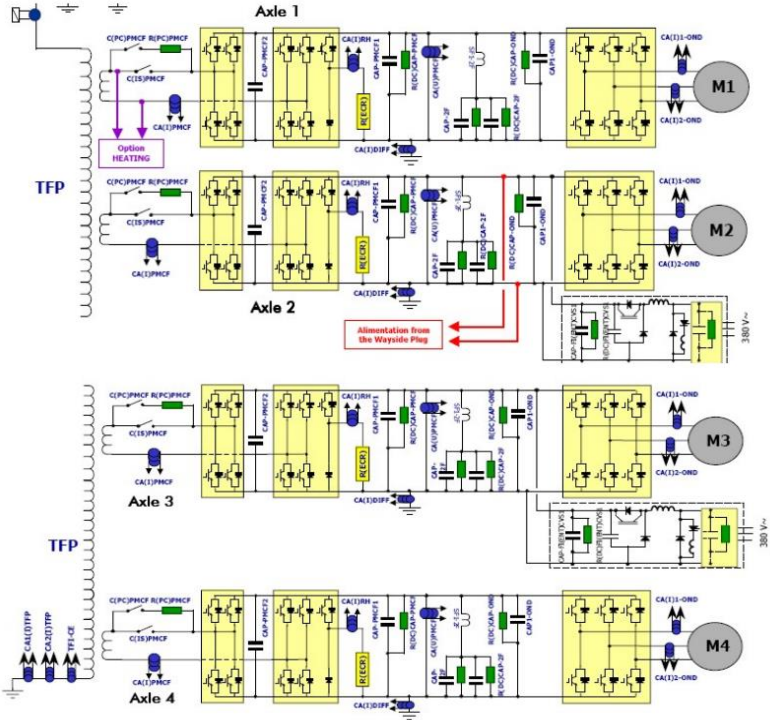

Figure 1. *Structural diagram of the electric traction drive system*

Lateral contact network circuits: The overhead voltage in my country is 25kV/50Hz single-phase AC, and the mains side circuit is basically implementing the overhead line into the car through the pantograph to power the locomotive.

Main traction transformer: The HXD2 electric locomotive main transformer uses ABB technology and is a combined transformer structure, consisting of the main transformer, auxiliary reactor, second harmonic filter reactor and other auxiliary equipment.

Traction converter: The HXD2 electric locomotive consists of two connected single machines. A single locomotive includes two bogies, each bogie includes two drive shafts. The single machine has 4 axles, and the whole car has an 8-axle structure. Each bogie contains two traction converters, the total locomotive has four bogies, and a total of 8 sets of independent traction converter units, which can realize one-to-one control of traction motors.

Asynchronous traction motor: The traction motor (YJ90A) of the HXD2 electric locomotive is an AC induction motor produced in cooperation with Alstom in France.

The rectifier part of the HXD2 electric locomotive adopts the structure of a single-phase PWM rectifier (VSR) as shown in figure 2, also known as a four-quadrant converter (4QC). The structure converts the single-phase AC input voltage on the secondary side of the main transformer to DC voltage to power the intermediate DC circuit. The term "four-quadrant converter" (4QC) means that the phase angle between voltage Vae and current IL is fully adjustable in both traction and braking conditions. By controlling the phase angle between voltage and current, four-quadrant AC operation can be achieved. Among them, L — the filter inductance on the AC side, C — the storage capacitor on the DC side, and R — the simulated load on the DC side.

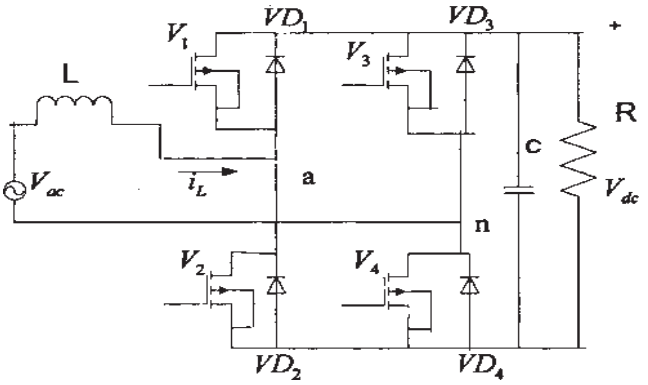

Figure 2. *Structure of a single-phase rectifier with PWM voltage source (VSR)*

For the HXD2 electric locomotive, the rectifier input voltage range is about AC900V (that is, the main transformer secondary voltage), the DC output side is about 1800V. It is worth noting that HXD1 and HXD3 also use this structure.

The so-called four-quadrant operation means: In the usual coordinate system, let the grid voltage be on the abscissa axis, and the grid current on the ordinate. Under traction and regenerative braking conditions, it is guaranteed that the grid voltage and current can operate in the four quadrants of the coordinate system according to positive and negative dependence.

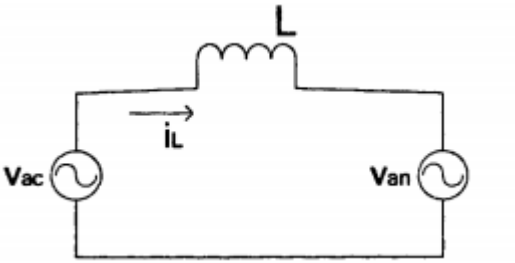

Figure 3. *Equivalent circuit diagram*

Basic principle: The amplitude of the output voltage Van on the AC side of the single-phase fully controlled four-quadrant bridge rectifier changes, and the change range switches between Vdc, 0 and -Vdc. If the appropriate control pulses are applied to the four switches of the circuit, then Van reacts accordingly to the change in the control pulse. If the control circuit is set to sinusoidal change, then on the Van side it will be equivalent to an AC source with variable phase and amplitude.

Power factor: The rectifier part of Chinese HXD electric locomotives uses single-phase PWM rectification without exception, this structure can realize four-quadrant operation, consists of two-phase modules (half-bridges). The rectifier part of the HXD2 electric locomotive also adopts this structure and performs AC/DC conversion at AC voltage of 950V on the secondary side of the main transformer.

This structure is suitable for large power converters. In the main circuit of the HXD2 locomotive, it can mainly provide stable DC power for the intermediate circuit. At the same time, it can cause less distortion on the grid side. Compared with the earlier method of phase-controlled rectification, the power factor of the four-quadrant rectifier is close to 1, so the interference and pollution of the power grid is less, and this structure is often used in modern high-power rectifier circuit.

Therefore, the power factor is of great importance for the circuit. In particular, for high power converter systems, the influence is especially noticeable. The locomotive itself is a powerful load, and its electrical energy comes from the contact network above the roof, and the power supply of the contact network from the

power grid, the locomotive itself has a huge impact on the power system as a source of power quality pollution.

Previous DC electric locomotives mostly used bridge rectifier circuits. Due to the frequent opening and closing of the switch tube and the limitation of the control strategy, the current supplied by the train back to the contact network during operation is seriously distorted, and the power factor is extremely low, which not only affects the normal operation of the surrounding communication equipment, but also affects the power grid, which in itself causes pollution. Although with the improvement of technology, some multi-segment bridge technology has been applied to the rectifier circuit of locomotives, but the effect is still not very good. So look forward to the emergence of a new type of schema application form and related control strategies.

To fully understand the circuit, you first need to understand the concept of power factor. By definition, in a circuit, the cosine value of the phase difference between voltage and current during operation is called the power factor, which is denoted by the symbol COSF. Power factor refers to the ratio of active power to the apparent power of a circuit.

$$\mathrm{COSF} = \frac{P}{S} \tag{1}$$

P-Active power S-Full power

The value of the power factor (COSF) is between 0 and 1, and the power factor is usually determined by the nature of the load. Loads such as incandescent lamps or electric resistance furnaces are purely resistive loads with a power factor of 1; Induction motor or synchronous motor refers to inductive load and capacitive load, and their power factor is less than 1.

In the mains, since the voltage is clamped by the mains, the distortion is small. But since the current waveforms are different, they are greatly affected by the load carried by the network.

Thus, its definition can be expressed as follows:

$$\lambda = \frac{P}{S} = \mathrm{UCOSF_1} \tag{2}$$

In the formula, U — the ratio of the root mean square value of the main wave current to the rms value of the total current, called the coefficient of the main wave, which reflects the distortion coefficient (degree of distortion) of the current;

P — active power, S — apparent power,

this is still the fundamental wave power factor angle.

At this time, the power factor must contain two factors:

1 - factor phase angle 2 - shape distortion factor.

The lower the power factor of the circuit, the more energy the circuit uses to

convert the alternating magnetic field, resulting in more reactive power. Ultimately, more reactive power will have many adverse effects on the power system. In addition, harmonic interference caused by a circuit with a low power factor will cause great harm to the power grid and electrical equipment.

In order to reduce this effect and damage, power factor correction technology has been developed, power factor correction technology ensures that the input voltage and current have the same frequency and phase, which effectively improves the performance of the circuit.

For traction converters, it consists of a single-phase rectifier and a three-phase inverter connected by a DC link capacitor. The pantograph is connected to the 25KV AC power through the traction network, and the 950V AC power is output through the traction transformer, after which it is converted into 1800V DC power through a single-phase rectifier, and then the 1800V DC power is supplied through the traction transformer, it turns out through an intermediate DC circuit and fed to a three-phase traction inverter to obtain a three-phase voltage of 950 V to drive the motor.

Modeling in Matlab a Single-Phase Rectifier with PWM (VSR)

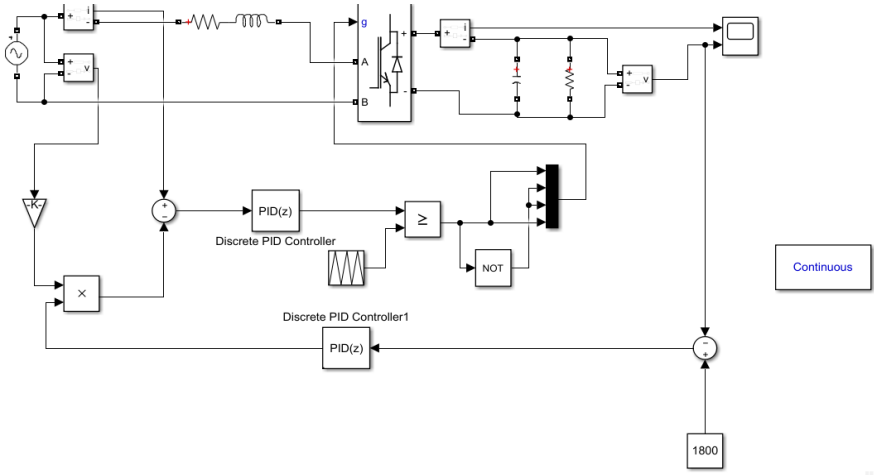

Figure 4. *Simulation model of a section of a single-phase traction rectifier*

From the results, it can be seen that the DC bus capacitor voltage is stable at 1800V, the AC side current of the single-phase traction rectifier can follow the grid voltage well, and the grid-side voltage-current power factor is 1.

References

1. Zhang Chongwei, Zhang Xing. PWM rectifier and its control [M]. Beijing: Engineering Industry Publishing House, 2003

2. Zhang Yucheng. Investigation of Single-Phase PWM Modulated Rectifier (VSR) [D], Huazhong University of Science and Technology, Wuhan City, Hubei Province, 2007

3. Zhang Shuguang - Chief Editor HXD2 Electric Locomotive / China Railway Press, 2009 (HXD Type High Power AC Locomotive Technology Series)

4. Wu Lin. Simulation study of the traction converter[D]. Southwestern Jiaotong University. 2010

5. Wu Xiaoyan, HXD2 Electric Locomotive Traction Converter Study [D], Southwest Jiaotong University, 2013.

DOI 10.34660/INF.2022.48.82.289

用激光选区熔化法研究GTE涡轮喷嘴工件制造断面的精度和稳定性

INVESTIGATION OF THE ACCURACY AND STABILITY OF MANUFACTURING SECTIONS OF THE GTE TURBINE NOZZLE WORKPIECES BY THE METHOD OF SELECTIVE LASER MELTING

Alekseev Vyacheslav Petrovich
Postgraduate
Kyarimov Rustam Ravilevich
Postgraduate
Samara University

抽象的。本文介绍了基于质量控制图，采用选择性激光熔化方法对涡轮喷嘴设备部分制造毛坯的精度和稳定性进行的研究结果。涡轮喷嘴部分的钢坯由 Inconel 738 材料在 SLM 280HL 装置上通过选择性激光熔化制成。对三坐标测量机上涡轮喷嘴装置截面的几何特性进行了控制。工艺过程的统计分析程序是使用定量数据的控制图和对工艺能力的评估及其满足规定要求的适用性进行的。作为产品质量的一个特征，选择了一个指标 – 喷嘴设备部分的羽毛叶片轮廓的几何形状的准确性，这显着影响产品的操作特性。作为统计分析的结果，发现该过程相对于内部可变性处于统计可控状态，该过程适合满足规定的要求并且具有有效过程控制所必需的足够的能力余量。

关键词：添加剂技术，选择性激光熔化，精度，质量，工艺稳定性，喷嘴部分。

Abstract. *This paper presents the results of a study of the accuracy and stability of manufacturing blanks for sections of the turbine nozzle apparatus, by the method of selective laser melting, based on quality control charts. Billets for the turbine nozzle section were made from Inconel 738 material by selective laser melting on an SLM 280HL unit. The control of the geometric characteristics of the sections of the turbine nozzle apparatus on a coordinate measuring machine was carried out. The procedure of statistical analysis of the technological process was carried out using control charts for quantitative data and an assessment of the capabilities of the process, and its suitability to meet the specified requirements. As a characteristic of the quality of the product, an indicator was chosen - the accuracy of the geometry of the profile of the feather blades of the section of the nozzle apparatus, which significantly affects the operational characteristics of the product. As a result of the statistical analysis, it was found that the process is in a*

state of statistical controllability with respect to internal variability, the process is suitable for meeting the specified requirements and has a sufficient margin of capabilities necessary for effective process control.

Keywords: additive technologies, selective laser melting, accuracy, quality, process stability, nozzle section.

Introduction

One of the most important and dynamically developing areas of additive technologies is the process of selective laser melting. Selective laser melting, SLM, SLM is one of the new additive manufacturing methods that uses high power lasers to create three-dimensional physical objects by fusing metal powders. The disadvantage of selective laser melting technology is large thermal deformations that occur due to the action of residual stresses due to a significant temperature gradient. As a result, large leashes, especially after the separation of the grown workpiece from the platform [1]. The main requirements for products obtained by additive technologies are to ensure the specified quality indicators for geometric accuracy, the state of the surface layer, phase composition, structure at micro-macro and meso levels, as well as the requirements for the absence of defects in the form of non-melting of powders, residual porosity, thermal leash.

One of the methods for managing a production or technological process, which has a certain variability due to the action of many factors on it, is statistical process control using quality control charts. Control charts are a tool for diagnosing the course of activity processes. They are used to analyze the production, technological or other process in order to determine the stability of the process, the accuracy of the equipment and its capabilities, to evaluate the quality of the products, to identify the causes of discrepancies.

In modern and promising GTE, special attention is paid to turbine nozzle blades in production. A characteristic feature of such parts is, first of all, the complexity of the technological process of their manufacture. At present, the tolerances of the shape of the feather of nozzle blades, regulated by the normative technical documentation, reach ± 0.2 mm. Increased requirements for the accuracy of manufacturing blades require taking into account the influence of technological factors on the stability of the manufacturing process. The noted fully applies to SLM technologies, which have not been fully studied in relation to GTE nozzle vanes.

In this regard, the goal was set to investigate the accuracy and stability of the technological process for manufacturing turbine nozzle sections by the method of selective laser melting using quality control charts.

Research methods and equipment

Manufacture of turbine nozzle sections grown from metal powder (average particle diameter is 15…53 μm) of heat-resistant alloy Inconel 738 was carried

out on an SLM 280HL unit. The location of the part must be set in such a way that the upper and lower shelves are at an angle relative to the platform with the construction of the support material on the leading edge of the blade. The presence of support material on the back and trough of the blade is unacceptable due to the high roughness after removal of the support structures.

The main parameters for manufacturing test samples of sections of the turbine nozzle apparatus by selective laser alloying from metal powder of heat-resistant alloy Inconel 738 on an SLM 280HL unit: power 325 W, scanning speed 677 mm/s [2]. The manufactured workpiece of the GTE turbine nozzle section is shown in fig. 1.

Figure 1. *Test workpiece of the nozzle section on the build platform*

The control of sections of the nozzle apparatus of the GTE turbine, manufactured using additive technology, was carried out on a DEA Global Performance 07.10.07 coordinate measuring machine at a temperature of 20 °C ±2 °C and a relative humidity of 80%. The airfoil profile of each blade of the turbine nozzle section was measured in three sections.

Statistical analysis of the data was performed using quality control charts for quantitative data. In some situations, it is not possible or not practical to use samples (subsets) of data to evaluate or manage a process. This is due to situations where measurements are expensive or when more than one measured indicator value cannot be obtained. In such situations, the process can be controlled based on individual values. Statistical analysis of the data obtained as a result of the experiments was performed in the commercial software product STATISTICA.

Research results

The evaluation of the quality of the product "section of the turbine nozzle apparatus" is carried out on a quantitative basis. As a characteristic of the quality of the product, an indicator was chosen - the accuracy of the geometry of the profile of the feather of each of the blades of the section of the nozzle apparatus, which significantly affects the operational characteristics of the product. Tolerance of the shape of the profile of the theoretical sections of the pen in diametric terms ±0.2 mm.

Fig. 2 shows individual value and moving range (MR) maps for pen profile deflection data. When using maps of individual values, an estimate of internal variability is determined on the basis of a measure of variation obtained from the sliding ranges of two consecutive observations. The sliding range MR is calculated as the modulus of the difference between the first and second measurements |X1 − X2|, the second and third measurements |X2 − X3|, etc. The number of sliding ranges MR is 1 less than the total number of measured values N, the sample size n is conditionally considered equal to 2 units [3]. Based on the moving ranges, the average moving range R is calculated, which is used to build control charts.

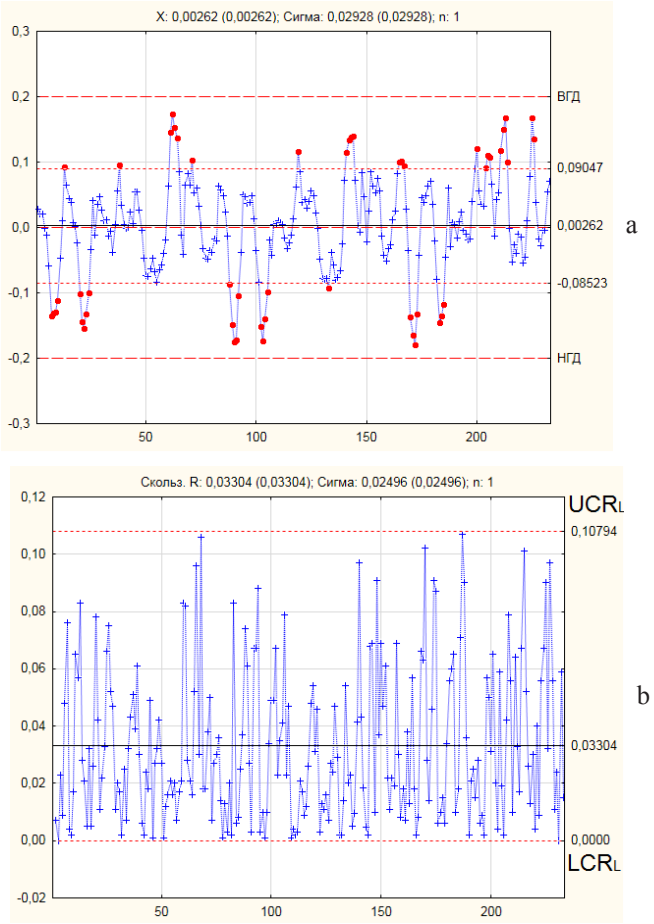

Figure 2. *Map of individual values (a) and moving range (b)*

First of all, it is necessary to assess whether the process is in a state of statistical control with respect to internal variability (process stability over ranges). The evaluation is performed using the UCL_R and LCL_R boundaries, as well as eight features [3]. In our case, the sample range points do not violate the boundary $UCL_R = 0.11$ and $LCL_R = 0$, i.e. there is no sign 1, and also there is no presence of special structures of points described in signs 2–8 [3]. Consequently, the process is in a state of statistical control over the sliding ranges MR, i.e. regarding internal variability.

Knowing the value of the standard deviation of internal variability σ makes it possible to calculate the suitability index (opportunity index) of the process $C_p = T / 6\sigma$. If $Cp > 1$, then the process is suitable for fulfilling the specified requirements and there is a margin of process capabilities. For our example $Cp = 2{,}3 > 1$, the process is suitable for meeting the specified requirements and there is a margin of opportunity sufficient to control the progress of the process to meet the specified requirements.

The control chart of individual values shows an unstable process. There is no state of statistical control over individual *X* values.

We will check the quality assurance conditions for compliance with the requirements. On fig. 3 shows the layout of the result scattering field in relation to the target.

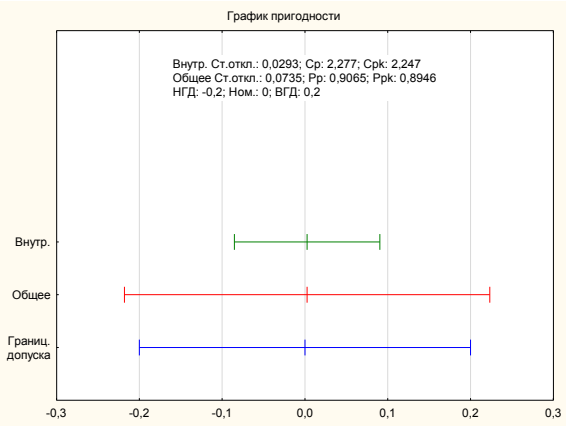

Figure 3. *Process suitability graph*

This figure shows that the scattering field of the results of the process $6\sigma = 0.44$ is greater than the tolerance $T = 0.4$. The upper and lower boundaries of the dispersion field of the results of the process go beyond the boundaries of the NGD

(Тн) and VGD (Тв) respectively. This process is shifted relative to the nominal value towards the upper tolerance limit Тв.

Checking the conditions for ensuring the quality of compliance with the requirements indicates that there may be *X* values that lie outside the tolerance limit and, as a result, product defects are possible. Therefore, it should be concluded that the quality of compliance with the requirements is not ensured.

Conclusions

As a result of the statistical analysis, it was established:

1) the process is in a state of statistical control with respect to internal variability (range-stable R);

2) the process is suitable to meet the specified requirements and has a sufficient margin of capabilities necessary to effectively manage the process: suitability index (capability index) Cp = 2.3;

3) the quality of the match for this sample is ensured. A slight shift of the scatter field of the scatter of the results of the process beyond the upper and lower tolerances did not lead to the appearance of marriage.

References

1. Stepanenko I.S., Pechenin V.A., Ruzanov N.V. Technique for improving the accuracy of GTE parts manufactured by selective laser sintering // IV International Conference and Youth School "Information Technologies and Nanotechnologies". — 2018. — P. 1672-1680

2. A. V. Sotov, A. V. Agapovichev, V. G. Smelov, Yu M. Anurov Investigation of the IN 738 superalloy microstructure and mechanical properties for the manufacturing of gas turbine engine nozzle guidevane by selective laser melting, International Journal of Advanced Manufacturing Technology (2020) 107:2525–2535.

3. Solonin S.I. Control chart method, electronic text edition. – Yekaterinburg: UFU, 2014.

DOI 10.34660/INF.2022.17.99.290
UDC 681.514

二阶Volterra级数非线性系统的极小极大自适应滤波算法
MINIMAX ADAPTIVE FILTERING ALGORITHM OF NONLINEAR SYSTEMS WITH VOLTERRA SERIES OF THE 2ND ORDER

Sidorov Igor Gennadievich
Candidate of Technical Sciences, Associate Professor at the Department of Software and Mathematical Methods of the Moscow Aviation Institute (National Research University)

抽象的。 本文利用二阶Volterra级数的非线性系统的极小极大自适应算法求解非线性系统的滤波问题，前提是根据最大根准则已知有用信号和干扰的自相关函数存在一定的误差。 -均方值过滤误差。

关键词：极小极大、滤波、线性、自相关、自适应、非线性、沃尔泰拉级数、干扰、梯度、强度、白噪声

Abstract. *The paper solves the problem of filtering nonlinear systems based on the minimax adaptive algorithm of nonlinear systems by Volterra series of the 2nd order, provided that the autocorrelation functions of the useful signal and interference are known with some errors according to the criterion of the maximum root-mean-square value filtering error.*

Keywords: *minimax, filtering, linear, autocorrelation, adaptive, nonlinear, volterra series, interference, gradient, intensity, white noise*

Introduction

In this paper, we study the problem of filtering nonlinear systems based on the minimax adaptive algorithm of nonlinear systems by Volterra series of the 2nd order, provided that the autocorrelation functions of the useful signal and noise are known with some errors. Quite a lot of approaches and methods have been developed to solve the problem of identification of nonlinear objects [1,2]. At the present stage, the requirements for the accuracy characteristics of the applied identification algorithms have increased. In this regard, classical approaches to solving the problem of identifying nonlinear systems are modified in order to increase their accuracy and reduce application restrictions [4], as well as universal search methods that require minimal a priori information about the identified system, but are difficult to implement. We also assume that the intercorrelation function of the useful signal and noise is equal to zero, and the random functions of the useful

signal and noise are stationary in the narrow sense [3] and are stationary related and have zero mathematical expectations. The quality criterion is considered to be the maximum root-mean-square filtering error. It is necessary to solve the problem of a minimax filtering structure in the form of a Volterra sequence, when a random signal at the input of the system is given with Gaussian white noise. The spectral intensities of the errors of the "noise additions" of the signal and interference are proportional to the magnitude of the errors with which the autocorrelation functions of the signal and interference are determined. It is shown that a 2nd order minimax Volterra filter (VF2) is equivalent to a parallel implementation of a minimax linear filter and a quadratic filter. A similar implementation of the VF2 filter was shown in [1,2] for the quality criterion in terms of the root mean square filtering error (MSFE). In the minimax formulation, the filtering problems by 2nd order Volterra series are solved for the first time, when efficiency is observed due to stable filtering with increasing intensity of white noise "additives", since the upper bounds in the MSFE asymptotic residual (MSFEAR) constraints for linear and quadratic filters are inversely proportional to the maximum eigenvalue for the autocorrelation matrix of the input signal with white noise in the presence of interference and its square, respectively. The purpose of this work is to study the convergence of the Volterra filter of the second order by the adaptive least mean squares (LMS) method. A Volterra filter with a constant step size μ at time-varying tuning is analyzed and a steady-state excess mean squared error (EMSE) quantification is performed, where the contributions of gradient misadjustment and tracking error are well characterized as a function of the maximum eigenvalue of the most unfavorable autocorrelation matrix of the input signal. In the first step, we quantify the excess mean square of the filtering error, and in the second step, we derive the optimal filter convergence learning step size. Similar problems are often encountered in radio engineering applications when estimating the amplitude of a deterministic signal with fluctuations in its shape and inaccurate noise corrections, that is, when it is hardly possible to determine the correlation function, which lies within a given convex-bounded family. Another example is the estimation of the regression parameters of a deterministic signal with an inaccurately known correlation function of both the main signal and the noise.

Formulation of the problem

Let's take a Volterra filter of the 2nd order, which consists of a parallel combination of linear and quadratic filters [1,2]:

$$y(n)=h_0+\sum_{j=0}^{N-1}a(j)x(n-j)+\sum_{j=0}^{N-1}\sum_{k=0}^{N-1}b(j,k)x(n-j)x(n-k), \qquad (1)$$

where $\{a(j)\}$ and $\{b(j,k)\}$ are called the linear and quadratic weights, respectively,

and N indicates the length of the filter (the filter's quadratic weights are assumed to be symmetric, i.e. $b(j,k) = b(k,j)$.. We will assume that the random signal $x(n)$ is an additive mixture of the useful signal and $s(n)$ of the noise $\xi(n)$

$$x(n) = s(n) + \xi(n), \tag{2}$$

moreover, $s(n)$ and $\xi(n)$ – are random stationary in the narrow sense [3] and stationary connected processes with zero mathematical expectation with a discrete parameter n, and their correlation functions are known with some errors δR_s and δR_ξ, respectively

$$\tilde{R}_s(n,n') = R_s(n,n') + \delta R_s(n.n'),$$

$$\tilde{R}_\xi(n,n') = R_\xi(n,n') + \delta R_\xi(n.n').$$

Here $R_s(n,n')$ and $R_\xi(n,n')$ - are assumed values (for example, some estimates of correlation functions). Everywhere below it is assumed that the cross-correlation function of the signal $x(n)$ and noise $\xi(n)$ is identically equal to zero, we also assume that $R_s(n,n'), \delta R_s(n,n'), R_x(n,n'), \delta R_x(n,n')$ is a symmetric function (in the class of generalized functions) of permutations of the arguments. These functions can be viewed as kernels of symmetric operators R_s, $\tilde{R}_s$, δR_s , R_ξ , $\tilde{R}_\xi$, δR_ξ on a Hilbert space. It is assumed, that $\xi(n)$ is the white Gaussian noise. It is believed that with respect to the errors δR_x and δR_ξ it is only known that they are bounded in the operator norm

$$\| \delta R_s \| \le \Delta_s, \| \delta R_\xi \| \le \Delta_\xi,$$

where operator norm $\| . \|$ is understood as the maximum eigenvalue of a symmetric operator.

Find the filter weights A and B, that minimize the maximum filter mean square error (MSFE) between $s(n)$ and the filter output $y(n)$, i.e.

$$e(A, B, R_s + \delta R_s, R_\xi + \delta R_\xi) = E[| s(n) - y(n) |^2] , \tag{3}$$

$$e_{макс}(A, B) = \max_{\|\delta R_s\| \le \Delta_s, \|\delta R_\xi\| \le \Delta_\xi} e(A, B, R_s + \delta R_s, R_\xi + \delta R_\xi) \tag{4}$$

VF2 implementation algorithm

In the definition of the minimum SEM of a 2nd order Volterra filter, there is a requirement for a driftless filter. Given the driftless filter output, in other words, it must be $E[y(n)] = 0$, since the main signal has zero mathematical expectation. Then we get the following relation for VF2 [2] :

$$y(n) = \sum_{j=0}^{N-1} a(j)x(n-j) + \sum_{j=0}^{N-1}\sum_{k=0}^{N-1} b(j,k)[x(n-j)x(n-k) - r_x(j-k)], \tag{5}$$

where

$$r_x(j) = E[x(n)x(n-j)]$$

denotes the autocorrelation function of $x(n)$, E - is the expectation symbol.

Expression (5) for VF2 can be represented in the equivalent matrix form

$$y(n) = \mathrm{A}^{\mathrm{T}}\mathrm{X(n)} + tr\{\mathrm{B}[\mathrm{X(n)X}^{\mathrm{T}}\mathrm{(n)} - \mathrm{R_x}]\}, \quad (6)$$

where trA denotes the trace of a square matrix $A = \{a_{kj}\}_{k=\overline{1,N}}^{j=\overline{1,N}}$, that is, the sum of its diagonal elements:

$$tr\mathrm{A} = \sum_{k=1}^{N} a_{kk},$$

and $\mathrm{R_x}$ denotes the size $N \times N$ autocorrelation matrix of the function $x(n)$, whose (j,k) -th element is equal to $r_x(j-k)$.

$$\mathrm{X}(n) = [x(n), x(n-1), ..., x(n-N+1)]^T,$$
$$\mathrm{A} = [a(0), ..., a(n-N+1)]^T,$$

$$\mathrm{B} = \begin{pmatrix} b(0,0) & \dots & b(0,N-1) \\ & \dots & \\ b(\mathrm{N}-1,0) & \dots & b(N-1,N-1) \end{pmatrix}$$

Taking into account the decomposition of the entire MSFE $e(\mathrm{A,B,R_s} + \delta\mathrm{R_s}, \mathrm{R_\xi} + \delta\mathrm{R_\xi})$ into a linear MSFE1 and a quadratic MSFE2, we obtain a representation of the linear and quadratic operators VF2 with the minimum MSFE in the form [6]:

$$\mathrm{A_0} = \mathrm{R_x^{-1}R_{sx}},$$

$$\mathrm{B_0} = \frac{1}{2}\mathrm{R_x^{-1}T_{sx}R_x^{-1}}, \quad (7)$$

where the cross-correlation and bi-cross-correlation elements of the R_{sx} and T_{sx} matrix functions, respectively, are defined as follows

$$r_{sx}(j) = E[s(n)x(n-j)],$$
$$t_{sx}(j,k) = E[s(n)x(n-j)x(n-k)] \quad (8)$$

It can be seen from (5) and (6) that the linear operator of the optimal VF2 is the same as the optimal minimax linear filter. Therefore, it is possible to design VF2 simply by adding a quadratic filter to the created optimal minimax linear filter without changing it, that is, as a linear filter in the sense of criterion (4), one can use the minimax filter A^*, which minimizes the maximum MSFE from (4) (in a given class of linear filters) over all the least favorable values of the correlation operators $\mathrm{R_s^*}$ and $\mathrm{R_\xi^*}$

$$e_{макс}(A^*) = \min_{A} \max_{\|\delta R_s\| \le \Delta_s, \|\delta R_\xi\| \le \Delta_\xi} e(A, R_s + \delta R_s, R_\xi + \delta R_\xi) =$$

$$= \min_{A} \max_{R_s^*, R_\xi^*} e(A, \tilde{R}_s, \tilde{R}_\xi) = \max_{R_s^*, R_\xi^*} \min_{A} e(A, R_s^*, R_\xi^*) = \min_{A} e(A, R_s^*, R_\xi^*), \quad (9)$$

Moreover, the least favorable values of the correlation operators will be equal to

$$R_s^* = R_s + \Delta_s I, R_\xi^* = R_\xi + \Delta_\xi I \quad (10)$$

Here I is the unit operator, Δ_s and Δ_ξ are the intensities of the "additives" of white noise. Let us explain the meaning of the term "additives" intensity of white noise. Since the error in the knowledge of the correlation function of fluctuations or a random signal is compensated by adding an additive in the form of white noise with a spectral intensity Δ_ξ or Δ_s, respectively, which increases with an increase in the error δR_ξ or δR_s, then the sum of $R_\xi + \Delta_\xi I$ or $R_s + \Delta_s I$ is equivalent to adding additional white noise to fluctuations or a random signal. The operator form of representation (10) is similar to the matrix correlation representation, in which the identity matrix I corresponds in operator form to the identity operator in the form of the Dirac delta function, and the matrices $\Delta_\xi I$ and $\Delta_s I$ are the correlation matrices of the white noise additives, respectively, of the spectral intensity Δ_ξ and Δ_s, and the kernels of the symmetric operators R_ξ and R_s represent the respective correlation matrices. As is known [7], the minimax filter in this case takes the form

$$A^* = R_s^*(R_s^* + R_\xi^*)^{-1}, \quad (11)$$

and its maximum MSFE is written as

$$e_{макс}(A^*) = \mathrm{tr} R_s^*(R_s^* + R_\xi^*)^{-1} R_\xi^*$$

Thus, it is possible to design VF2 simply by adding a quadratic filter in parallel to the created minimax filter without changing it and losing significant accuracy.

Therefore, by introducing “noise additions” to the main signal and noise, we can achieve a significant gain for the asymptotic residual of the MSFEAR root-mean-square error, due to an increase in the maximum eigenvalue of the auto-correlation matrix, which is equivalent to a decrease in the training adaptation coefficient in inverse proportion to this maximum eigenvalue , due to the choice of the least unfavorable noisy signal and noise correlation matrices, respectively, for the minimax linear filter. Let the value of the variance according to the criterion of the worst mean square error for the implementation of VF2 be limited by the value ξ_{opt} [f-la (12), 6]

$$\xi_{opt} = r_s(0) - R_{sx}^{\mathrm{T}}(R_x^*)^{-1} R_{sx} - (\frac{1}{2})\mathrm{tr}[R_x^{-1} T_{sx} (R_x^*)^{-1} T_{sx}], \quad (12)$$

where $R_x^* = R_x + \Delta_x I$,

$$r_s(0) = E[s^2(\mathrm{n})], R_{sx} = R_x^* A, \mathrm{T_{sx}} = 2\mathrm{R_x^* B R_x^*}$$

Here Δ_x corresponds to the intensity of the total "additives" of white noise in the input signal $x(n)$.

The least squares method for linear and quadratic weights of the adaptive filter VF2, respectively, A(n) and $B(n)$ can be represented as a stochastic version of the steepest descent method (LMS) in the following form [6]

$$\mathrm{A(n+1) = A(n) - 2\mu A e(n) X(n)}$$

$$\mathrm{B(n+1) = B(n) - 2\mu B e(n) X(n) X^T(n)} \quad (13)$$

The learning constants $\mu\mathrm{A}$ and $\mu\mathrm{B}$ determine the stability and convergence of the adaptive filter, $e(n) = y(n) - s(n)$. Note that the linear and quadratic optimal weighting coefficients VF2 change in this case according to the following dependence

$$\mathrm{A_0(n+1)=A_0(n)+\delta A_0(n)},$$

$$\mathrm{B_0(n+1)=B_0(n)+\delta B_0(n)}, \quad (14)$$

where $\delta\mathrm{A_0(n)} = \mathrm{A_0(n)} - \mathrm{A_0}$ and $\delta\mathrm{B_0(n)} = \mathrm{B_0(n)} - \mathrm{B_0}$ – essence of deviation and $\mathrm{A_0(n)}$ and $\mathrm{B_0(n)}$ from their optimal values.

As shown in [6], in the adaptive implementation of VF2, fluctuations of the linear and quadratic filter operators add some additional SEM to the output value of the filter even when the adaptive process is in a stable position, that is, the asymptotic SEM of the adaptive VF2 is generally greater than the SEM of the optimal VF2. To estimate the residual SEM, we write the adaptive VF2 SEM as

$$\xi(\mathrm{n}) = \xi_{opt} + \xi_A(n) + \xi_B(\mathrm{n}),$$

where excess rms residuals $\xi_A(n)$ and $\xi_B(\mathrm{n})$ in the adaptive implementation of VF2 have the form

$$\xi_A(n) = E[tr\{\delta\mathrm{A^T(n) R_x \delta A(n)}\}]$$

$$\xi_B(\mathrm{n}) = E[tr\{\delta\mathrm{B^T(n) R_x \delta B(n)}\}]$$

The asymptotic MSFE estimates for the linear minimax and quadratic filters of the VF2 implementation can be estimated from above through the estimate of $r_s(0)$ as follows [6]

$$\xi_\mathrm{A} \le 4\mu\mathrm{A}\xi_\mathrm{opt}\mathrm{N r_s(0)},$$

$$\xi_\mathrm{B} \le 3\mu\mathrm{B}\xi_\mathrm{opt}\mathrm{N^2 r_s(0)} \quad (15)$$

The training steps μA and μB for the linear minimax A quadratic filters B are respectively chosen from the conditions

$$0 \le \mu A \le \lambda_{\max}^{-1}, 0 \le \mu B \le \lambda_{\max}^{-2},$$

where $\lambda_{\max}$ is the maximum eigenvalue of the matrix R_x^*, which is greater than the maximum eigenvalue $\lambda_{\max}$ of the matrix R_x by the value Δ_x according to Weyl's theorem [Weil's theorem (4.3.1.), 8]. It can be seen from the representation estimates for MSFEAR in (12) that by increasing the maximum eigenvalue of the matrix R_x^* it is possible to increase the stability and convergence of the algorithm and obtain a gain η in terms of root-mean-square errors, which shows the presence of additional information about disturbances in the correlation matrix R_x of the main signal and the correlation matrix R_ξ, in particular, for the case of jointly Gaussian random processes $x(n)$ and $s(n)$ we have

$$T_{sx} = 0$$

and the expression for the gain η by the minimax mean square error with respect to the mean square error for the filter built according to the proposed values of R_s and R_ξ, takes the form in matrix form similar to that in operator form [f-la (5), 7]

$$\eta = 1 + \frac{\mathrm{tr}(\Delta_s R_s - \Delta_\xi R_\xi)^2 (R_s + R_\xi)^{-2} (R_s + R_\xi + \Delta_x I + \Delta_\xi I)^{-1}}{\mathrm{tr}(R_s + \Delta_s I)(R_s + R_\xi + \Delta_s I + \Delta_\xi I)^{-1}(R_\xi + \Delta_\xi I)} \qquad (16)$$

The larger Δ_s or Δ_ξ, the greater the efficiency of the minimax filter, and hence the 2nd order Volterra filter (VF2). In particular, for $\Delta_\xi I >> R_\xi$, $\Delta_s = 0$ the gain estimate η will be linearly dependent on the value of the noise additive Δ_ξ and will be equal to

$$\eta \cong 1 + \Delta_\xi \frac{tr R_\xi^2 (R_s + R_\xi)^{-2}}{tr R_\xi} \qquad (17)$$

Similarly to this case, we can consider another extreme case for $\Delta_s I >> R_s$, $\Delta_\xi = 0$ and obtain an estimate for the payoff η in the form

$$\eta \cong 1 + \Delta_s \frac{tr R_s^2 (R_s + R_\xi)^{-2}}{tr R_s} \qquad (18)$$

It can also be shown that with a slow change in the parameters of the learning adaptation model VF2, the optimal value of the training step will be equal to

$$\mu_{opt} = \mu A = \mu B = \sqrt{\frac{N(\sigma_{NSA}^2 + \sigma_{NSB}^2)}{J_{\min}[4N\sigma_x^2 + 2tr(R_x^2) + N^2(\sigma_x^2)^2]}}, \qquad (19)$$

where

$$\sigma_x^2 = E[x^2(n)],$$

$$J_{\min} = \mathrm{cov}(e(n)),\ e(n) = y(n) - s(n),$$

$$\sigma_{NSA}^2 = \mathrm{cov}(\Delta A_0(n)) = \tfrac{1}{N} E[\mathrm{tr}(\Delta A_0 \Delta A^T{}_0)],$$

$$\sigma_{NSB}^2 = \mathrm{cov}(\Delta B_0(n)) = \tfrac{1}{N} E[\mathrm{tr}(\Delta B_0 \Delta B_0^T)]$$

that is, as it follows from (18), the efficiency of the obtained 2nd order optimal Volterra filter (VF2) in terms of the training adaptation step is also inversely proportional with a significant increase in the level of noise additives in disturbances in the correlation matrix R_x of the main signal.

An example of the efficiency of a 2nd order Volterra filter with the simultaneous implementation of a linear minimax filter

To illustrate the effectiveness of the algorithm, computer simulations were carried out. A linear minimax filter as an equivalent replacement for a linear filter was used to evaluate a second-order Volterra system with Gaussian input $x(n)$, i.e. there is additive Gaussian white noise in the input signal $x(n)$ and output $y(n)$ in a non-stationary and noisy environment on a model example:

$$y(k) = x(k) - 0.5x(k-1) + x^2(k) + 0.1x^2(k-1) - 0.4x(k)x(k-1) + n(k)$$

In the output signal $y(n)$, $n(k)$ denotes white noise of known intensity. Fig. 1 shows a plot of the optimal learning step size μ_{opt} versus value J_{min} on various intensities of the "noise additive" Δ_x in the noise of the input signal $x(n)$ with constant covariances σ^2_{NSA} and σ^2_{NSB} of the deviations of the parameters of the weight coefficients A(n) and $B(n)$ and a constant signal-to-noise ratio SNR in observing the output signal $y(n)$ equal to 25 dB.

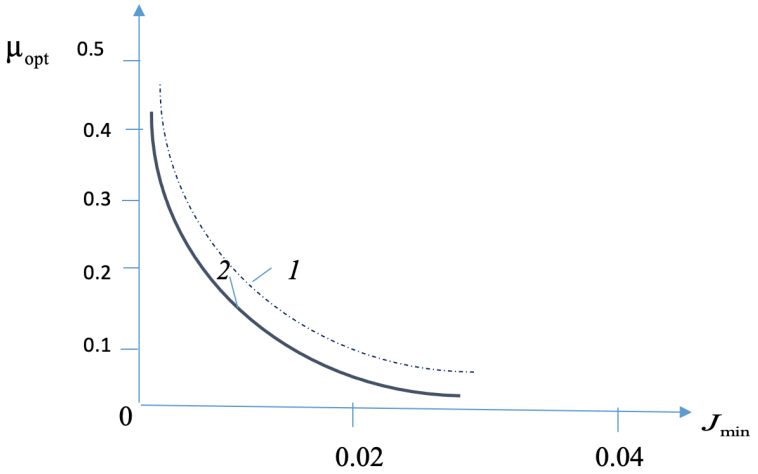

Figure 1. *A graph of the dependence of the optimal size of the learning step* μ_{opt} *on the magnitude* J_{min} *of the various values of the intensities of the "noise additive". 1) dotted graph –* Δ_x *=10; 2) solid graph -* Δ_x *= 5 SNR=25 dB,* $\sigma^2_{NSA} = \sigma^2_{NSB} = 2.5*10^{-6}$, $\sigma_x = 0.0017$

From plotting the dependence of the optimal size of the learning step μ_{opt} on the value J_{min} on various values of the intensities of the "noise additive" Δ_x in the noise of the input signal $x(n)$ it can be seen that with an increase in the level of intensities Δ_x the value of the optimal learning step monotonically decreases and reaches the optimal constant level on the second learning curve, which is consistent with the theoretical conclusions made above in the context of the article on the optimal behavior of the adaptation step depending on the level of change in the intensities of noise additives in an additional increase in the noise level of the input signal.

Conclusion

Thus, the problem of determining the linear and quadratic Volterra filter operators of the 2nd order with a minimax mean square error for identifying nonlinear stationary systems has been solved and implemented in an algorithmic form. The efficiency of the adaptive stable Volterra filter of the 2nd order is shown for jointly Gaussian random processes of useful and observed signals under conditions of an inaccurately known signal in noise and with inaccurately known correlation properties. The next task will be to improve this method and use the Volterra filter to identify multidimensional dynamic nonlinear control systems with interval parameters in the problems of estimating regression interval parameters of a useful signal.

References

1. Pupkov K.A., Kapalin V.I., Yushchenko A.S. Functional series in the theory of nonlinear systems.-Moscow:Nauka,1976.448 p.

2. Pupkov K.A., Tsibizova T.Yu. Implementation of the second-order Voltaire filter for identification of nonlinear control systems // technomag.edu.ru : Science and Education: electronic scientific and technical publication. — 2006. — Issue 6. — URL - http://technomag.edu.ru/doc/58741.html. (accessed 19.01.2015)

3. Pugachev V.S. Theory of random functions, Fizmatgiz, 1962.

4. Lukyanova N.V., Kuznetsov I.A. Identification of nonlinear dynamic systems based on the decomposition of functionals by the Wiener method // Materials of the conference "Management in marine and aerospace systems" (UMAS-2014).— St. Petersburg, 2014.

5. Sidorov I. G., Levin V. I. Linear minimax interpolation of a stationary random process with interval parameters // Control, communication and security systems. 2021. No. 1.pp. 215-242.

6. Taiho Koh, Edward J.Powers, "Second-Order Volterra Filtering and its Application to Non-Linear System Identification," IEEE Transaction on acoustics, speech, and signal processing, vol. ASSP-33, no. 6, pp. 1445-1455, December 1985.

7. Kuznetsov V.P. On stable linear filtering of random signals // Radio Engineering and electronics. 1975. No. 1.pp. 2405-2408.

8. Horn R., Johnson Ch. Matrix analysis. Moscow: Mir, 1989.

DOI 10.34660/INF.2022.20.29.291

惯性运动的物理解释
PHYSICAL EXPLANATION OF INERTIA MOTION

Tiguntsev Stepan Georgievich
Candidate of Technical Sciences, Associate Professor
Irkutsk National Research Technical University

抽象的。牛顿第一定律被接受为假设，即没有证据和实验支持的陈述。假设中的陈述可能是错误的，随后被认为是不正确或不准确的。科学的基本任务是要么证明一个假设，要么用另一个由证据和实验证实的陈述代替它。

陈述 – 真正的惯性现象（物体的惯性运动）仅由于外力的径向性质 – 球体上的重力，即地球或其他空间物体的曲线表面，才可能发生。在局部绝对参考系（LARS）中考虑惯性而不是 IFR，即 RS，其原点位于具有重力的物体 – 引力物体（GO）的中心。

惯性运动存在的条件（据说是物体的“先天属性”）被制定——这是重力的存在，这是 GO 的球形度，这是对特定 GO 的绑定。

牛顿惯性定律中不存在这些条件。而且，惯性现象的发现者伽利略在描述这种现象时，指出了地球的球形，而牛顿却忽略了伽利略的指示。

惯性定律的以下表述被提出：“每个物体保持其静止状态或沿等势轨迹围绕引力物体中心的均匀曲线运动，直到其他物体通过它们的动作改变这种状态”。

关键词：假设，牛顿第一定律，惯性运动，引力物体，局部绝对参考系。

Abstract. *Newton's first law is accepted as a postulate, i.e. a statement not supported by evidence and experiments. The statements made in the postulates may be erroneous and subsequently recognized as incorrect or inaccurate. The fundamental task of science is the task of either proving a postulate, or replacing it with another statement confirmed by evidence and experiments.*

The statement - the real phenomenon of inertia (movement of bodies by inertia) is possible only due to the radial nature of the external force - gravity on the spherical, that is, the curvilinear surface of the Earth or other space object. Instead of IFR, inertia is considered in the Local Absolute Reference System (LARS), i.e. RS, the origin of which is located in the center of an object that has gravity - a gravitating object (GO).

The condition for the existence of motion by inertia (supposedly an "innate property" of bodies) is formulated - this is the presence of gravity, this is the sphericity of GO, this is a binding to a specific GO.

None of these conditions exist in Newton's law of inertia. Moreover, the discoverer of the phenomenon of inertia, Galileo, pointed to the sphericity of the Earth when describing this phenomenon, but Newton ignored Galileo's instructions.

The following formulation of the law of inertia is proposed: "Every body retains its state of rest or uniform and curvilinear motion around the center of a gravitating object along an equipotential trajectory until other bodies change this state by their action".

Keywords: *postulate, Newton's first law, inertial motion, gravitating object, local-absolute frame of reference.*

Newton's first law is accepted as a postulate, that is, a statement not confirmed by evidence and experiments. Usually, on the basis of a postulate, a theory is created that explains a particular phenomenon. The postulate is necessary in the case when the observed phenomenon cannot be explained on the basis of known physical concepts and available theories. Science is the art of understanding nature. The statements made in the postulates may be erroneous and subsequently recognized as incorrect or inaccurate.

At the heart of the modern understanding of the world are observations and measurements. Theories are built on them, which are then tested by experience. In research, the scientific method is usually used, namely, this sequence of actions: observation, reasoning (theory) and experience (testing the theory - proving its validity).

The theory establishes a connection between various facts and must take into account all available information. However, in the case of the phenomenon of inertia, all the information and the connection between the facts were not taken into account. The fundamental task of science is the task of either proving a postulate, or replacing it with another statement confirmed by evidence and experiments.

For the first time, the concept of real inertia was formulated by the Italian scientist Galileo Galilei (1564-1642) as a short term for the ability of a body to move curvilinearly (along the circumference of the Earth's surface) and uniformly, but for no reason.

This is stated in the work of G. Galileo "Dialogue on the two main systems of the world - Ptolemaic and Copernican", second day:

Salviati. Therefore, a ship moving on the surface of the sea is one of those moving bodies that slide on one of these surfaces without inclination and rise, and which therefore tend, if all accidents and external obstacles are eliminated, to move constantly and evenly with the momentum received?

Simplicino. Seems like it should be…".

It should be noted that in almost all physics textbooks G. Galileo for some reason is credited with the formulation of the concept of inertia, which refers to

the straightness of motion.

The English physicist and mathematician Isaac Newton (1643-1727) formulated the law of abstract inertia (literally): "Every body remains at rest or moves in **a rectilinear** fashion at a constant speed, unless it is acted upon by a force that changes the speed of the body" (Newton's first law), in the modern formulation "Every body retains its state of rest or uniform and **rectilinear** motion until unbalanced external forces (or until the influences of other bodies) force it to change this state". Since that time, in my opinion, the prejudice has **come into physics** that the movement by inertia is rectilinear, and the prejudice remains that such a movement **does not need** an external influence to maintain it.

So what is inertia? First of all, it is a real physical phenomenon that each of us feels in everyday activities. Inertia is manifested in the "unwillingness" of the body to change its state in space. If the body is in a state of rest, then to transfer it to a state of motion, the action of a force is necessary; if the body is in a state of motion, then an application of a force is also necessary to change its state. At the same time, the manifestation of inertia is most noticeable on a daily basis when the body moves along a horizontal surface after the end of the application of force - for example, the movement of a car with the engine turned off.

I propose the statement that the real phenomenon of inertia (movement of bodies by inertia) is possible only due to the radial nature of the external force - gravity on the spherical, i.e., curvilinear surface of the Earth or another space object. In addition, the ability to single out one frame of reference (the surface of the Earth) in relation to others (moving relative to the surface) by simple experiments refutes the essence of Galileo's principle of relativity. And this reference system is the Local Absolute Reference System (LARS), i.e. CO, the origin of which is located in the center of an object with gravity - a gravitating object (GO).

Below is an explanation of how the force of gravity is converted into a force that causes inertial motion. A body with mass **m** is affected by the force of gravity $\dot{F}$, which is equal to the product of the mass **m** and the gravitational acceleration vector (GAV) $\dot{g}$**.** The forcen $\dot{F}$, being the product of a scalar quantity and a vector quantity, is also a vector quantity. At two points 1 and 2 spaced apart from each other, on a horizontal (for each point) surface of the Earth, a body with mass **m** is affected by gravity forces $\dot{F}_1$ and $\dot{F}_2$, equal to the product of the mass **m**, respectively, by the vectors of gravitational accelerations $\dot{g}_1$ and $\dot{g}_2$, whose modules are the same. In this case, we will assume that the vectors $\dot{g}_1$ and $\dot{g}_2$, converge at the center of the Earth at an angle φ (Fig.1), placing them on the scale of the Earth's radius R from the Earth's surface to its center (point O). The force vectors $\dot{F}_1$ and $\dot{F}_2$ are also equal in absolute value and converge in the center of the Earth at an angle φ to each other (Fig.1). For clarity, the figures show the vectors at a sufficiently large angle to each other, although this angle can be arbitrarily small.

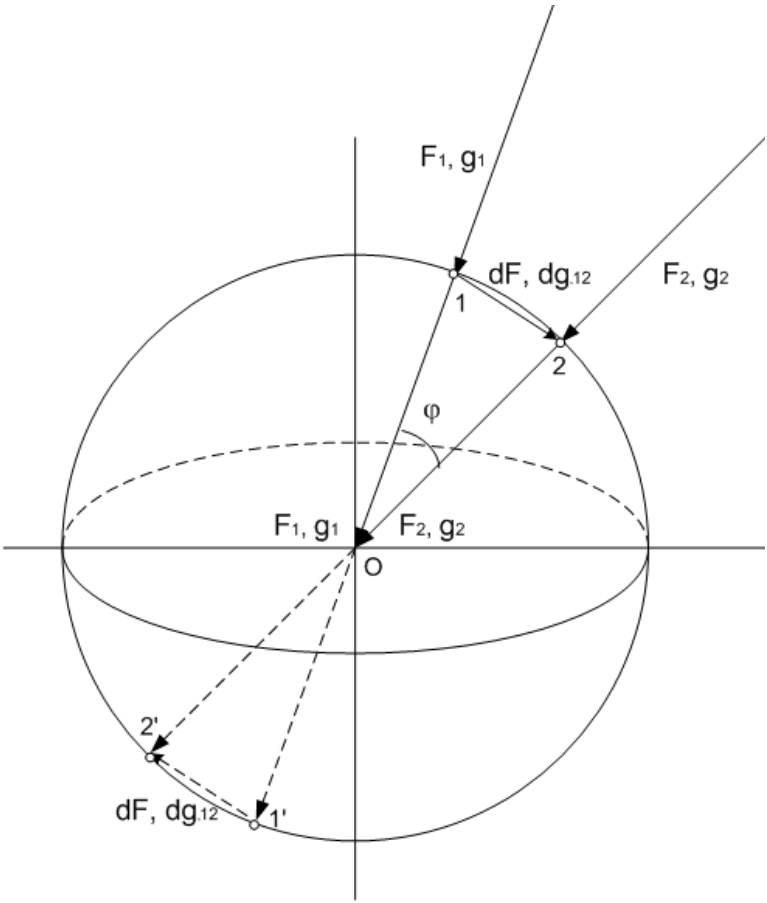

Figure 1

Let us assume that the body, after applying the force impulse, is in a state of uniform motion along the "horizontal" (essentially curvilinear) surface of the Earth from point 1 to point 2 in the absence of braking effects of the surface and air. Moreover, it will be horizontal at point 1, at point 2, but the path between these points is curvilinear, even in a section of 1 meter or less in length, with a radius of curvature equal to the radius of the Earth and a very specific value of the angle between the two radii.

During its uniform motion from point 1 to point 2, this body is constantly affected by a force equal to the difference between the forces $\dot{F}_2$ and $\dot{F}_1$ (in accord-

ance with Fig.1, we move the origin of the vectors $\dot{F}_2$ and $\dot{F}_1$ to point 0, for two vectors $\dot{F}_2$ and $\dot{F}_1$, having a common point 0, we can apply the rule for subtracting force vectors). The vector $\Delta\dot{F}$ (in the figure *dF*), equal to the difference between the vectors $\dot{F}_2$ and $\dot{F}_1$ represents a force that, being external to the body, acts from point 1 to point 2 and ensures uniform movement of the body along the curvilinear surface of the Earth, arbitrarily long in the absence inhibitory reasons.

Thus, the force acting on a body of mass **m** is determined by the formula:

$$\Delta\dot{F} = m * (\dot{g}_2 - \dot{g}_1) \quad (1)$$

In expression (1), the difference of the vectors $\Delta\dot{g} = (\dot{g}_2 - \dot{g}_1)$ (in Fig. 1 - dg) represents the acceleration, which is constantly provided by the force $\Delta\dot{F}$. **The indicated acceleration is related to the free fall acceleration, with the only difference being that the free fall acceleration always acts, and this acceleration only from the moment when the body is in a state of uniform motion after the application of force.**

In order to be able to operate with the force $\Delta\dot{F}$ in the aggregate of other forces, it should be reduced to a single dimension, for which it is necessary to determine the angle φ between the free-fall acceleration vectors $\dot{g}_1$ and $\dot{g}_2$, directed from the surface of the GO to its center, which is formed between the vectors when the body passes along equipotential trajectory of distance *S* in 1 second in a state of uniform motion. Uniform motion can continue for an arbitrarily long time, so it is necessary to choose a time interval that would be commensurate with the dimension of other physical quantities. Since the second is used in the dimension of force and acceleration of free fall, we consider the path in 1 second.

$$S=V*1\ sec. \quad (2)$$

From geometry, knowing the length of the arc S, the angle can be determined by the formula:

$$\varphi = S/R. \quad (3)$$

The same angle through g and Δg is defined as:

$$\varphi = \Delta g/g. \quad (4)$$

Further, from (3) and (4) we obtain:

$$\Delta g = g * S/R. \quad (5)$$

Or magnitude

$$\Delta g = g * V * 1c/R. \quad (6)$$

The acceleration vector $\Delta\dot{g}$ has the direction of velocity, i.e. every 1 second is directed along the chord of the circumference of the Earth.

Under the influence of this constantly acting force ($\Delta\dot{F}$) the body is in a state of uniform motion with a speed:

$$\dot{V} = (\dot{g}_2 - \dot{g}_1) * R/\dot{g} * 1c \quad (7)$$

Each value of the speed V of the uniform motion of the body corresponds to its own value of the value obtained by (6), let's call this value the acceleration of "tiguntia" (the term "tiguntia" was proposed by opponents during a discussion on forums on the Internet).

The specified value is called acceleration, because it has the dimension m/s^2, however, given that the movement occurs in a circle, it is uniform at a given acceleration.

It follows from this that, having ensured the uniform movement of the body along the "horizontal" (i.e. along the curvilinear, spherical) surface of the Earth, we provide a certain amount of acceleration "tiguntia", which remains constant throughout the entire path of uniform movement of the body, up to non-stop movement around the circumference of the Earth, naturally, in the absence of inhibitory causes. This constancy is maintained by the forces of gravity, due to their radial nature.

It will be more clear if we consider the process in terms of the intensity of the gravitational field (GF). The GF tension always exists, even if there is no mass. Tension is a vector quantity equal to GAV. How the vectors are located - can be seen in Fig. 1.

Accordingly, between any two points on an equipotential spherical surface, there is always a vector difference in strengths GF, due to the presence of an angle between the vectors. Accordingly, this vector difference acts on any body moving along this surface. Here you should pay attention to the most significant point that needs to be understood - therefore, I will repeat once again the text of my previous explanation "... **there is always a vector difference of strengths GF between any two points on an equipotential spherical surface, due to the presence of an angle between the vectors** ...". That is, it does not matter if there is a body or not, but it is important that the vector difference of intensities GF (or GAV) between any two points ALREADY EXISTS. And as soon as a moving body falls into the conditions of this difference, the movement of which arose as a result of the action of the applied force, this vector difference begins to act on this body.

I repeat the thought once again - there are many points on the equipotential surface, between each of them there is ALWAYS tension GF (vector difference of radial tensions GF). As soon as a body that has some speed falls into the conditions of this difference, then the vector difference of intensities GF will continue to maintain this movement with this speed FOREVER (if there are no forces of resistance to movement).

Let me remind you that the force of gravity moves the body accelerated radially, and the force due to the vector difference in the forces of gravity moves the body uniformly along the equipotential surface.

Let us show on the calculation example the magnitude of accelerations for uniform motion on the surface of the Earth. Let a body moving uniformly with a speed of V=10 m/s, We obtain by formula (6) that in this case the body moves with a constant acceleration directed along the chord of $\Delta g=0.0000153$ m/s^2 . For the first cosmic velocity near the Earth's surface $\Delta g=0.0215$ m/s^2

One of the main issues in the dynamics of motion is the question of the dependence of the force ΔF on the force F_{pr}, applied to the body, determined by Newton's second law. Let's consider the processes occurring at the occurrence of the physical phenomenon INERTIA. A body with a mass **m**, located on a "horizontal" platform in the absence of braking causes, is subjected to a contact effect in the form of an applied force F_{pr}. At the moment of impact of the applied force, it will be counteracted by a force unknown to the science of nature, which is called the "force of inertia" (the nature and reason for this resistance is not known).

What is the nature of this resistance? - counteracts the gravitational field, or rather one of its properties, due to the radial nature of gravity. The magnitude of this counteraction is determined by the mass of the body and the acceleration that the body acquired, overcoming the action of the gravitational field. In physics, it is customary to call this force the force of inertia.

Simultaneously, the applied force F_{pr} is converted into a force ΔF**.** aking into account the difference in the nature of the forces, we introduce a new concept - the force of "tiguntia" (the name was proposed by opponents during a discussion on forums on the Internet) $F_{tg} = \sum \Delta F$**,** which is directed in the same direction as the applied force (the force of inertia is directed oppositely applied force and acts only at the moment of application of the force, and the "tiguntia" force acts after the end of the application of force in the direction of the applied force) in accordance with the expression:

$$F_{tg} = F_{pr} * g * \Delta t * t/R \quad (8)$$

Where: g – GAV module; Δt – coefficient of time dimension (corresponds to 1 second if the second is used in the dimension of force and g); t – is the time during which the force F_{pr} was applied to the body; R – the distance to the center of the gravitating object (here the Earth).

As a result of the applied force F_{pr} the body will acquire a uniform motion velocity V and will continue to move at this velocity for an infinitely long time under the influence of the "tigunting" force:

$$F_{tg} = m * g * V * 1c/R \quad (9)$$

The constancy of this force is provided by the gravitational field, the force effect of which is infinite. Here it should be clarified that the "tiguntia" force arises and gradually increases during the transformation of the applied force. The transformation mechanism is as follows: the applied force acts on the body, this force

is counteracted by the inertia force, these forces are equal in magnitude only at the first moment of time, however, the applied force increases and the inertia force does not "keep up" with the applied force by the value ΔF and the body starts to move. As soon as the body has moved from its place, the first portion of ΔF goes to the treasury of the force F_{tg}. The applied force again becomes equal to the inertia force, which accordingly decreased by ΔF, but the applied force increases again - the body increases speed, the next portion of ΔF goes to the F_{tg} force treasury, and so on until the applied force acts. Thus, the mechanism of formation of the force "tiguncia" is discrete-constant.

Summarizing the above, we note that:

1. There is no place anywhere in the universe where there is no gravity. Those. any movement occurs with the OBLIGATORY participation of gravity. This means that it is unacceptable to exclude gravity from the problems of motion. Accordingly, the law about this most innate property of bodies, in which there is no indication of gravity, should be considered limited, incomplete (defective).

2. Everywhere in the Universe, the source of gravity is gravitating objects (GO), as a rule, having the shape of a ball (or close to this shape). This means that in the law about the "innate property" of bodies there should be an indication of the sphericity of GO.

3. A body can be at rest only on the surface of the GO; in any other case, the body moves either relative to the GO or together with the GO.

Thus, it is possible to formulate the condition for the existence of an allegedly "innate property" of bodies - this is the presence of gravity, this is the sphericity of the GO, this is binding to a specific GO.

None of these conditions exist in Newton's law of inertia. Moreover, the discoverer of the phenomenon of inertia, Galileo, pointed to the sphericity of the Earth when describing this phenomenon, but Newton ignored Galileo's instructions.

The following formulation of the law of inertia is proposed: **"Every body retains its state of rest or uniform and curvilinear motion around the center of a gravitating object along an equipotential trajectory until other bodies change this state by their action".**

DOI 10.34660/INF.2022.10.79.292

用博弈论工具对自然垄断市场进行国家调控

STATE REGULATION OF THE NATURAL MONOPOLY MARKET WITH THE GAME THEORY APPARATUS

Shamsivaleev Timur Nailevich
Postgraduate

Panyukov Anatoly Vasilievich
Doctor of Physico-mathematical Sciences, Full Professor, Lead Research Officer

Chelyabinsk Mechanics and Technology Institute

抽象的。 该研究的目的是开发一种模型算法，旨在提高国家对自然垄断市场中商品分配的监管方法的有效性。 作为监管方法，考虑使用非价格杠杆，同时假设系统是封闭的，即国家只在市场内重新分配资金。

关键词：非合作博弈； 国家监管； 自然垄断市场； 平衡。

Abstract. *The aim of the study is to develop an algorithm for a model aimed at increasing the effectiveness of methods of state regulation of the distribution of goods in the natural monopoly market. As methods of regulation, the use of non-price levers is considered, while it is assumed that the system is closed, i.e. the state only redistributes funds within the market.*

Keywords: *non-cooperative game; state regulation; natural monopoly market; equilibrium.*

Introduction

State regulation of markets with a high degree of monopolization is one of the most important economic problems both at the level of the state and any administrative-territorial entity. The most effective way to regulate monopolized markets is tariff regulation. At the moment, tariffs are formed exclusively by the cost method, which does not allow monopolies to receive excess profits, but at the same time the competitive component of the market is not regulated in any way. In this regard, the regulation of natural monopoly markets is of particular difficulty.

The greatest difficulty in developing methods for regulating monopolized markets (especially markets with a natural monopoly) is created by an unstable situation related to the opposition of the interests of the state as a guarantor of the supply of the population with benefits for life support, the supplier of which is

usually a natural monopolist, and, on the other hand, as a defender of the market free competition [1]. This situation requires constant state intervention in order to balance the interests of society and the monopoly [2].

1. Model of the market environment of the state

The apparatus of game theory is used to analyze the situation on the market and resolve the conflict. Player *M* (monopoly) offers a product to consumers, seeking to maximize profits by increasing the price of the product. Player *П* (consumers), comparing the characteristics of the goods and the benefits from them with the requested price, determines the amount of demand for each of the goods. A decrease in the demand for the product of player *П* affects the amount of profit received from the sale of this product by player *M*.

Since player *П* has a multiple structure, the need for each product is formed independently by each of the consumers. Since all consumers in the natural monopoly market are characterized by similar properties (the impossibility to single-handedly influence the market, the impossibility of creating meaningful coalitions in its pure form, etc.) and the same goal (maximizing consumer utility), we will consider the entire set of consumers as a single player.

From the standpoint of the game-theoretic approach, the game process in the market can be expressed in general form as a tuple

$$\Gamma = (\{M, \Pi\}\{X_M, X_\Pi\}\{H_M, H_\Pi\}), \quad (1)$$

where *M* – monopolist; $X_M = I = \{1, 2, ..., n\}$ – set of monopolist strategies, and each strategy $i \in X_M$ determines the product and its price *P*(*i*); *П* – many consumers; $X_\Pi = J = \{1, 2, ..., m\}$ – set of consumer strategies, where each strategy $j \in X_\Pi$ defines a group of consumers and volumes of their consumption $V(j)$; $H_M = PV^T + \Delta_M$ – payoff matrix of the game *Г* for a monopolist, where elements of the matrix $H_{M_{ij}} = P(i)V(j) + \Delta_M(i, j)$ – profit of the monopolist in the event of a situation (i, j), $P(i)$ – price set by the monopolist, *V*(*j*) – the amount that consumers are willing to buy at advertised prices, Δ_M – matrix of state influence on a monopolist; $H_\Pi = -PV^T + \Delta_\Pi$ – the payoff matrix of the game *Г* for buyers, whose elements represent the total utility of the corresponding situation for consumers, Δ_Π – is the matrix of government impact on consumers.

The impact on the players from the state is not necessarily the same $\Delta_M \neq \Delta_\Pi$. he system is assumed to be closed, when the state redistributes part of the funds of the monopolist and consumers, i.e.

$$\sum_{i\in I, j\in J} \Delta_M(i,j) + \sum_{i\in I, j\in J} \Delta_П(i,j) = 0. \quad (2)$$

Within the framework of the study, not direct price setting is considered as a method of regulation, but the use of non-price levers: subsidies, excises, tariffs, etc. Thus, the state can influence the payoff matrices by adjusting Δ_M and $\Delta_П$, but cannot completely eliminate the conflict between the buyer and the monopolist by setting the price in the market (fig. 1).

In fact, the problem is reduced to an analogue of the arbitrage scheme, which consists in finding matrices Δ_M and $\Delta_П$, such that the bimatrix game

$$\Gamma = \left(\{M, П\}, \{X_M, X_П\}, \{H_M = PV^T + \Delta_M, H_П = -PV^T + \Delta_П\}\right.$$

had the desired (i.e. given) equilibrium situation for the state (*i, j*).

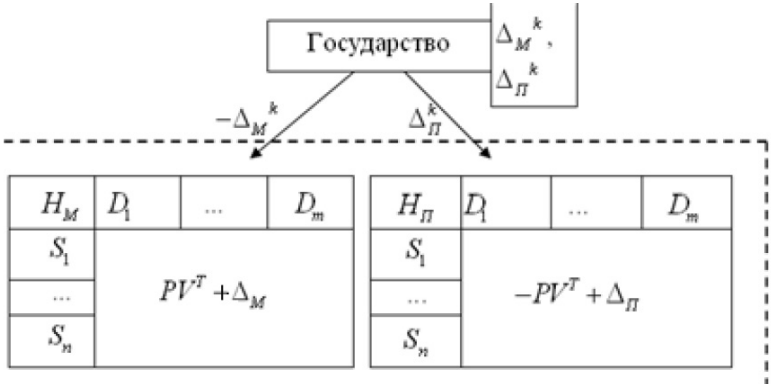

Figure 1. *Market situation management*

Finding correction matrices

The construction of adjusted (desired) payoff matrices $H_M = PV^T + \Delta_M$ and $H_П = -PV^T + \Delta_П$, for which situation (i^*, j^*) is a Nash equilibrium in pure strategies is reduced to the construction of matrices Δ_M and $\Delta_П$ such that

$$(\forall i \in I, j \in J)(P(i)V(j) + \Delta_M(i,j) \le P(i^*)V(j) + \Delta_M(i^*, j)) \quad (0)$$

$$(\forall i \in I, j \in J)(-P(i)V(j) + \Delta_П(i,j) \le -P(i)V(j^*) + \Delta_П(i, j^*)) \quad (2)$$

$$\sum_{i\in I, j\in J} \Delta_M(i,j) + \sum_{i\in I, j\in J} \Delta_П(i,j) = 0 \quad (3)$$

Conditions (1) and (2) mean that strategies i^* and j^* are acceptable for the monopolist and consumers, respectively, and condition (3) reflects the closed na-

ture of the system – the state redistributes part of the funds of the monopolist and consumers.

The policy that leads to the minimization of the distribution of funds by the state seems to be optimal. In this case, the corrected matrices can be found as a solution to the convex programming problem

$$\sum_{i\in I, j\in J} \left|\Delta_M(i,j)\right| + \left|\Delta_\Pi(i,j)\right| \to \min_{\Delta_M, \Delta_\Pi}. \quad (4)$$

Problem (1)-(4) has an optimal solution [3].

The Visual Studio programming environment [4] was used to solve the problem.

To store the P and V vectors, one-dimensional dynamic arrays are used, because this built-in data type meets the needs of the task. To store the values of λ (the Lagrange multiplier used in solving the problem by the decomposition method), the set container from the $< set >$ [5], library [5] is used, since it provides the ability to add non-repeating elements.

The P and V vectors are filled randomly using the Generation function, which adds random increments to a randomly generated positive seed. This method corresponds to the accepted rule of ordering the values of vectors in ascending order.

To store matrices Δ_M, Δ_Π dynamic two-dimensional arrays are used. To output and input information, the capabilities of the <iostream> and <fstream> libraries are used.

The algorithm for calculating the functions $G_\Pi(\lambda)$ and $G_M(\lambda)$ obtained as a result of applying the decomposition scheme is implemented in the C++ programming language (fig. 2).

```
int G(float L, int N, int* A, int S, bool isP){ //Вычисление функций Gm и Gn
	int k = 0; //индекс k/l
	int val;
	if (isP){
		k = 1 + ceil((1 - L)*N / 2);
		if (k > N)
			k = N;
		val = -A[k - 1] * (-L*N - 2 * k) - L*S + rVal(A, N, k) - lVal(A, k);
	}
	else{
		k = 1 + ceil((1 + L)*N / 2);
		if (k > N)
			k = N;
		val = A[k - 1] * (-L*N + 2 * k) + L*S + rVal(A, N, k) - lVal(A, k);
	}
	return val;
}
```

Figure 2. *Algorithm for calculating $G_\Pi(\lambda)$ and $G_M(\lambda)$*

The input of the function is the value $\lambda(L)$, the number of array elements, a reference to the array, the value S – the sum of all elements of the array, and the boolean

variable is*P*. The boolean variable is*P* determines which value ($G_{П}(\lambda)$ or $G_{М}(\lambda)$ should be calculated.

The *rVal* and *lVal* functions are also used in the calculations. The *rVal* function calculates the sum of the array elements located to the right of the given element, the *lVal* function – to the left of the given element.

The computational complexity of the algorithm is $O(1)$, the computational complexity of the initialization procedure is – $O(|I|)$ or $O(|J|)$.

The function of finding the value of λ, at which the function $G_{П}(\lambda)\cdot\sum_{i\in I}P(i)+G_{М}(\lambda)\cdot\sum_{j\in J}V(j)$ is maximum, includes enumeration of all values of the function from λ (fig. 3).

```
for (auto i : MAP){
	temp = G(i, J, V, vS, true)*pS + G(i, I, P, pS, false)*vS;
	if (temp > maxV){
		maxV = temp;
		maxL = i;
	}
}
```

Figure 3. *Finding the maximum value of* λ

Since $|\Lambda|=|I|+|J|$, and the complexity of calculating the value of $G_{П}(\lambda)$ and $G_{М}(\lambda)$ does not exceed $O(1)$, then the computational complexity of finding the maximum value of λ does not exceed $O(|\Lambda|)=O(|I|+|J|)$.

As a result of executing the program with the given parameters, such matrices $\Delta_{М}$, $\Delta_{П}$, are constructed that the payoff matrices $H_{М}$, $H_{П}$ make up the game, where each situation is Nash optimal, since the values in the columns have the same value in the matrix $H_{М}$ and the values in the rows in the matrix $H_{П}$. Thus, the given algorithm solves the problem in such a way that it brings the game to a state where each situation is Nash optimal.

References

1. Konovalova, E.D. Analysis of the efficiency of adaptation of state regulation instruments to changes in situations in markets with a high degree of monopolization / E.D. Konovalova // Mathematical and statistical study of socio-economic processes: a collection of scientific papers / ed. A.V. Panyukov. – Chelyabinsk: SUSU Publishing Center, 2011. – Iss. 3. – P.5-12.

2. Maltseva, E.D. Principles of adaptation of the state to the regulation of the degree of monopolization of the market in conditions of imperfect competition / E.D. Maltseva // Mathematical and statistical study of socio-economic processes: a collection of scientific papers / ed. A.V. Panyukov. – Chelyabinsk: SUSU Publishing Center, 2009. – Iss. 2. – P. 36-51.

3. Panyukov, A.V., Konovalova E.D. Stackelberg equilibrium control in the problems of state regulation of the natural monopoly market / A.V. Panyukov, E.D. Konovalova // Bulletin of SUSU. Series: Computational Mathematics and Informatics – 2013. – V.2 №4. – P. 2–10.

4. Gelmers S.A. Microsoft Visual Studio 2013. Step by step / S.A. Gelmers – M.: Ekom, 2014. – 612 P.

5. MSDN Development Center. [Electronic resource] URL: https://msdn.microsoft.com.

DOI 10.34660/INF.2022.45.79.294

霍奇金-赫胥黎模型的数值研究
NUMERICAL STUDY OF THE HODGKIN-HUXLEY MODEL

Nguyen Thi Thu
Master's student
Bakhtieva Lyalya Uzbekovna
Candidate of Physical and Mathematical Sciences, Associate Professor
Kazan Federal University

抽象的。 已经研究了一种众所周知的数学模型，该模型描述了可兴奋细胞（例如神经元和心肌细胞）中的电位作用，该模型基于细胞膜与电路的比较。 为了求解模型的方程，使用了高级编程环境 Matlab。 已经开发了一个用户界面，允许您以交互模式使用模型。 获得了实际重要的结果，得出了结论。

关键词：数学模型，心脏活动，微分方程的数值解。

Abstract. *A well-known mathematical model describing the action of potentials in excitable cells, such as neurons and cardiomyocytes, based on a comparison of the cell membrane with an electrical circuit, has been studied. To solve the equations of the model, the high-level programming environment Matlab was used. A user interface has been developed that allows you to work with the model in an interactive mode. Practically important results are obtained, conclusions are drawn.*

Keywords: *mathematical model, cardiac activity, numerical solution of differential equations.*

Introduction

The development of mathematical models related to medical problems is a very urgent task. Of particular importance are studies related to heart disease. Below are the results of modeling a qualitative picture of human cardiac activity, based on the study of the properties of the action potential of myocardial cells.

It is known that cardiomyocyte contraction is directly related to the behavior of the action potential [1]. Therefore, the nature of the heartbeat can be judged by the pattern of changes in the action potential of myocardial cells (Figure 1).

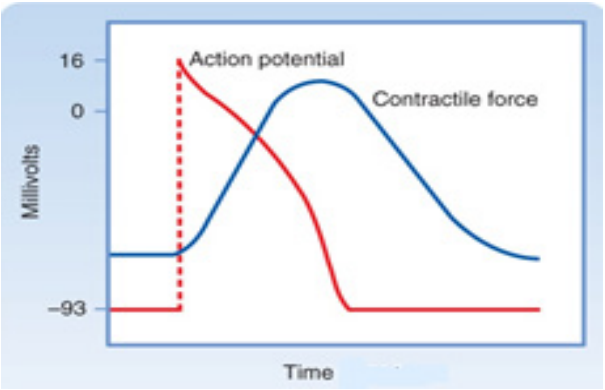

Figure 1. *The relationship of the action potential with the contraction of the cardiomyocyte.*

Description of the model

The model of Hodgkin and Huxley [2] describes the action potential in nerve cells (in particular, in myocardial cells). Within the framework of this model, the cell membrane is considered as a flat capacitor, the equivalent electrical circuit of which is shown in Figure 2. The capacitive current through the cell membrane can be described as the sum of changes in the membrane voltage V_m and ion currents, primarily due to sodium *(Na),* potassium *(K)* and other leaks *(L),* mainly chloride ions. Ionic currents are determined by their conductivities g, their equilibrium potentials *(E),* and how the channel gates open and close *(m, n, h)*.

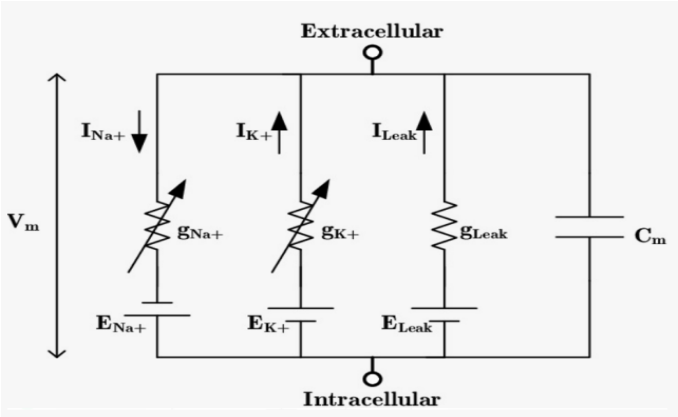

Figure 2. *Electrical diagram of the cell membrane*

The differential equations of the model [2] are the result of non-linear interactions between the membrane voltage V_m and the gating variables m, h, n for Na^+, K^+ and leakage L ions. The basic equation of the Hodgkin-Huxley model has the form

$$C_m \frac{dV_m}{dt} = -G_{Na} m^3 h(V_m - V_{Na}) - G_k n^4 (V_m - V_{Na}) - G_L (V_m - V_L) + I_{st}, \quad (1)$$

the variables m, h, n are related to the voltage V_m by the equations

$$\begin{aligned} \frac{dn}{dt} &= \alpha_n(V_m)(1-n) - \beta_n(V_m)n, \\ \frac{dm}{dt} &= \alpha_m(V_m)(1-m) - \beta_m(V_m)m, \\ \frac{dh}{dt} &= \alpha_h(V_m)(1-h) - \beta_h(V_m)h, \end{aligned} \quad (2)$$

system parameters (2) are determined by dependencies

$$\alpha_n(V_m) = 0.01 \frac{10 - V_m}{exp\left(\frac{10 - V_m}{10}\right) - 1}, \quad \beta_n(V_m) = 0.125 exp\left(\frac{-V_m}{80}\right),$$

$$\alpha_m(V_m) = 0.1 \frac{25 - V_m}{exp\left(\frac{25 - V_m}{10}\right) - 1}, \quad \beta_m(V_m) = 4 exp\left(\frac{-V_m}{18}\right),$$

$$\alpha_h(V_m) = 0.07 exp\left(\frac{-V_m}{20}\right), \quad \beta_h(V_m) = \frac{1}{exp\left(\frac{30 - V_m}{10}\right) + 1},$$

V_m is membrane potential, C_m is membrane capacitance, I_{st} is stimulating (external) current, t is time, G_K is maximum potassium conductance in the cell, occurring at $n = 1$, G_{Na} is maximum sodium conductance in the cell, occurring at $m = 1$ и $h = 1$, $V_{Na} = E_{Na} - E_r$, $V_K = E_K - E_r$, $V_L = E_L - E_r$, E_r is value of the resting potential (for most neurons this value is on the order of -60 to -70 mV), E_{Na}, E_K, E_L is equilibrium potentials for sodium, potassium and leakage ions.

Simulation results

The system of equations (1) - (2) was solved numerically using the Matlab program. For the convenience of calculations and the possibility of interactive work with the model, a user interface was developed (Figure 3).

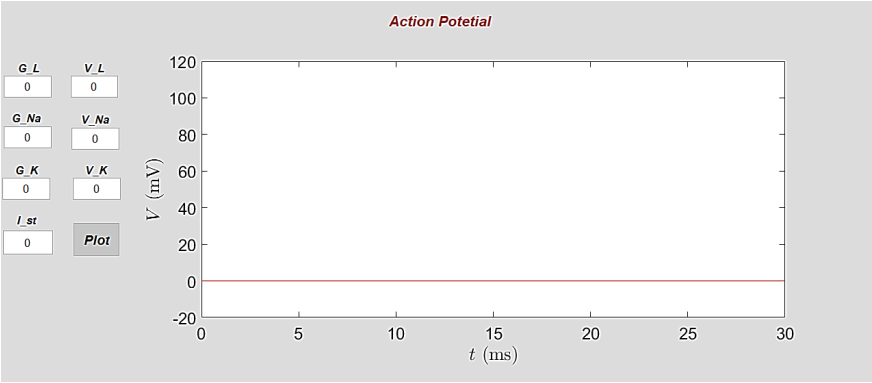

Figure 3. *User interface*

Figure 4 shows the simulation results for the parameter values given in [2] at $I_{st} = 6\ mA/sm^2$ (table 1), in the follows we will take these values as reference values (corresponding to the normal functioning of myocardial cells).

Table 1.

V_{ions}	$V_{Na} = 115$	$V_K = -12$	$V_L = 10{,}6$
g_{ions}	$g_{Na} = 120$	$g_K = 36$	$g_L = 0.3$

For resting potential $E_r = -60\ mV$, $E_{Na} = 55\ mV$, $E_K = 72\ mV$, leakage potential $E_L = -49{,}387\ mV$ respectively, $C_m = 1\mu F/sm^2$.

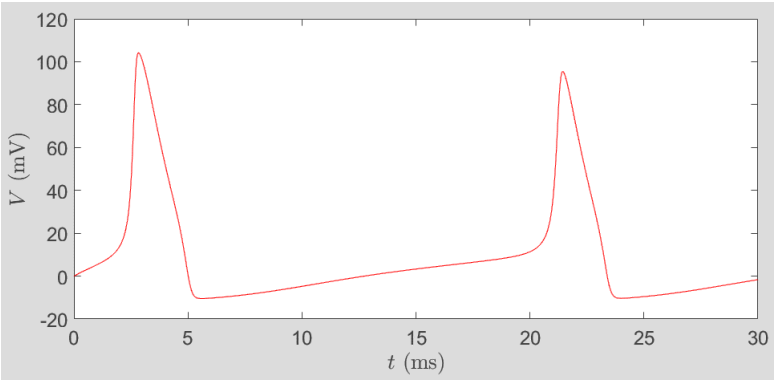

Figure 4. *Simulated action potential according to the Hodgkin-Huxley model*

Figures 5 - 7 show the results of numerical experiments with parameters that differ from the reference ones. Analysis of Figure 5 shows that a change in the magnitude of the external current significantly affects the picture of the heartbeat. In case of insufficient supply of an electrical impulse (Fig. 5a, $I_{st} = 2.6\ mA/sm^2$) the process completely attenuates and additional stimulation of myocardial cells is required, with an increase in the external current strength, the heartbeat becomes more frequent and its amplitude decreases (Fig. 5b, $I_{st} = 30\ mA/sm^2$), when the external current is too high (Fig. 5c, $I_{st} = 100\ mA/sm^2$), the heart palpitations with small amplitude occur.

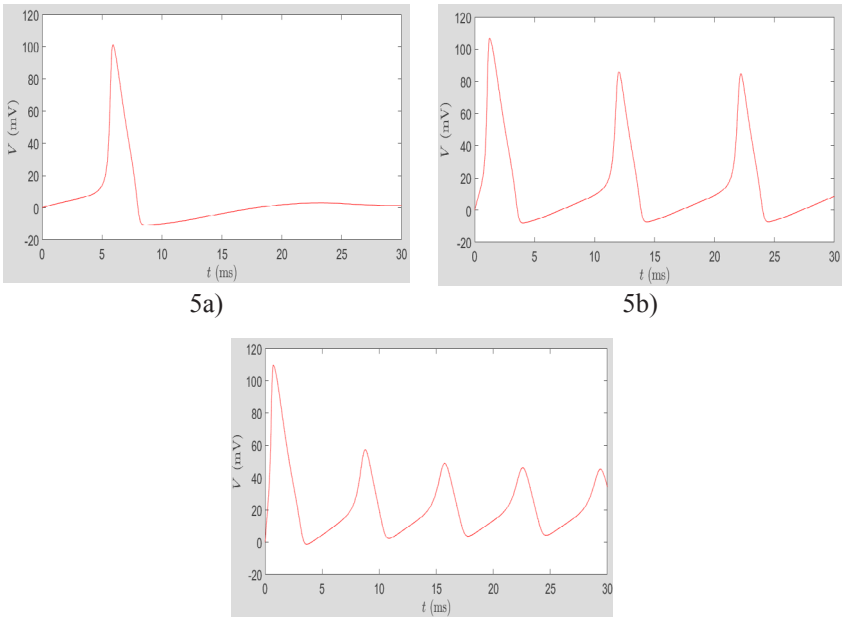

5a) 5b)

5c)

Figure 5. *Simulated action potential with a change in current*

Figure 6 shows the results of a study on the effect of sodium ions on the value of the action potential. With a decrease in the amount of sodium ions (Fig. 6a, $V_{Na} = 60\ mV$) there is no heartbeat process. When increasing the amount of sodium ions (Fig. 6b, $V_{Na} = 200\ mV$), the heartbeat becomes stronger and more frequent compared to the reference value.

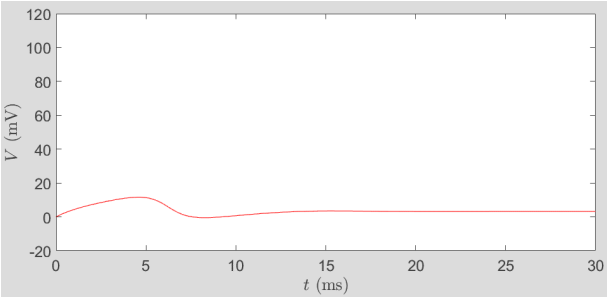

6a)

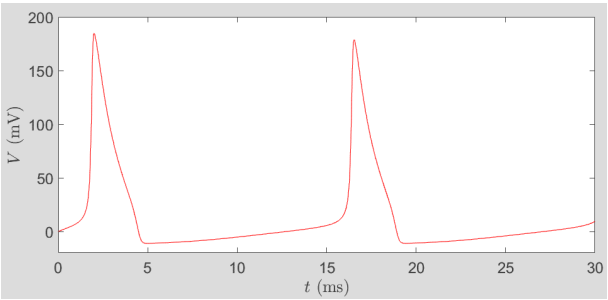

6b)

Figure 6. *Simulated action potential with changes in sodium ions*

Figure 7 shows that changes in the amount of potassium ions also significantly affects the picture of the heartbeat. Figure 7a corresponds to an increase in the amount of potassium ions ($V_K = -20\ mV$), figure 7b shows the attenuation of the heartbeat process with a decrease in the amount of potassium ions ($V_K = -10\ mV$).

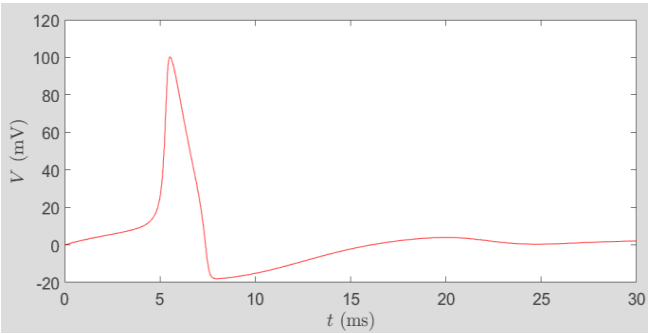

7a)

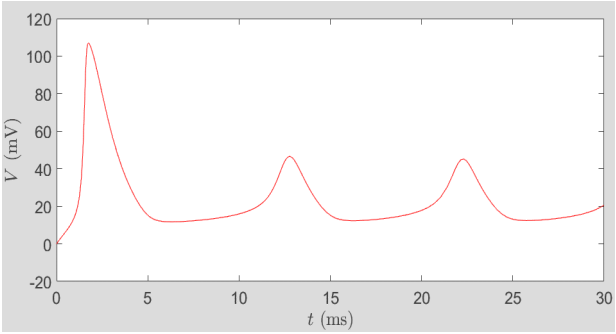

7b)

Figure 7. *Simulated action potentials with changes in potassium ions*

Conclusions

Based on the well-known model [2], with the support of modern programming tools, the authors developed an effective tool for analyzing the influence of various factors on the magnitude of the action potential of excitable cells of the body, in particular, cardiomyocytes. Since the nature of myocardial contractility is directly related to changes in action potentials, the results obtained allow us to judge the qualitative picture of changes in the human heartbeat depending on the values of the model parameters. This can be helpful when checking for heart abnormalities and making medical recommendations. The results obtained are in good agreement with the available data of other scientists [3].

References

1. *Electrical properties of the heart, http://users.atw.hu/blp6/BLP6/HTML/C0169780323045827.htm*
2. *The Journal of Physiology - 1952 - Hodgkin - A quantitative description of membrane current and its application to conduction and excitation in nerve (By A. L. Hodgkin and A. F. Hyxley), https://doi.org/10.1113/jphysiol.1952.sp004764*
3. *The Premier Undergraduate Neuroscience Journal 2015, The excitatory effect of temperature on the Hodgkin-Huxley model.*

NOTES

科学出版物

上合组织国家的科学研究：协同和一体化

国际科学大会的材料

2022年6月8日。中国北京

编辑A.A.Siliverstova
校正A.I.尼古拉耶夫

2022年6月8日。中国北京
USL。沸点：98.7。 订单253.流通500份。

在编辑和出版中心印制
无限出版社